Investigation of B cell and T follicular helper cell responses following priming with immunogens designed to trigger VRC01-class neutralizing antibodies to HIV-1

by

Alekhya Josyula Venkata

B.Tech., SreeNidhi Institute of Science and Technology, 2014

Thesis Submitted in Partial Fulfillment of the
Requirements for the Degree of
Master of Science

in the
Department of Molecular Biology and Biochemistry
Faculty of Science

SIMON FRASER UNIVERSITY
Fall 2017

Approval

Name: **Alekhya Josyula Venkata**

Degree: **Master of Science**

Title: **Investigation of B cell and T follicular helper cell responses following priming with immunogens designed to trigger VRC01-class neutralizing antibodies to HIV-1**

Examining Committee:

Chair: **Dr. Esther Verhayen**
Professor

Dr. Ralph Pantophlet
Senior Supervisor
Associate Professor
Faculty of Health Sciences

Dr. Jonathan Choy
Co-Supervisor
Associate Professor

Dr. Jamie Scott
Supervisor
Professor

Dr. Mark Brockman
Internal Examiner
Faculty of Health Sciences and
Department of Molecular Biology and Biochemistry

Date Defended/Approved: November 30, 2017

Ethics Statement

The author, whose name appears on the title page of this work, has obtained, for the research described in this work, either:

a. human research ethics approval from the Simon Fraser University Office of Research Ethics

or

b. advance approval of the animal care protocol from the University Animal Care Committee of Simon Fraser University

or has conducted the research

c. as a co-investigator, collaborator, or research assistant in a research project approved in advance.

A copy of the approval letter has been filed with the Theses Office of the University Library at the time of submission of this thesis or project.

The original application for approval and letter of approval are filed with the relevant offices. Inquiries may be directed to those authorities.

Simon Fraser University Library
Burnaby, British Columbia, Canada

Update Spring 2016

Abstract

Antibodies are one of the host's main defences against invading pathogens. The antibody response to Human Immunodeficiency Virus type 1 (HIV-1) infection elicited against the viral envelope (Env) spike can be categorised into non-neutralizing, narrowly neutralizing and broadly neutralizing, based on the relative breadth of circulating HIV-1 strains that the antibodies can neutralize in vitro. There has yet to be a vaccine that can elicit broadly neutralizing antibodies (bnAbs) against HIV-1. The general inability of germline (gl) precursors of these bnAbs to bind recombinant forms of the Env spike used in prospective vaccine formulations has been identified as one of the likely obstacles to achieving a bnAb response by vaccination. The design or identification of antigens that are able to engage gl precursors of bnAbs, dubbed "gl targeting", is a strategy currently being explored to elicit bnAbs. The VRC01-class of bnAbs, which target the highly conserved CD4 binding site on the HIV Env spike, are attractive templates for vaccine design owing to their tremendous neutralization potency and breadth and common mode of antigen recognition. Here, we investigated a panel of antigens, derived from the 45_01dG5 strain of HIV-1, for their ability to engage VRC01-class gl precursors. Additionally, we assessed their capacity to stimulate T follicular helper (Tfh) cell and B cell responses in C57BL/6 mice after a single priming immunization, using assays developed with two model immunogens. Specifically, we assessed the influence, on Tfh and B cell responses, of appending a single copy of the PanDR helper epitope (PADRE) to select immunogens in comparison to immunogens without the PADRE motif. We found that several constructs bind mature and gl-reverted versions of the VRC01 bnAb, as well as one of two VRC01-class precursor antibodies tested here. The immunizations revealed that immunogens with a glycan-masked V3 elicit a very weak Tfh response, which may have led to correspondingly weak B cell responses. Appendage of the single PADRE motif was insufficient to reverse the otherwise weak Tfh cell responses observed with the V3-masked immunogens used here, supporting the need for multiple copies of the motif to adequately provide Tfh cell mediated B cell help. In sum, this work provides insight into the early immune response to priming by HIV-1 candidate immunogens as part of a first phase of explorations toward eliciting VRC01-class bnAbs.

Keywords: HIV-1; VRC01; T follicular helper cells; immunization; antibodies

Dedication

I dedicate this thesis to my grandfather. Thank you Tata for your love, support and faith.

Acknowledgements

Firstly, I thank my supervisory committee: thank you Ralph for giving me this opportunity and for your mentorship and patience; thank you Jonathan for your invaluable advice and guidance; thank you Jamie for your kindness and encouragement. I sincerely thank all the past and present members of the Pantophlet, Choy, Scott and Brockman/Brumme labs, especially Naiomi, Sreedevi, Ruth, Fatima, Kevin, Aniqa, Natalie and Gursev for their support and encouragement over the past three years. I also thank my friends Pooja, Gayathri, Ali, Rashmi, Eshan, Poonam, Vivek, Tony and Tereyza for bearing with me, and my family Nathan, Kartik, Deepika, Aditya, Natasha, Leo, and my parents and grandparents for their unconditional love, support and understanding.

Table of Contents

List of Tables

List of Figures

List of Acronyms

Abs	Antibodies
Ad5	Adenovirus vector 5
ADCC	Antibody-dependent cellular cytotoxicity
AID	Activation-induced cytidine deaminase
AIDS	Acquired ImmunoDeficiency Syndrome
ANOVA	Analysis of variance
AP	Alkaline phosphatase
ASCs	Antibody secreting cells
BcR	B cell receptor
bnAbs	Broadly neutralizing antibodies
BSA	Bovine serum albumin
CD4bs	CD4 binding site
CDR	Complementarity determining region
CM	Central memory
CTLs	Cytotoxic T lymphocytes
DMEM	Dulbecco’s minimal essential medium
ELISA	Enzyme-linked immunosorbent assay
ELISPOT	Enzyme-linked Immunospot (assay)
EM	Effector memory (T cell)
Env	Envelope
FBS	Fetal bovine serum
FDCs	Follicular dendritic cells
GCs	Germinal centers
gl	Germline
Gp	Glycoprotein
HA1	Influenza haemagglutinin surface subunit
HBSS	Hank’s balanced salt solution
HIV	Human Immunodeficiency Virus
HPV	Human papilloma virus
iLN	Inguinal lymph node
ICOS	Inducible co-stimulator
Ig	Immunoglobulin

ITC	Isothermal Calorimetry
KLH	Keyhole limpet haemocyanin
MPER	Membrane proximal external region
MSM	Men who have sex with men
nAb	Neutralizing antibody
NIH	National Institutes of Health
Ni-NTA	Nickle-nitrilotriacetic acid
OD	Optical density
PADRE	PanDR helper epitope
PBS	Phosphate buffer saline
RT	Room temperature
SAP	SLAM-associated protein
SLAM	Signaling lymphocyte activation molecule
SHM	Somatic hypermutation
SPR	Surface plasmon resonance
Tfh	T follicular helper
TLR	Toll-like receptor
VH	Variable heavy chain domain
VL	Variable light chain domain

Chapter 1.

Introduction

1.1 Development of antigen-specific antibody responses

Antibodies are generated in response to immune stimulation, such as infections or immunizations; they mediate protection by several mechanisms, including (i) the direct neutralization of infectious pathogens, (ii) activation of the complement pathway or of antibody-dependent cellular cytotoxicity, leading to the death of infected cells, and (iii) opsonization leading to phagocytosis of infectious pathogens [1,2]. A first wave of antibodies (IgM and IgG) is produced by extrafollicular B cell subsets (B1 and marginal-zone B cells) that typically respond to antigens that do not stimulate T helper cells (T-independent antigens) and, as a result, do not undergo affinity maturation and class-switching [3,4]. Follicular B cells which are more specialized in sustained and high affinity antibody responses, and are responsible for mounting faster responses upon re-exposure to antigen, unlike extrafollicular B cells. The affinity maturation of antibodies and generation of humoral immune memory is governed by critical interactions between follicular B cells and T follicular helper (Tfh) cells in germinal centres (GCs)[5,6].

1.1.1 B Cell Participation in the GC Reaction

All B cells originate from progenitor cells in the bone marrow and mature in secondary lymphoid organs. These B cells populate compartments (follicles) in all lymph nodes and are surrounded by T cells, which originate in the thymus. Particulate antigens are captured from lymph by subcapsular macrophages and are shuttled to follicular dendritic cells (FDCs) by extrafollicular (bystander) B cells [7]. The FDCs then present antigen to follicular B cells. Antigen-specific follicular B cells migrate to the T-B cell border (Figure 1.1) to interact with

antigen-experienced Tfh cells, which come from the surrounding T cell zone [8]. Some B cells with relatively higher affinity for antigen differentiate into short-lived antibody-secreting cells, and relatively low affinity clones enter the GC pathway where they improve in affinity [9] (Figure 1.1). GCs are transient structures that typically form in response to T-dependent antigens and incorporate B cell follicles (Figure 1.1) [10,11]; they facilitate cognate B and T cell interactions and are critical for the selection of B cells with high affinity for antigen [12]. B cells that are primed to enter the GC pathway and Tfh cells migrate to the GC in response to cytokines produced by FDCs. Tfh cell provide signals to GC B cells in the form of CD40-CD40L interactions and cytokines for survival, proliferation and differentiation. B cells also undergo multiple rounds of affinity maturation in GC with Tfh aid and increase in affinity for their target epitopes by somatic hypermutation (SHM; accumulation of nucleotide mutations in antibody genes). As a result of clonal selection in GC, high affinity B cell clones are selected for clonal expansion, whereas low affinity clones undergo apoptosis [10,13]. B cells with relatively higher affinities for antigen differentiate into long-lived plasma cells and memory B cells [12].

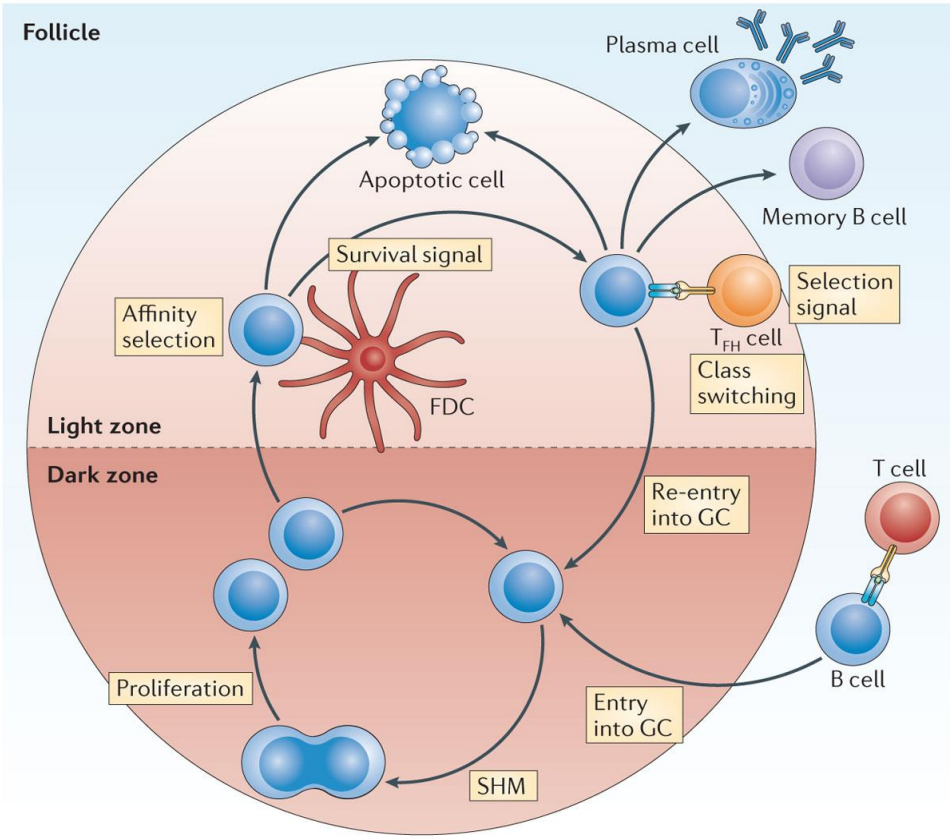

Figure 1.1 Schematic representation of the GC reaction

The GC is compartmentalized into dark and light zones. The dark zone is packed with B cells that enter the GC pathway and appears relatively darker when examined under a microscope [10]. It is the site of GC B cell proliferation and where the GC B cells undergo SHM. These B cells then enter the light zone, where they encounter antigen presented by FDCs, interact with antigen-specific Tfh cells leading to differentiation into plasma cells or memory B cells, or re-enter the dark zone for further SHM [7]. Image reused with permission from the Nature Publishing Group.

1.1.2 Tfh Cell Participation in the GC reaction

T cells are functionally divided into two broad subsets: cytotoxic T lymphocytes (CTLs) and helper T cells, and they are typically identified by their expression of the molecules CD8 and CD4, respectively, on their cell surface. CD4+ T cells are initially primed in the T cell zones of secondary lymphoid structures by antigen-presenting dendritic cells, and receive cytokine signals that

induce their commitment to a specialized subset such as Th1, Th2, Th17, Tfh, regulatory T (Treg), or regulatory T follicular helper cells (Tfr) cells [144]. Among the various CD4 T cell subsets, Tfh cells specialize in providing B cell help [14]. T cells that commit to the Tfh lineage are at this point pre-Tfh stage; they migrate to the T-B border present on the outskirts of the follicle to engage B cells (Figure. 1.1) [15]. Tfh cells express Bcl6, a master transcriptional regulator that prevents differentiation into non-Tfh phenotypes such as Th1, Th2, Th17, and Treg cells [16]. The PD-1 receptor, specific for PD-1 ligand expressed on B cells, is also upregulated on Tfh cells. Tfh cells furthermore express CD40L (CD40 ligand), inducible co-stimulator (ICOS), and SLAM-associated protein (SAP), which are involved in cognate interactions with B cells [17]. Tfh cells also secrete IL-21, which drives the survival, proliferation, and differentiation of GC B cells by inducing the intracellular expression of molecules such as Bcl6 and the plasma cell master regulator BLIMP-1 [18]. Another Tfh-secreted cytokine, IL-9, regulates memory B cell development by activating the transcription factor STAT1 [19]. A general consensus is that Tfh cells that provide cognate help to B cells within GCs can be identified as CD4+ cells with high-level expression of the surface markers CD44 (which identifies antigen-experienced T cells), PD-1, and CXCR5 [20–22].

Given their role in promoting the development of high affinity B cells, Tfh cells are of considerable interest to vaccine research, including the work described in this thesis; investigations into early immune responses related to the design of immunogens for eliciting antibodies to human immunodeficiency virus (HIV). In the following section, the HIV-1 pandemic as well as the structure of the HIV envelope (Env) spike are reviewed with relevance to vaccine design.

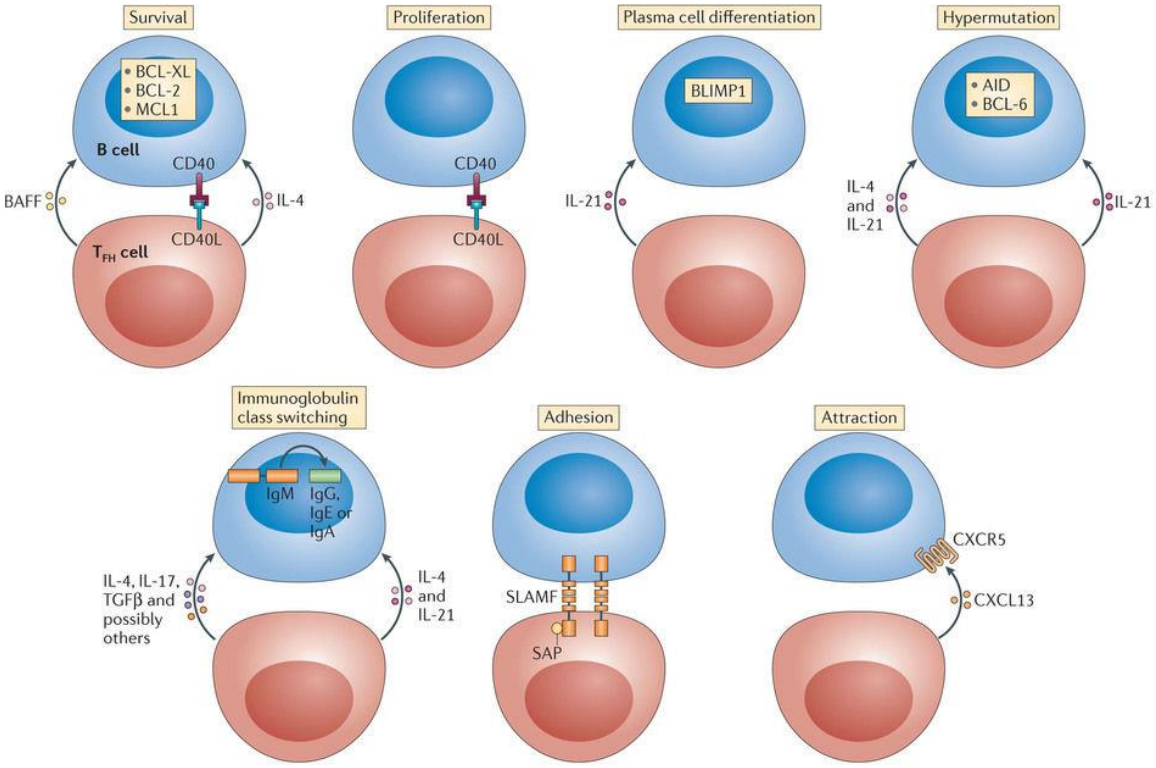

Figure 1.2 Tfh-mediated B cell help.

Tfh cells provide help to B cells for a variety of functions including survival, proliferation, and differentiation. Some of the help is mediated by Tfh-secreted cytokines such as IL-4, which activates transcription factors such as BCL-XL, BCL-2, and MCL-1, as well as IL-21, which promotes BLIMP-1 expression which in turn regulates the plasma B cell program. Activation induced cytidine deaminase (AID) is also activated by IL-4 and IL-21 and mediates the affinity maturation of antibodies through hypermutation of the antibody genes. Class-switching from IgM to IgG is also dependent on Tfh signaling. Cell adhesion molecules such as SLAM and SAP help establish cognate interactions, and Tfh migration to GCs is mediated by CXCR5 in response to CXCL13 produced by B cells. Image reused with permission from the Nature Publishing Group.

1.2 HIV and the search for a vaccine

HIV is a single-stranded RNA retrovirus within the genus *Lentivirus*, which is a member of the *Retroviridae* family of viruses. HIV preferentially infects activated CD4+ T lymphocytes, the loss of which weakens the immune system [23] and often leads to a debilitating disease called acquired immunodeficiency syndrome (AIDS). There are two distinct types of HIV: type-1 (HIV-1), which is primarily responsible for the global AIDS pandemic, and type-2 (HIV-2), which is prevalent mainly in West Africa [24,25]. Given the prevalence of HIV-1 infection, it is of greater relevance to vaccine research and as such is the primary focus of the following review.

1.2.1 The HIV-1 Pandemic

The first case of AIDS was reported in the United States in 1981, and a virus originally assigned to a family of human T cell leukemia retroviruses was identified as the causative agent in 1983 [26]. This virus was reclassified as HIV in 1986 [26–28]. As of 2016, there were an estimated 36.7 million people worldwide living with HIV, and 1 million of those infected died from AIDS-related illnesses by the end of 2016 (http://www.unaids.org).

HIV infection is no longer considered fatal provided that individuals receive adequate medical care. Over the years, combination anti-retroviral therapy (cART) has led to improved quality of life and an increase in life expectancy of HIV-positive individuals. Furthermore, the documented case of an HIV-infected individual who was declared HIV-negative after receiving a hematopoietic stem cell transplant from a donor carrying a homozygous deletion for a HIV-1 co-receptor gene CCR5Δ32 showed that HIV infection can be cured [29]. However, bone marrow transfusion from CCR5Δ32 donors is not a viable treatment option for most HIV-infected individuals, and cART is expensive and unavailable in sub-Saharan Africa where HIV infection is rampant but infected individuals lack adequate economic support and access to healthcare [30,31]. The stigma

associated with HIV-1 infection in such countries further promotes poor adherence to ART, even when it is available [32]. In developed countries such Canada, HIV-1 infection is mostly prevalent among high-risk populations, notably sex-workers and injection drug users (http://www.canada.ca/public-health/services). As of 2014, there were an estimated 75,500 people in Canada living with HIV-1 (http://www.catie.ca).

With an aim to eliminate the need for expensive and prolonged therapy, current research is focused on developing curative treatments: cell and gene therapy to eliminate integrated HIV genomes; technology to detect latent reservoirs of HIV-1; and T cell engineering to reduce T cell susceptibility to HIV-1 infection [33–36]. Furthermore, given the success of vaccines in eradicating epidemics such as smallpox [37], and the relative ease of accessibility to the general public, massive efforts are underway to design a vaccine that can prevent HIV-1 infection. The HIV Env spike is critical for viral infectivity and is targeted by antibodies that can neutralize a wide breadth of circulating HIV-1 strains, making it the central focus of vaccine efforts aiming to elicit such antibodies. However, the challenges of designing a vaccine that can elicit a robust and sustained neutralizing antibody (nAb) response are many [38,39]. An understanding of the structure and function of Env spike as well as how existing nAbs bind their targets on Env spike is deemed critical to vaccine design for eliciting similar types of antibodies.

1.2.2 Structure and function of HIV-1 Env spike

HIV entry is mediated by the Env spike, a glycoprotein (gp) consisting of a trimeric complex of heterodimers comprising the subunits gp120 and gp41; it forms the “spikes” that stud the surface of HIV particles [40]. The linear structure of gp120 is traditionally divided into five conserved (C1-C5) and five variable loop regions (V1-V5) [41]. Gp41 comprises an ectodomain or extracellular region, as well as cytoplasmic and transmembrane regions. The ectodomain is further divided into five functionally distinct regions: i) fusion peptide, ii) the polar region,

iii) N- and C-terminal heptad repeats (HR;HR1 and HR2, respectively), and iv) the membrane proximal external region (MPER) [42]. To initiate infection, the Env spike first interacts with adhesion molecules on the host-cell membrane, such as Siglec-7 and sometimes $\alpha_4\beta_7$ integrins, which bring the Env spike closer to the primary receptor, CD4 [43,44]. Binding to CD4 rearranges the V1/V2 and V3 loops that normally cover up the co-receptor binding site on gp120, thus exposing it to enable engagement of the requisite co-receptor, which, depending on the tropism of the virus, is generally CXCR5 or CXCR4 [45]. Co-receptor engagement results in further conformational changes in gp120 and exposure of the gp41 fusion peptides, which then shoot into the target cell membrane, ultimately creating a fusion pore and enabling entry of viral RNA into the target cell [45–47].

NAbs to HIV are directed against the Env spike, as it is the only exposed element on the viral coat. NAbs can be broadly categorized as strain-specific (*i.e*., of narrow breadth) and heterologous (of broader breadth) [48]. Broadly neutralizing antibodies (bnAbs) are heterologous nAbs that neutralize a broad spectrum of HIV strains. Thus, a significant goal of HIV vaccine research is to produce vaccines that can elicit bnAbs.

1.3 Non-neutralizing and neutralizing antibodies to HIV-1

Non-nAbs against HIV-1 develop in the first few weeks of infection. They are typically elicited against epitopes on Env spike fragments, such as solubilized gp120 or gp41 stumps attached to the viral membrane, but cannot bind the native Env spike, which is generally viewed as a prerequisite for virus neutralization [49–51]. However, it is believed that some non-nAbs may exhibit antiviral activity *via* Fc-mediated effector mechanisms, such as antibody-dependent cell-mediated cytotoxicity (ADCC) or antibody-dependent cell-mediated phagocytosis (ADCP) [52,53].

Strain-specific nAbs develop subsequent to non-nAbs (from weeks to months after infection). This delay is attributed to inadequate T cell help during

HIV infection [58–60]. Although strain-specific nAbs can exhibit some level of cross-reactivity, they predominantly target regions on Env spike that tend to be fairly variable. Such antibodies are thus incapable of neutralizing diverse strains [57,61–63].

As mentioned above, bnAbs are capable of neutralizing a diverse array of virus strains by targeting relatively conserved sites on the Env spike. They tend to develop only in a subset of HIV-infected individuals and, in adults, not until at least one year post-infection. In some children born to HIV-infected mothers, bnAbs seem capable of developing faster (i.e., <1 year) [221]. BnAbs appear to co-evolve with the virus, resulting in extensive SHM [64,65]. The following section focuses on the characteristics of bnAbs and their importance to vaccine design.

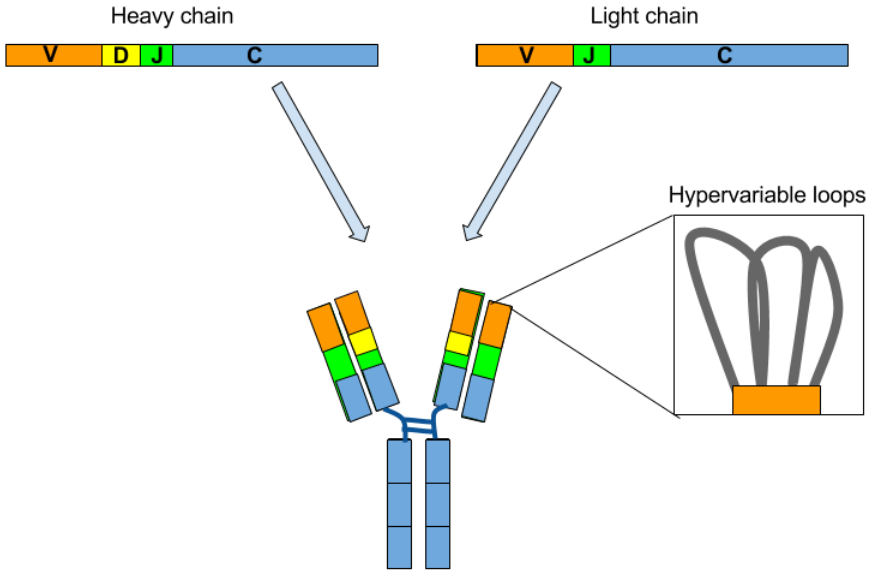

Figure 1.3 Structure of an antibody.

Shown here is the recombined heavy and light chain gene segments encoding the variable (V), diversity (D), joining (J) and constant (C) domains of an antibody. The heavy chain comprises multiple C domains as well as the V, D and J domains, whereas the light chain lacks a D region and only contains one C domain. The hypervariable loops constitute the antigen-interface region on both the heavy and light chain V domains.

1.3.1 Broadly neutralizing antibodies

BnAbs are produced in ~20% of chronically HIV-infected individuals [66]. BnAbs target conserved epitopes on the HIV Env spike [67]. Several bnAbs have been identified that target the same epitope, allowing them to be grouped into classes based on certain commonalities such as V gene usage and complementarity determining region (CDR) features [66,68]. Five regions on the Env spike are now recognized as bnAb targets: the CD4bs, glycans on the V1/V2 variable loops, glycans on the V3 loop, the MPER, and the gp120:gp41 interface region [66].

In addition to exhibiting broad and generally potent neutralization *in vitro*, passively transferred bnAbs have also been shown to confer protection from simian-human immunodeficiency virus (SHIV) challenge in non-human primates or HIV-1 challenge in studies with mice reconstituted with human immune cells [69–72]. Studies suggest that the bnAbs confer protection in these model systems by neutralization of cell free virus and ADCC activity against infected cells [73–75].

Among the numerous bnAbs that now have been discovered, it has become clear that some display exceptional neutralization breadth. Among the most notable are hose targeting the CD4 binding site on gp120 (CD4bs). This aspect, together with the functional conservation of the CD4bs, has led to substantial interest in vaccine design efforts to target the CD4bs.

Table 1 Features of CD4bs-targeting bnAbs.

Class	VH gene	VL gene	CDRL3 length (amino acids)
VRC01	VH1-2	Vκ3-20, Vκ1-33, Vκ1-5, Vκ3-15, Vλ2-14	5
8ANC131	VH1-46	Vκ3-20	9
IOMA	VH1-2	Vλ2-23	8
CH103	VH4-61	Vλ3-1	13
HJ16	VH3-30	Vκ3-30	8
VRC13	VH1-69	Vλ2-14	6
b12	VH1-3	Vκ3-20	9

BnAbs that target the CD4bs can be grouped into seven classes based on their ontogenies. These classes are named after and represented by: VRC01, 8ANC131, IOMA, CH103, HJ16, VRC13, and b12. These bnAb classes are further categorized as VH gene-restricted (blue) or CDRH3-restricted (yellow) based on their mode of antigen recognition [76]. VRC01, 8ANC131, and IOMA-class bnAbs are classified as VH gene-restricted, meaning that their interactions with antigen are dictated by their VH gene usage, whereas bnAbs belonging to CH103, HJ16, VRC13, and b12 classes make contact with antigen chiefly via their CDRH3s [77].

VRC01-class nAbs to the CD4bs of HIV-1

The CD4bs is targeted by seven classes of bnAb, which are subdivided into two groups based on their mode of contact with target epitopes: (i) VH (variable heavy chain domain) gene-restricted classes, comprising 8ANC131,

VRC01, and IOMA [76,77]; and (ii) those that primarily utilize their CDRH3s, represented by antibodies b12, CH103, HJ16, and VRC13 (Table 1). Of these, the class represented by antibody VRC01 is the largest and exhibits the greatest neutralizing potency and breadth. The antibody VRC01 was isolated from a chronically infected individual designated donor 45. The evolution of this antibody and the diversity of VRC01 lineage antibodies was studied using samples collected over 15 years [78]. This study showed that prolonged affinity maturation occurred during natural infection thus accounting for the high SHM observed with bnAbs such as VRC01 [78]

Antibodies of the VRC01 class have been recovered from a variety of individuals. They derive from the VH gene *VH1*-2*02 that encodes Trp, Asn, and Arg residues at positions 50, 58, and 71 that are critical for antigen recognition, and have characteristically short CDRL3s (five amino acid residues), and a similar mode of antigen recognition [79]. Another commonality is their extensive SHM, which is ~33% in VH and ~23% (at the amino acid level) in VL (variable light chain domain), as compared to ~6% in antibodies produced early on in infection [78–80]. Such commonalities have fuelled the idea that immunogens that can activate VRC01 class-specific precursor B cells might aid in eliciting equivalent bnAbs by immunization [81–84].

There are, however, several challenges to eliciting VRC01-class bnAbs, including: (i) the need for immunogens that can prime naïve B cells expressing VRC01-class immunoglobulin (Ig) receptors in many different people; (ii) the limited number (<1%) of such B cells in humans; (iii) the possible presence of distracting epitopes on the immunogen and (iv) the design of an immunization schedule to achieve the level of affinity maturation that may be required for neutralization breadth [85]. To approximate naïve bnAb precursors, gl antibodies of VRC01-class bnAbs have been inferred computationally and these then used to investigate antigen binding.

Studies with VRC01-class gl-reverted antibodies show that some of them exhibit autoreactive features [86,87], implying that priming immunogens might have to provide enough stimulus to precursor B cells to overcome tolerance checkpoints. Additionally, antigen-specific B cells in transgenic mice expressing the gl-reverted VRC01-class antibody 3BNC60 were found to be anergic [82]. The design of immunogens that can overcome the aforementioned hurdles is currently being investigated [85,88].

Before discussing ongoing immunogen design efforts to elicit VRC01-like bnAbs, past and ongoing vaccine trials are reviewed in the following section.

1.3.2 HIV-1 vaccine trials to date

The primary expectation from an HIV vaccine is an immune response that endures and protects against infection [38]. However, developing an effective HIV vaccine has proven to be immensely challenging [38,89]. The hurdles for inducing a protective immune response include, but are not limited to, the high genetic diversity of HIV, the capacity of the virus to evade immune surveillance, the relatively low accessibility of some conserved neutralization-sensitive epitopes on the Env spike [38]. There have been seven HIV-1 vaccine clinical trials to date, which aimed to confer protection by eliciting either bnAbs or CTLs through a variety of vaccination strategies [89].

Vaccines to elicit bnAb responses to HIV-1

VAX003 and VAX004 were the first HIV-1 clinical efficacy trials aimed at eliciting nAb responses to HIV-1. VAX003 tested a vaccine consisting of recombinant gp120s derived from subtype B strain MN and CRF01_AE strain CM244 (dubbed AIDSVAX B/E) in injection drug users in Thailand [90,91]. VAX004 used a bivalent formulation consisting of two subtype B gp120s from strains MN and GNE8 (AIDSVAX B/B), and tested efficacy in men who have sex with men (MSM) and high risk heterosexual women in North America and The Netherlands [92,93]. Both the VAX003 and VAX004 trials failed to demonstrate efficacy in

preventing HIV infection or disease progression, which was attributed to an overall inability of the elicited antibodies to effectively neutralize HIV strains representative of contemporaneous circulating viruses [93].

A more recent third trial, RV144, reported ~31% efficacy in preventing acquisition of HIV infection in vaccine recipients, excluding seven participants who were infected at the time of enrolment, relative to the placebo group [90,94]. This trial combined priming with a canarypox vector expressing the (vCP1521) CRF01_AE gp120 92TH023 fused to transmembrane portion of gp41, and boosting with the gp120 AIDSVAX B/E vaccine used in the VAX003 trials; it was conducted in heterosexual men and women in Thailand. A strong priming effect was observed with vCP1521, with a stronger and more durable antibody response following two protein boosts in this trial compared to the earlier VAX003 and VAX004 trials in at least a subset of recipients [90,93]. The nAb responses in RV144 to neutralization-sensitive (tier 1) HIV strains [95] were lower than those seen in VAX003 and VAX004, and mostly targeted V1V2 loop epitopes [90,93,96]. The IgG response observed in RV144 recognized linear epitopes on the V2 and V3 regions of gp120, correlated with reduced risk of infection, and exhibited antibody-dependent cell-mediated cytotoxicity (ADCC) activity [93]. Additionally, low levels of IgA seemed to correlate with a lower risk of acquiring infection in RV144 [90,93,96,97]. Given the modest success of the RV144 trial and to investigate if the responses observed in the RV144 trial in Thailand could be replicated in other regions, a phase-1b trial, designated HVTN 097, was initiated utilizing the RV144 regimen in combination with hepatitis B or tetanus toxoid vaccines in South Africa; early results indicate that the responses elicited in HVTN 097 are comparable to those of RV144 [98]. Another clinical trial, designated HVTN 702, is also underway in South Africa currently; it tests a prime-boost regimen modified from RV144 to include locally prevalent subtype C strains in both priming and boosting immunizations, *i.e*., two priming immunizations with canarypox vector (vCP2438) expressing subtype C gp120 (ZM96), and two boosting

immunizations with vCP2438 plus bivalent subtype C gp120s (TV1.C and 1086.C) formulated in the MF59 adjuvant (http://www.avac.org/trial/hvtn-702).

Vaccines to elicit broadly reactive CTL responses to HIV-1

Aside from the aforementioned trials designed to elicit bnAb responses, there have been three trials so far aimed at eliciting broadly reactive CTL responses (HVTN 502, 503, and 505). The HVTN 502 trial, also termed the STEP trial, tested an adenovirus type-5 (Ad5) vector vaccine, designated MRK Ad5 subtype B HIV-1 *gag/pol/nef*, in MSM and high-risk heterosexual men and women in clade B pre-dominant regions of the world (North America, South America, and Australia). The HVTN 503 trial, dubbed the Phambili trial, tested the same Ad5 vector vaccine in heterosexual men and women in clade C-dominant South Africa [99,100]. Both studies were terminated when preliminary analyses showed failure to reduce early viral loads [101]. Further analyses revealed an elevated risk of infection in Ad5 seropositive or uncircumcised men in the STEP study, which *in vitro* analyses suggested could be due to an expansion of Ad5-specific CD4+ T cells that were readily susceptible to HIV infection [102]. A later study tested a DNA/rAd5 (DNA prime and rAd5 boost) vaccine in fully circumcised and Ad5 seronegative men and transgender women in the United States [102]. The DNA prime expressed clade-B Gag, Pol, Nef, and Env proteins from clades A, B, and C, while the rAd5 boost expressed a Gag-Pol fusion protein in addition to the multi-clade Envs [103]. This study, designated HVTN 505, was designed to minimize the risk of infection observed in the STEP trial by excluding Ad5 seropositive and uncircumcised men from the test subjects. The HVTN505 trial was, however, terminated early due to its failure to reduce viral load set points [104].

Given the explosive discovery of numerous bnAbs in the last several years [64,105], there has been an increased focus on designing vaccines that can elicit such antibodies [106,107].

1.4 Engineered immunogens to elicit bnAbs to HIV-1

As reviewed above, vaccine trials to date have not been successful in eliciting robust and sustained levels of nAbs. However, the recovery of numerous bnAbs from HIV-infected individuals in recent years and studies of their interactions with Env spike have led to increased efforts to tailor immunogens for the induction of bnAbs [66]. Thus far, attempts at eliciting bnAbs in animal models, such as non-human primates or humanized mice—immunodeficient mice implanted with human hematopoietic stem cells that can develop into all blood cell lineages have largely been unsuccessful [82,108,109]. This has been attributed to several factors, including the limited antibody repertoire in humanized mice, differences between human and primate antibody repertoires in the case of non-human primates, the inability of the immunogens to prime the right precursor B cells, and inadequate Tfh cell help [38]. The use of intentionally designed or selected antigens to activate precursor B cells of bnAbs are dubbed gl-targeting. Antigens capable of promoting the elicitation of PGT121-like bnAbs, which targets the N332-glycan-supersite, and VRC01-class bnAbs to the CD4bs are some of the most prominent examples currently being explored [110].

The two most notable attempts at designing VRC01-class gl-targeting antigens yielded the 426c core and eOD-GT8 [110] proteins. 426c core was designed to lack glycans at three critical N-linked glycosylation sites (AA positions 276, 460, and 463) in addition to truncations of the V1V2 and V3 loops. As a result, it bound to a majority of gl-reverted VRC01-class antibodies. The gp120 outer domain-based construct, eOD-GT8, was used to isolate VRC01-class precursor B cells from healthy individuals. Thus, both these constructs show great promise as candidate priming immunogens. Furthermore, they highlighted features of gl-reverted VRC01-class antibodies that are relevant to vaccine design efforts, such as the subtle differences in binding preferences. For instance, the 12A21gl and 3BNC60gl antibodies have a greater net-negative charge on their CDRLs than other VRC01-class antibodies, such as VRC01gl and NIH45-46gl, resulting in weaker binding to constructs carrying negatively-

charged amino acid residues at key contact sites [86,82,111]. Other features, such as differences in light-chain V-gene usage (*Vκ1-33*, *Vκ3-20, Vκ3-15,* and *λ2-14*) and CDRH3 amino-acid composition are also believed to contribute to the varied binding to different antigens [86]. It must be noted that the inferred gl antibodies used in these studies contain mature CDR3s.

Novel strategies, including the use of nanoparticle-based multimeric immunogens, glycan-masking of unwanted B cell epitopes, deletion of the N276 glycan to enable better access to the CD4bs, and surface stabilization of proteins to activate precursor B cells, have also been investigated [112,110,88,113]. The glycan-masking of undesired epitopes was first proposed as a means to focus the antibody response to the CD4bs, to improve the chances of activating VRC01-like precursor antibodies while preserving the conformation of the immunogen.

In the following section, a component of vaccine design that has shown promise for improving Tfh-mediated B cell help and the subsequent antibody response are reviewed.

1.5 T helper epitopes to promote antibody responses

Crucial to the strategy of successive immunization are the formation of memory and shaping of B cell lineages during affinity maturation, requiring GC reactions. The memory Tfh cells generated in the primary response support memory B cells in the recall response [114]. Optimal Tfh cell involvement is critical to antibody generation and B cell survival [115]. Abrogated Tfh cell function correlates with impaired GC development and subsequent antibody generation, as is seen in HIV infection [58,59]. Furthermore, the promotion of Tfh function has been associated with robust antibody responses [116–120]. Thus, the efficacy of vaccines that promote T cell-mediated B cell help is being evaluated in the context of infectious diseases such as malaria, dengue, influenza, human papilloma virus (HPV), HIV, and cancer immunotherapy [117,121–125]. Multiple studies have shown that T cell responses can be improved with the use of

oligonucleotides or short peptide fragments [125–127]. Examples of such elements include Toll-like receptor agonists, such as CpG, short interfering RNAs (siRNAs), and peptides bearing T cell epitopes [128–131].

Besides promoting T cell responses, T helper epitope peptides can augment interactions between T and B cells. The PanDR helper epitope (PADRE) is a 13-amino acid motif (AKFVAAWTLKAAA) that binds to at least 10 different human HLA-DR molecules, and I-A^b molecules of mice [129,132]. PADRE has been shown to improve protective antibody responses when fused to a wide range of protein antigens, including for HIV, malaria, dengue, pneumonia, and *Burkholderia* [121,124,133,134].

1.6 Thesis overview

Several factors have been found to contribute to the inability of vaccines to elicit bnAbs. Briefly, some of these are: the inability of immunogens to engage gl precursors of bnAbs; the inaccessibility of relevant, conserved epitopes to antibodies; the presence of distracting B cell epitopes; and inadequate Tfh cell help [66]. This thesis explores the importance and possible improvement of Tfh cell-mediated B cell help during the priming response to a panel of immunogens designed to engage VRC01-class gl antibody precursors.

Chapter 2 discusses the validation of assays to phenotypically and functionally identify Tfh cells and B cells. The glycoproteins keyhole limpet haemocyanin (KLH) and influenza haemagglutinin HA1 were used as sentinels for priming immunizations in mice, and subsequently tissue was collected and used to assay for antigen-specific Tfh cells and GC B cells. These two proteins were chosen because immune responses to these immunogens have been well characterized. Enzyme-linked immunospot assays were also developed to enable enumeration of cytokine (IL-21)-secreting cells and antibody-secreting cells. These experiments enabled the optimization of protocols and provided

reference points to compare results from priming immunizations with HIV-1 Env spike-derived immunogens.

In Chapter 3, the design of the abovementioned HIV-1 Env spike-derived immunogens are presented and discussed, and their ability to engage VRC01-class precursors, as well as their capacity to elicit Tfh cell and B cell responses following priming immunizations in mice are investigated. Specifically, the ability of a PADRE-appended immunogen carrying a glycan-masked V3 to elicit Tfh and B cell responses following a priming immunization is compared to variants without PADRE, those with and without the glycan-masked V3, as well as to the positive-control, classical immunogens mentioned above. The results suggest that V3 glycan-masking significantly reduced the Tfh cell response, possibly affecting B cell responses, such as GC B cell proliferation and antibody production, and was not restored by appending a single copy of the PADRE motif. Lastly, in Chapter 4, key conclusions from the data presented in Chapters 2 and 3 are summarized, with suggestions for further investigations to improve Tfh cell-mediated B cell help to 45_01dG5-derived candidate priming immunogens.

Chapter 2. Investigation of T and B cell responses to priming immunizations with model immunogens

Alekhya Josyula Venkata[1] and Ralph Pantophlet[1,2]

[1]Department of Molecular Biology and Biochemistry and [2]Faculty of Health Sciences

2.1 Abstract

Priming with protein immunogens typically induces Tfh cells, which interact with antigen-primed B cells in germinal centres (GCs) and promote antibody production. The accurate measurement of Tfh and B cell responses is crucial to estimating the immunogenicity of Human Immunodeficiency Virus type-1 (HIV-1) envelope (Env) spike-derived candidate priming immunogens. To this end, we tested protocols to assess Tfh and B cell phenotype and function following priming mice with two unrelated and commonly used glycoproteins, keyhole limpet haemocyanin (KLH) and HA1 from H1N1 Influenza viruses. KLH was found to elicit superior Tfh and GC B cell frequencies. HA1 elicited modest antibody and antibody secreting cell (ASC) responses despite seemingly poor Tfh and GC B cell induction at Day 7 post-prime, suggesting that Tfh and GC B cell frequencies had appreciated at later time points following HA1 immunization. In conclusion, this work enabled the validation of protocols to phenotypically identify Tfh and GC B cells, measure antibody titers, and enumerate ASCs in addition to providing points of comparison for future immunizations with HIV-1 Env spike-derived priming immunogens.

2.2 Introduction

GCs develop within the follicles of secondary lymphoid organs following immunization and are comprised primarily of B cells [10]. Dendritic cell-primed Tfh cells, a subset of CD4+ T cells specialized for providing B cell help, gain entry to the GC compartment by upregulating CXCR5, a receptor for CXCL13 [135], and provide help to antigen-specific GC B cells [6,9]. Tfh cells also co-express

programmed death ligand-1 (PD-1), which regulates activation through the PD-1:PD-1L pathway [136]. Commitment to the Tfh lineage is regulated by the transcription factor B cell lymphoma 6 (Bcl6) [135,137,138]. The GC reaction is regulated by T follicular regulatory (Tfr) cells that share common cell surface markers with Tfh cells [139]. The Tfr cell program is regulated by FoxP3, a transcription factor that also serves to distinguish this subset from Tfh cells [140]. IL-21 secretion is another characteristic feature of Tfh cells [5], which serves as a proliferation and differentiation signal for GC B cells [18]. Similar to Tfh cells, GC B cells are also driven by Bcl6 expression [141]. Upon commitment to this B cell phenotype, the activation marker GL7 is upregulated. Fas (CD95) is co-expressed and regulates GC B cell homeostasis [142]. The GC reaction peaks around Day 7 post-immunization and declines thereafter, as is visible from the Tfh and GC B cell frequencies measured at Day 7 and later [10]. During the course of the GC reaction, GC B cells that have differentiated into ASCs exit the lymph node and accumulate in the bone marrow and other sites (*e.g.*, mucosal subepithelia) [143].

Here, I validated Tfh cell and GC B cell staining protocols using two model immunogens; KLH, and recombinant HA1 subunit from A/California/04/2009 and A/Brevig Mission/1/1918. Additionally, I developed and tested ELISPOT assays to detect IL-21-secreting cells and ASCs. A plethora of markers have been described for phenotypic identification of Tfh and GC B cells by flow cytometry, but only a select few have been deemed necessary and sufficient and as such are the focus of this report [144–146]. Protein engineering and transfections (section 2.3.1) were performed by R.P. The flow cytometry, ELISPOT assays and ELISAs were performed by A.J.V. with guidance from R.P.

2.3 Methods

2.3.1 Expression of recombinant soluble antibody in mammalian cells to mimic antibody-secreting cells

The HIV gp120 V3-specific antibody, B4e8 [147,148], and the flu HA stem-specific antibody, CR6261 [149], were produced in 293T cells to imitate antibody-secreting cells. Plasmids encoding the B4e8 heavy and light chains were obtained from Lisa Cavacini [150], and codon-optimized CR6261 heavy and light chain gene constructs were synthesized by DNA 2.0 from published sequences [149]. DNA encoding the antibody heavy and light chains were subcloned into pFUSEss-CHIg-hG1 and pFUSEss-CLIg-hk (Invivogen), respectively. The 293T cells were maintained in Dulbecco's minimal essential medium (DMEM)/F-12 (Lonza) supplemented with 5% (v/v) fetal bovine serum (FBS; Thermo Fisher). For transfection, cells were trypsinized (TrypLE Express; Life Technologies), pelleted by centrifugation (0.1 rcf for 5 min at 15º C), re-suspended in DMEM/F-12 supplemented with 10% FBS, counted, seeded at a density of $2x10^5$ cells/well in a 6-well plate (Corning), and then cultured overnight at 37 ºC. The next day, plasmid DNA (2-4 µg per well) was mixed with polyethyleneimine "Max" (PEImax; Polysciences Inc.; 4-8 µl per well) in DMEM/F-12 without FBS (0.2 ml per well). Following a brief incubation, the mixtures were added dropwise to the cells and then cultured at 37 ºC. At three days post-transfection, cells were trypsinized (TrypLE Express; 1 ml per well), pelleted as described above, and then re-suspended in RPMI 1640 (Lonza) supplemented with 10% (v/v) FBS and used to mimic antibody-secreting cells (ASCs) for the development of an ASC Enzyme-Linked ImmunoSpot (ELISPOT) assay (see below).

2.3.2 Immunizations

Recombinant HA1 surface subunit from H1N1 Influenza viruses A/California/04/2009 and A/Brevig Mission/1/1918 (Sino Biologicals Inc.) as well as keyhole limpet haemocyanin (KLH; Sigma) were used for immunizations. Approximately 6- to 8-week-old female C57BL/6 (n=5/group; Charles River) or

BALB/c (n=2-3/group; Jackson Labs) mice were immunized subcutaneously at the base of the tail, and tissue and blood recovered at Days 7 and 28 post-immunization. Each animal received a total of 20 µg HA1 (Sino Biologicals Inc.) or KLH (Sigma) formulated in 200 µl endotoxin-free phosphate buffer saline (PBS) (Lonza) plus 20 µg QuilA (Brenntag Biosector), distributed into two injections of 100 µl each. Formulations were mixed on a shaker for 1 h at room temperature (RT) prior to injection and administered on the same day. All experiments were approved by the Animal Care Committee at Simon Fraser University (protocol 1098HS-13).

2.3.3 Flow cytometric analysis of Tfh and GC B cells

Inguinal lymph nodes (iLNs) were recovered from naïve and immunized mice (seven days post-immunization). Single-cell suspensions were prepared by passing tissue through a 70-µm cell strainer (VWR). Samples were then washed and re-suspended in Hank's Balanced Salt Solution (HBSS; Lonza) supplemented with 10% (v/v) FBS (Thermo Fisher). The following antibody conjugates, specific for the noted cell-surface molecules, were used to identify Tfh cells: CD4 (PerCP-Cy5.5; RM4-5), CXCR5 (biotinylated; 2G8) (both from BD), CD44 (PE-Cy7; IM7), and PD-1 (APC; J43 or RMP1-30) (both from Thermo Fisher). A CD19-specific antibody (APC-Cy7; 1D3; BD) was used to exclude B cells for Tfh staining. GC B cells were identified using the same APC-Cy-conjugated CD19 along with conjugated antibodies specific for: IgD (FITC; 11-26c), GL7 (PE-Cy7; GL-7), and CD95 (PE; 15A7) (all from Thermo Fisher). The aforementioned PerCP-Cy5.5-conjugated CD4-specific antibody was used to exclude CD4+ T cells for GC B cell staining. For CXCR5 and GL7 staining, cells were incubated first with biotinylated antibody for 30 min, followed by incubation with streptavidin-conjugated PE-Cy7 or PE (both from Thermo Fisher) along with fluorophore-conjugated antibodies. Intracellular staining for FoxP3 was performed using the FoxP3/transcription factor staining buffer set (Thermo Fisher) or the fixation/permeabilization solution kit (BD), as per the manufacturer's instructions. All incubation steps for cell surface staining were

performed on ice. Reagents for flow cytometry were used at the manufacturer's recommended concentration or pre-titrated to determine the optimal concentration for usage. Following staining, data were acquired on a BD FACSJazz and analyzed with FlowJo v10 software (Treestar).

2.3.4 Enzyme-Linked ImmunoSpot (ELISPOT) Assays

IL-21

A prospective ELISPOT to detect IL-21-secreting cells was developed using 293T cells transfected with a plasmid encoding murine IL-21 (pUNO1-mIL21) (Invivogen). Transfection of cells and harvesting at three days post-transfection were performed as described above for recombinant antibodies. To assay for IL-21 expression, 96-well multiscreen filter plates (Millipore) were coated with unconjugated anti-mouse IL-21 (FFA21; Thermo Fisher) at 5 µg/well and incubated overnight at 4 ºC. Plates were then washed eight times with PBS containing 0.02% Tween (Bioshop) (PBS-T) and blocked with 5% (w/v) skimmed milk (Bioshop) dissolved in PBS for 1 h at RT. Following the blocking step, cell suspensions were added in triplicate to the wells starting at 10^5 cells/well in RPMI 1640 (Lonza) supplemented with 10% FBS (Thermo Fisher) and serially diluted. Plates were then incubated for 48 h at 37 ºC in a CO_2 incubator. After washing as before, PE-conjugated anti-mouse IL-21 (mhalX21, Thermo Fisher) diluted in PBS-T and supplemented with 5% (w/v) skimmed milk (diluent) was added (0.5 µg/well) and incubated for 1 h at RT, followed by washing as before and then the addition of biotin-conjugated anti-PE antibody (Thermo Fisher) diluted 1:2,000 in diluent. After 1 h of incubation at RT, the plates were again washed as before, then alkaline phosphatase (AP)-conjugated streptavidin (Jackson ImmunoResearch) diluted 1:2,000 in diluent was added and incubated for 30 min at RT. Plates were then washed as before and rinsed (four times) with distilled water. Nitro-blue tetrazolium/5-bromo-4-chloro-3-indolylphosphate (NBT/BCIP; Sigma) substrate, dissolved in AP buffer (0.1 M $NaHCO_3$, 2 mM $MgCl_2$, pH 9.8), was added to plates and spot development was monitored every 15-30 seconds.

The reaction was stopped by pipetting off the solution and rinsing with distilled water. Washed plates were left to dry in the dark. The number of spots per well was calculated as the average of two independent counts performed using a dissecting microscope.

IL-21-secreting cells in iLN from naïve and immunized mice were assayed by ELISPOT as described above. Cell suspensions were prepared as described above for flow cytometry.

Antibody-Secreting Cells (ASCs)

A prospective ELISPOT assay for measuring antigen-specific ASCs was developed using 293T cells expressing antibodies B4e8 (gp120 V3 specific) or CR6261 (flu HA stem specific). Ninety-six-well multiscreen filter plates (Millipore) were coated in duplicate with antigen at 1 µg/well and anti-mouse or human IgG Fc-specific capture antibody (Jackson ImmunoResearch) at 0.5 µg/well and incubated overnight at 4 ºC. Washing and blocking were performed similar to the IL-21 ELISPOT. Cell suspensions were added to the wells and serially diluted in media starting at 10^5 cells/well. Plates were incubated for 4 h at 37 ºC in a CO_2 incubator and washed as described above for the IL-21 ELISPOT. Subsequently, biotinylated anti-mouse or -human IgG Fc-specific antibody (Jackson ImmunoResearch) diluted 1:2,000 in diluent was added to antigen-coated wells, and anti-mouse or -human $F(ab')_2$-specific antibodies (Jackson ImmunoResearch) diluted 1:2,000 in diluent was added to capture antibody-coated wells. The plates were incubated for 1 h at RT, then washed as before and incubated for 30 min with AP-conjugated streptavidin diluted 1:2000 in diluent. The reaction was stopped by pipetting out the solution and rinsing with distilled water. Plates were developed, stored, and spots enumerated as described above for the IL-21 ELISPOT.

ASCs in bone marrow from naïve and immunized animals were measured by ELISPOT using the protocol described above. Cell suspensions were prepared by first incubating bone marrow samples with red blood cell lysis buffer

(155 mM NH_4Cl, 10 mM Tris/HCl, pH 7.5) for 5 min, followed by centrifugation at 0.1 xg for 5 min at 15 ºC and then re-suspension in RPMI 1640 (Lonza) supplemented with 10% FBS.

2.3.5 Enzyme-Linked ImmunoSorbent Assay (ELISA)

Antigen-specific IgG levels in the sera of naïve and immunized mice were determined by ELISA as described elsewhere [151]. Antigen-specific serum IgM was measured in a similar manner using anti-mouse IgM µ chain-specific antibody (Jackson ImmunoResearch).

2.3.6 Statistical Analysis

Statistical significance of T and B cell frequencies, as well as ASCs between the different groups of mice was determined by one-way analysis of variance (ANOVA) followed by Tukey's multiple comparisons test (****p <0.0001, *** p < 0.001, **p < 0.01, and *p <0.05), performed using Graphpad Prism 6 software [152,153]. Fitness of data, for performing one-way ANOVA, was assessed using JMP v12 software (SAS) in consultation with Ian Bercovitz (Department of Statistics, Simon Fraser University).

2.4 Results

2.4.1 Optimization of staining protocol enables identification of Tfh cells in KLH-immunized mice at seven days post-prime

Tfh cells drive the formation of GCs, which are essential for B cell differentiation and antibody production [5]. To validate staining protocols for identifying Tfh cells, we first primed BALB/c mice with HA1 derived from H1N1 Influenza virus A/Brevig Mission/1/1918. Tfh cells were defined as the PD-1+ CXCR5+ subset of activated (CD44hi) CD4+ T lymphocytes (Figure 2.1A) [14,16]. Although we were able to identify a Tfh population, this result could not be replicated in C57BL/6 mice (Figure 2.1A). In parallel, we changed the staining

strategy in an attempt to exclude regulatory T cells from the Tfh cell population in iLN of immunized mice using the marker FoxP3 [146]. However, this staining protocol (CD4+ CD44hi FoxP3+ PD-1+ CXCR5+), which was investigated initially in C57BL/6 mice and subsequently in BALB/c mice immunized with A/California/04/2009 HA1 subunit, did not allow for the detection of Tfh cells in either mouse strain. Because C57BL/6 mice were to be used in future immunizations (Chapter 3), we only used this mouse strain in subsequent protocol validations.

Immunizing KLH which has been shown to elicit strong Tfh cell responses[154], and excluding FoxP3 from the gating scheme also did not enable the identification of Tfh cells in C57BL/6 mice (Figure 2.1C). Based on suggestions that CXCR5+ cells in a Tfh gating scheme are best detected with a substantially brighter fluorophore [120], we revised our Tfh gating scheme to use the fluorophore PE for detecting CXCR5+ cells instead of the relatively dimmer APC-Cy7. This revision indeed allowed the detection of Tfh cells, albeit only in KLH but not HA1-immunized C57BL/6 mice (Figure 2.1C).

In sum, the KLH immunization showed that Tfh cells can indeed be identified using our revised staining scheme in draining iLN at seven days post-prime. Comparison of the results from the BALB/c and C57BL/6 immunizations with the HA1 from A/Brevig Mission/1/1918 suggested that the T helper cell epitopes on this immunogen might be predominantly I-A^d restricted, consequently eliciting higher Tfh cell frequencies in BALB/c mice relative to C57BL/6 mice. Furthermore, there is some evidence indicating that Tfh cell (and B cell) responses following immunization with A/California/2009 HA1 may be delayed in C57BL/6 mice [128,155], thus further explaining our inability to detect a Tfh cell response in these mice seven days after priming with antigen.

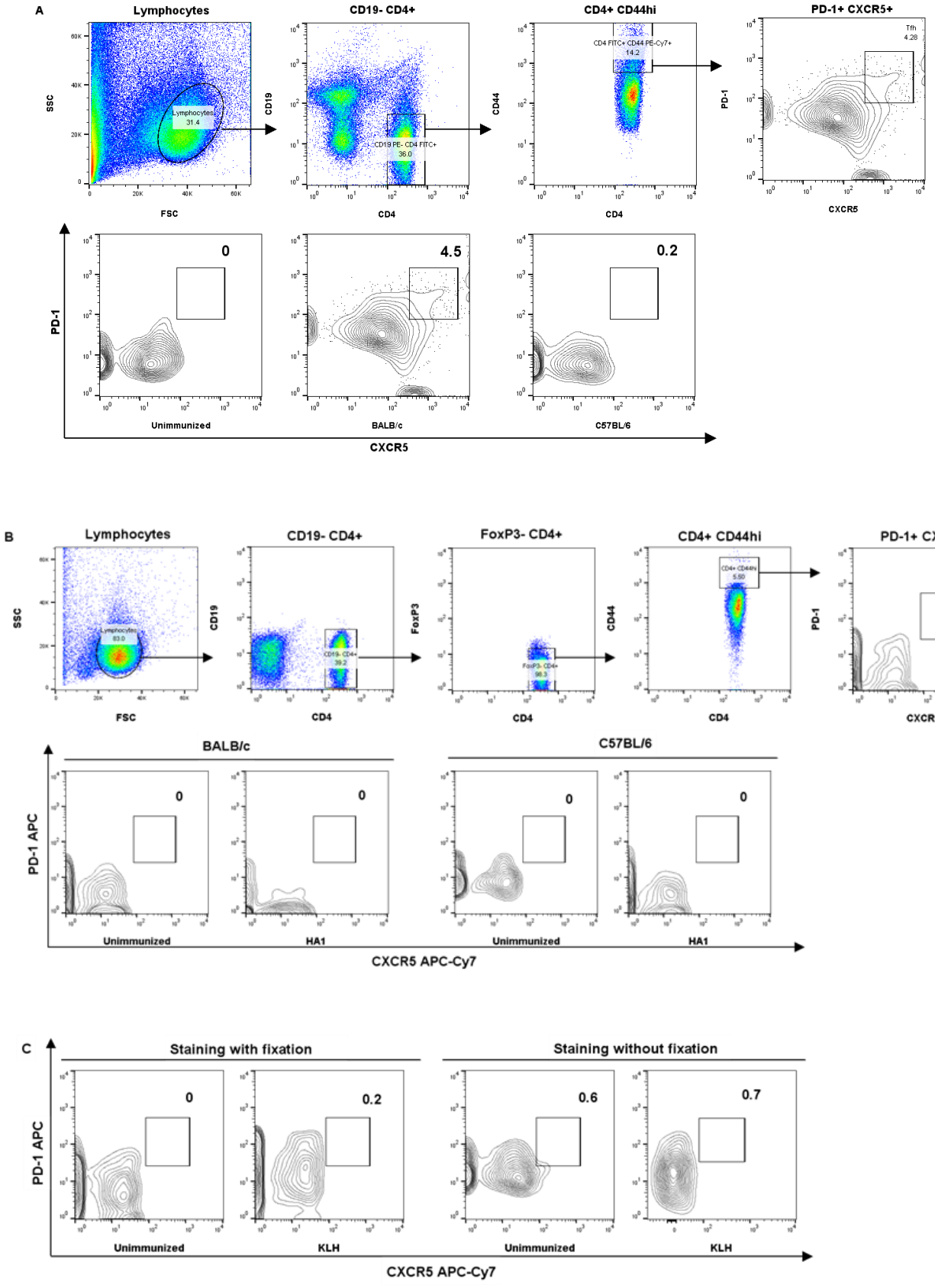
A
Lymphocytes
CD19- CD4+
CD4+ CD44hi
PD-1+ CXCR5+
SSC
FSC
CD19
CD4
CD44
PD-1
CXCR5
Lymphocytes
31.4
CD19 PE- CD4 FITC+
36.0
CD4 FITC+ CD44 PE-Cy7+
14.2
Tfh
4.28
0
4.5
0.2
Unimmunized
BALB/c
C57BL/6
B
Lymphocytes
CD19- CD4+
FoxP3- CD4+
CD4+ CD44hi
PD-1+ CXCR5+
FoxP3
Tfh
0.10
BALB/c
C57BL/6
PD-1 APC
Unimmunized
HA1
CXCR5 APC-Cy7
C
Staining with fixation
Staining without fixation
0
0.2
0.6
0.7
KLH

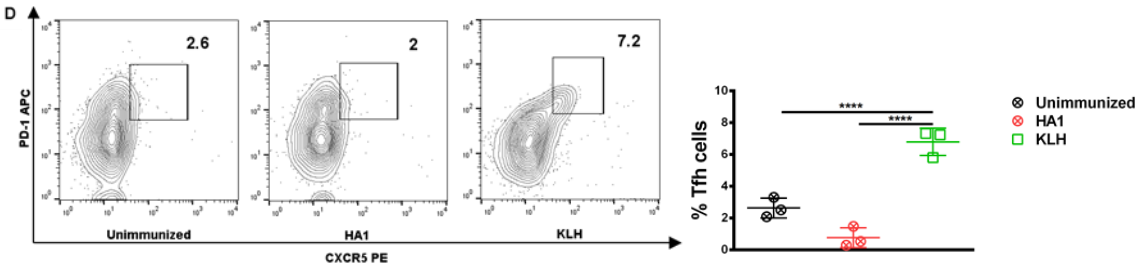

Figure 2.1 Optimization of staining protocol enables the identification of Tfh cells in KLH-immunized mice.

A) Shown here is the gating strategy used to identify Tfh cells (CD4+ CD44hi PD-1+ and CXCR5+) and representative Tfh cell plots from unimmunized mice and mice immunized with the HA1 subunit from A/Brevig Mission/1/1918. Tfh cells could be identified in BALB/c mice (n=2), but not C57BL/6 (n=3) mice immunized seven days previously. B) Shown here is the strategy used to exclude Treg cells (CD4+ CD44hi FoxP3+ PD-1+ and CXCR5+) from the Tfh cell population, and final plots from HA1 (A/California/04/2009)-immunized BALB/c (n=3) and C57BL/6 (n=3) mice at Day 7 post-prime. Data from C57BL/6 mice are representative of two independent experiments. C) Tfh cell frequencies in KLH-immunized C57BL/6 mice when stained with and without fixation at Day 7 post-prime. D) Representative flow cytometry plots and dot plots comparing the Tfh cell frequencies in unimmunized mice, and mice immunized days previously with KLH or HA1 (A/California/04/2009). Tfh cells were identified using PE-conjugated CXCR5. Data are from a single experiment unless indicated otherwise. Statistical significance was assessed by one-way ANOVA followed by Tukey's multiple comparisons test (****p <0.0001, *** p < 0.001, **p < 0.01, *p <0.05). Only statistically significant differences are denoted.

2.4.2 KLH elicits greater GC B Cell frequencies relative to flu HA1 at seven days post-prime.

The frequency of GC B cells is partially a measure of the help provided by Tfh cells to mature follicular B cells that have encountered antigen [22]. GC B cells can be identified phenotypically by their expression of GL7 and CD95 (Fas) [21]. A subset of this population expresses IgD, a marker typically associated with naïve and IgM+ B cells [141,156]. To minimize ambiguity regarding the activation state of the B cells, we defined GC B cells as the GL7+ and CD95+ subset of IgD-

CD19+ B lymphocytes (Figure 2.2A), which is consistent with other reports [21,141]. The staining protocol for GC B cells was validated with HA1 (A/California/04/2009) and KLH, as was done for Tfh cell staining. We found, as with the Tfh cell analysis, that KLH elicited a robust GC B cell response, thus further supporting the use of KLH for protocol validation in our experimental system. In contrast, GC B cells were not detected at the same time point in HA1-immunized mice (Figure 2.2B). The presence of GC B cells in naïve mice, although somewhat peculiar, may be indicative of low-level immune responses to environmental stimuli in these mice. The lack of observable GC B cells in HA1-immunized mice was not entirely unexpected, given that Tfh cells were also undetectable in these mice at Day 7 post-prime (Figure 2.1D).

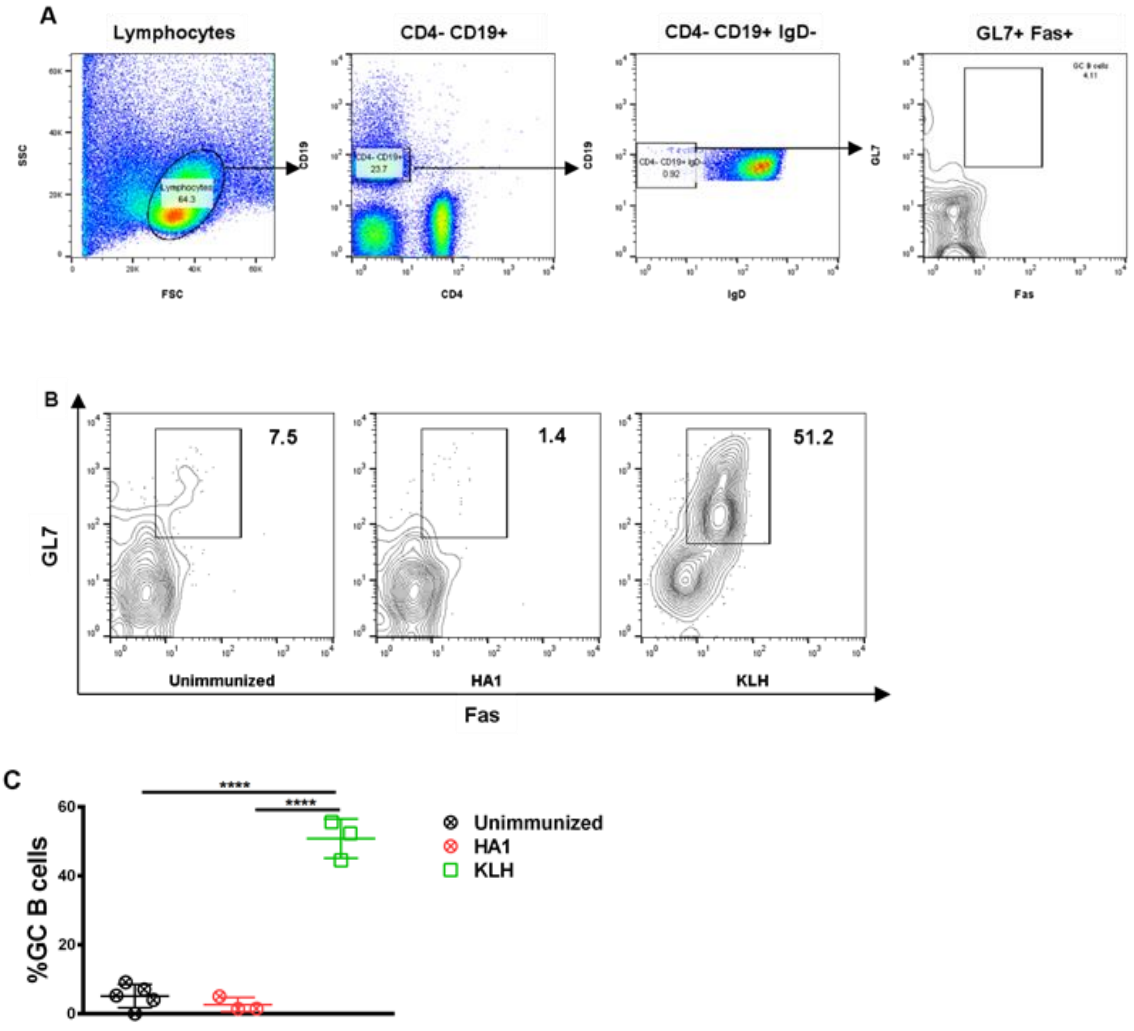

Figure 2.2. KLH elicits greater GC B cell frequencies relative to HA1 at Day 7 post-prime.

A) Gating strategy used to identify GC B cells (CD19+ IgD- GL7+ CXCR5+) in C57BL/6 mice immunized seven days previously. B) Representative flow cytometry plots showing GC B cell (GL7+ Fas+) frequencies in unimmunized (n=5), and KLH- (n=3) and HA1- (n=3) immunized mice. C) Dot plots comparing IgD- GC B cell frequencies in immunized and unimmunized mice. Data are representative of a single experiment. Statistical significance was assessed by one-way ANOVA followed by Tukey's multiple comparisons test (****p <0.0001, *** p < 0.001, **p < 0.01, *p <0.05). Only significant comparisons are shown.

2.4.3 ELISPOT assay enables enumeration of ASCs

B cells that differentiate into ASCs enter circulation and eventually reach the bone marrow [9]. While secreted antibodies can be measured in serum by ELISA, ASCs can be enumerated by ELISPOT. Similar to GC B cell proliferation, the differentiation of GC B cells into ASCs is not just indicative of B cell function; it is also a measure of the Tfh cells' aid to B cells [145,157–159]. We first developed an ELISPOT protocol for the detection of ASCs using 293T cells expressing the gp120-specific antibody B4e8 and the flu-specific antibody CR6261 together with gp120 as antigen. As per the assay design, antigen-specific spot formation was observed only with B4e8 (Figure 2.3A).

Having developed the ELISPOT protocol, we then used it to assay cells recovered from the bone marrow of naïve mice and those immunized 28 days earlier with HA1 (A/California/04/2009) or KLH. We observed antigen-specific ASCs in both HA1- and KLH-immunized mice (Figure 2.3B), although only the latter group had significantly higher ASC levels relative to naïve mice. The average percentage of KLH-specific ASCs was also higher for KLH-immunized mice than for HA1-immunized ones.

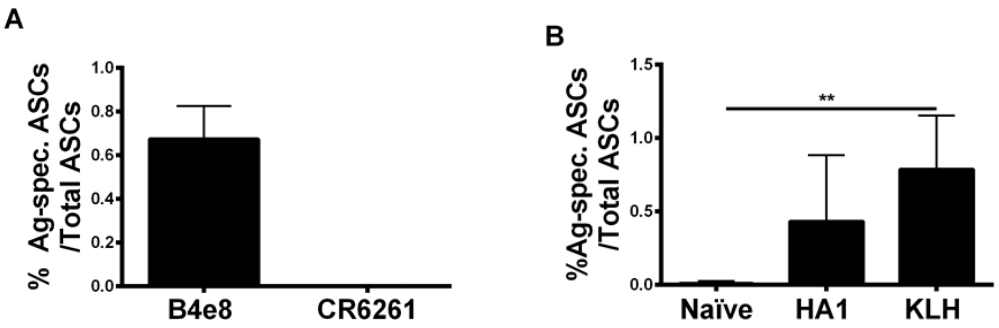

Figure 2.3. Enumeration of antigen-specific ASCs by ELISPOT.

A) 293T cells expressing gp120-specific anti-V3 antibody B4e8 and the flu HA-stem specific antibody CR6261 were assayed using full-length JR-FL gp120 as antigen. Error bars indicate deviation from the mean from a single experiment with two technical replicates. B) Bone marrow samples from naïve (n=4), and A/California/04/2009 HA1- (n=3) and KLH- (n=5) immunized C57BL/6 mice (28 days post-prime) were assayed in ELISPOT with homologous antigen. Error bars indicate deviation from the mean from a single experiment with three to five replicates.

2.4.4 ELISPOT assay enables enumeration of IL-21-secreting cells

ELISPOT is a commonly used method to assess IL-21 secretion by Tfh cells [20]. We first developed a protocol to enumerate IL-21-secreting cells using 293T cells transfected with a plasmid encoding mouse IL-21 (Figure 2.4). We unexpectedly observed a higher frequency of spots if 0.5 µg plasmid DNA was used for transfection compared to 4 µg; this suggested that the transfection with the greater amount of plasmid was incompatible with the cells. We then used this protocol to assay cells prepared from iLNs of HA1-immunized mice at Day 7 post-prime, but were unable to detect any IL-21 secretion (data not shown). This outcome was not entirely unexpected, given that Tfh cells were undetectable at the same time point by flow cytometry (Figure 2.1D).

However, in other published protocols, cells are stimulated with antigen prior to measuring IL-21 secretion [20,160]; such a step was not included in our first iteration of the IL-21 ELISPOT protocol. In retrospect, KLH stimulation might

have better enabled us to determine the suitability of this protocol for enumerating IL-21-secreting cells. We have since modified this protocol to include the antigen stimulation step and validation of this revised protocol is planned.

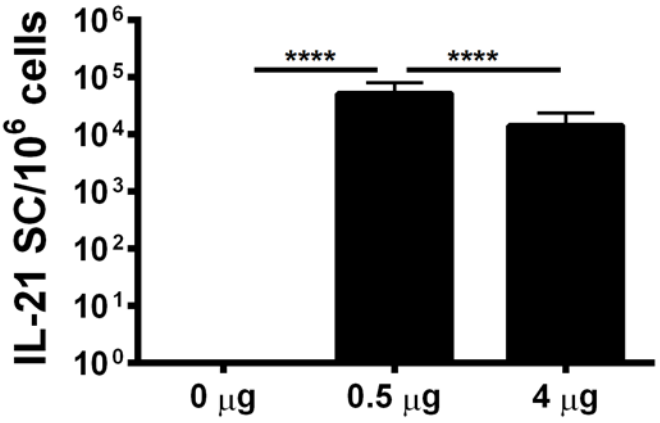

Figure 2.4. ELISPOT assay enables the enumeration of IL-21-secreting cells.

Shown here is the average number of spot-forming cells per 10^6 plated cells. 293T cells transfected with 0.5 µg plasmid encoding mouse IL-21 appeared to have a greater number of spot-forming cells than those transfected with 4 µg of the plasmid. Error bars indicate deviation from the mean. Data are from a single experiment.

2.4.5 KLH elicits greater magnitudes of IgM and IgG responses relative to HA1

IgM and IgG are the most common antibody isotypes elicited in response to immunization with a T-dependent antigen [10]. To measure IgM and IgG responses, we assayed serum samples recovered at 7 and 28 days post-prime from HA1- and KLH-immunized mice with homologous antigen in ELISA (Figure 2.5). KLH immunization yielded robust IgM and IgG responses by Day 7. IgM levels in KLH-immunized animals diminished by Day 28, whereas IgG levels increased as expected. For HA1, we were somewhat surprised to find IgG at Day 28, given that Tfh and GC B cell frequencies were very low/undetectable at Day 7 (Figures 2.1 and 2.2). However, as noted earlier, Tfh cell and B cell responses

following immunization with A/California/2009 HA1 have been found to be delayed in C57BL/6 mice [128,155]. Thus, our findings here are consistent with those of past reports. Importantly, they verify the use of HA1 as a “sentinel immunogen”, for detecting relatively weak T-dependent immune responses and, as such, it is at the opposite end of the spectrum relative to Tfh responses elicited by KLH.

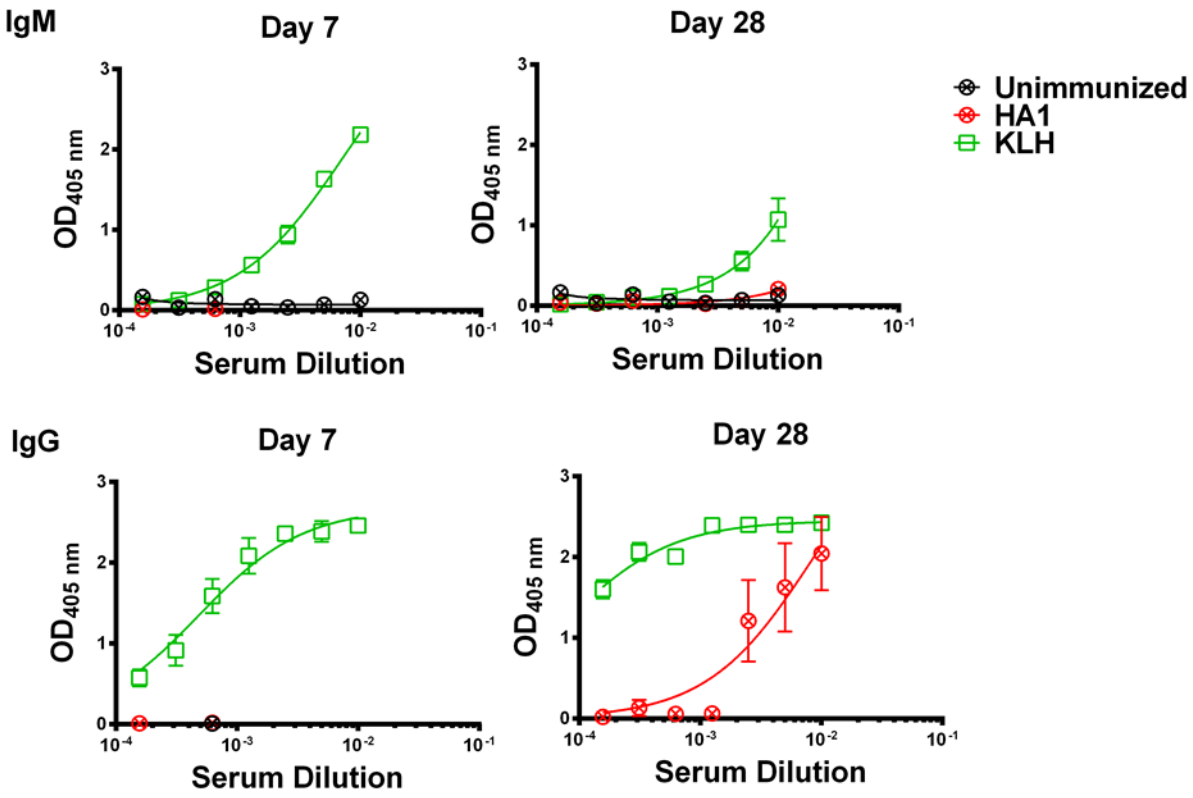

Figure 2.5 KLH elicits greater magnitudes of IgM and IgG responses relative to HA1.

Sera from HA1- (n=3) and KLH- (n=3-5) immunized mice recovered at Days 7 and 28 post-prime were assayed in ELISA with homologous antigen. Sera from unimmunized mice (n=5) were assayed similarly for comparison. Each data point on a curve is representative of the mean optical density (OD) measured at the corresponding serum dilution. Error bars indicate deviation from the mean obtained from two independent experiments.

2.5 Discussion

Model immunogens are widely used to characterize T and B cell responses. In this thesis, we performed priming immunizations with KLH and HA1, assessed Tfh and GC B cell frequencies, enumerated ASCs, and measured serum antibody in naïve and immunized mice.

For immunizations, mice received subcutaneous base-of-tail injections of antigen adjuvanted in QuilA. Following immunization, the local draining lymph nodes, which in this case were the iLN (Harrell et al. 2008), were then recovered for Tfh and GC B cell analyses seven days later [8]. The early Tfh and B cell responses to KLH and HA1 were strikingly different. KLH appeared to be more immunogenic and elicited greater frequencies of Tfh and GC B cells than HA1 (Figures 2.1 and 2.2). Additionally, KLH also elicited IgM and IgG responses at Day 7 (Figure 2.5). Although Tfh and GC B cell frequencies in HA1 immunized mice were barely above baseline at Day 7, an IgG response was observed at Day 28 (Figure 2.5). ASCs were also enumerable in the bone marrow of KLH- and HA1-immunized mice at 28 days post-prime (Figure 2.3).

HA1 was initially used for testing Tfh and GC B cell staining strategies for flow cytometry, but soon proved to be insufficient for validating the various protocols. HA1 from the A/Brevig Mission/1/1918 virus elicited a Tfh cell response in BALB/c mice but not in C57BL/6 mice, whereas the HA1 from A/California/04/2009 did not elicit Tfh cells in either strain (Figure 2.1). The reason for this was unclear at the time, but further investigation of the response to the A/California/04/2009 HA1 informed us that GC induction might have been slower in A/California/04/2009-immunized mice, thus producing an IgG response at 28 days post-prime, despite poor Tfh and GC B cell induction. Other studies have shown that Tfh induction occurred as late as Day 10 post-prime [149,155]. Our preliminary attempts at identifying Tfh cells in C57BL/6 mice proved fruitless and prompted us to investigate the use of KLH, a potent immunogen commonly used for characterizing T and B cell responses [21,162]. However, initial experiments with KLH showed that our staining protocol did not allow the detection of Tfh cells. To

address this, we replaced the fluorophore on CXCR5, one of the cell surface markers on Tfh cells, with the relatively brighter PE, and were able to identify Tfh cells in KLH-immunized C57BL/6 mice (Figure 2.1D).

In addition to *ex vivo* assessments, we also validated ELISPOT protocols. The assay to detect IL-21-secreting cells was developed using IL-21-secreting 293T cells. Using this assay, we successfully enumerated IL-21 secretion *in vitro,* but not in samples recovered from HA1-immunized mice. This was not unexpected, since Tfh cells could not be identified in these mice at the same time point. In retrospect, samples from KLH-immunized mice would have better informed the protocol design and development for enumerating IL-21-secreting cells *ex vivo*. The ELISPOT procedure was also modified to detect ASCs. This protocol was developed using 293T cells that secrete the gp120-specific antibody B4e8 [150], and was later tested with bone marrow recovered from HA1- and KLH-immunized mice at 28 days post-prime (Figure 2.3). The ASC responses to HA1 and KLH were similar, which was unexpected, given the difference in magnitude of IgG responses observed by ELISA at Day 28. In conclusion, the immunizations with KLH and HA1 allowed the verification of various protocols and also established reference points for the comparison of results from future experiments.

Chapter 3. A single copy of the PanDR helper epitope is insufficient to restore the T follicular helper cell response to V3-hyperglycosylated, HIV-Env spike-derived germline-targeting immunogens

Alekhya Josyula Venkata[1] and Ralph Pantophlet[1,2]

[1]Department of Molecular Biology and Biochemistry and [2]Faculty of Health Sciences

3.1 Abstract

Germline (gl)-targeting is a strategy that aims to elicit broadly neutralizing antibodies (bnAbs) such as the CD4 binding site (CD4bs)-targeting VRC01-class antibodies. This entails activation of naïve, B cells bearing “gl”-precursors to the VRC01-class antibodies (gl-VRC01). This strategy has not yet been successful, perhaps because gl-targeting is impeded by the presence of distracting B cell epitopes, such as those on the V3 region of gp120. To this end, we constructed immunogens with a glycan-masked V3 to eliminate unwanted B cell epitopes. To compensate for the loss of any T helper epitopes that might have resulted from V3 glycan-masking, we appended a pan DR helper epitope (PADRE) to a V3 glycan-masked antigen. We found that these antigens were bound by gl-reverted VRC01, and one of two tested (B046 and B053) precursor antibodies in the VRC01 lineage (VRC01lin), justifying further investigation into their use as priming immunogens. Immunizations with these gl-targeting immunogens revealed that the V3-unmasked variant elicited superior T follicular helper (Tfh) cell frequencies relative to the immunogens carrying the glycan-masked V3. However, B cell responses were decreased in mice immunized with this V3-unmasked immunogen relative to the classical immunogen, keyhole limpet haemocyanin (KLH); this suggests that the two antigens differ in the quality of the Tfh cell-mediated B cell help they elicit. In sum, this work provides further insights into factors influencing the elicitation and assessment of Tfh and B cell responses to priming with immunogens that target VRC01-class precursor antibodies.

3.2 Introduction

Studies exploring broadly neutralizing antibodies (bnAb) responses to human immunodeficiency virus type-1 (HIV-1) have helped identify hurdles to eliciting with greater clarity, and strategies have been proposed to overcome such hurdles [112,163]. Eventually, it was proposed that immunogens capable of recognizing unmutated precursors of bnAbs should be designed and used as primes in vaccine studies[164]. This approach, dubbed gl-targeting, is currently being explored to elicit bnAbs of various specificities, including the CD4binding site (CD4bs)-targeting VRC01-class [165,166,110,111].

To this end, we investigated an approach to focus the antibody response against the CD4bs. Engineering such immunogens entails trimming off or blocking unwanted epitopes to minimize unwanted antibody responses [113]. However, this can potentially diminish T follicular helper (Tfh) cell support and subsequent B cell responses if T helper cell epitopes are removed or destroyed in the process. Here, we examined the effect of appending the PanDR helper epitope (PADRE) to gl-targeting HIV immunogens on Tfh cell responses. PADRE is a 13 amino acid T helper epitope that is known to bind at least 10 HLA-DR molecules in humans [167], and I-A^b molecules in mice. PADRE has been researched extensively in several bacterial and viral vaccine studies and was shown to improve antibody responses [129,168,133,169] possibly by facilitating Tfh cell-mediated B cell help. Here, we tested a panel of immunogens derived from the 45_01dG5 strain of HIV, whose gp120 envelope (Env) protein had been shown to bind the VRC01gl antibody with µM affinity [170]. PADRE was appended to a 45_01dG5 gp120-derived immunogen, which we suspected elicited insufficient Tfh cell help on its own (Figure 3.1). In the following sections I present the methods used to assess these immunogens. Protein engineering and transfections were performed by R.P. The flow cytometry, ELISPOT assays and ELISAs were performed by A.J.V. with guidance from R.P.

3.3 Methods

3.3.1 Construction, expression, and purification of HIV gp120-derived 45_01dG5 antigens

The HIV antigens used in this thesis were derived from HIV-1 strain 45_01dG5, the gp120 of which had been shown to bind gl-reverted VRC01 [78]. Several modifications were introduced into the 45_01dG5 gp120 backbone (Figure 3.1) to minimize antibody responses to unwanted epitopes, in anticipation of future investigations to probe the ability of these antigens to elicit VRC01-class antibodies. First, construct 45_core-V3cho was designed. It contains truncated V1/V2 loops, and lacks portions of the N and C termini, analogous to similar constructs made by others [171–173]; it also carries four additional glycans and two alanine substitutions in V3 [113]. This construct was synthesized by DNA 2.0. The V3 modifications were later removed by PCR mutagenesis to generate construct 45_core. Three copies of the PADRE motif [133,169] were appended by PCR to the 45_core-V3cho construct, thus yielding 3XPADRE-45_core-V3cho. An S375Y mutation was later introduced by QuikChange site-directed mutagenesis (XL II kit; Agilent Technologies) in the 45_core and 45_core-V3cho constructs, as well as a 45_core-V3cho construct with one PCR-appended PADRE motif (1XPADRE-45_core-V3cho) to generate corresponding variants.

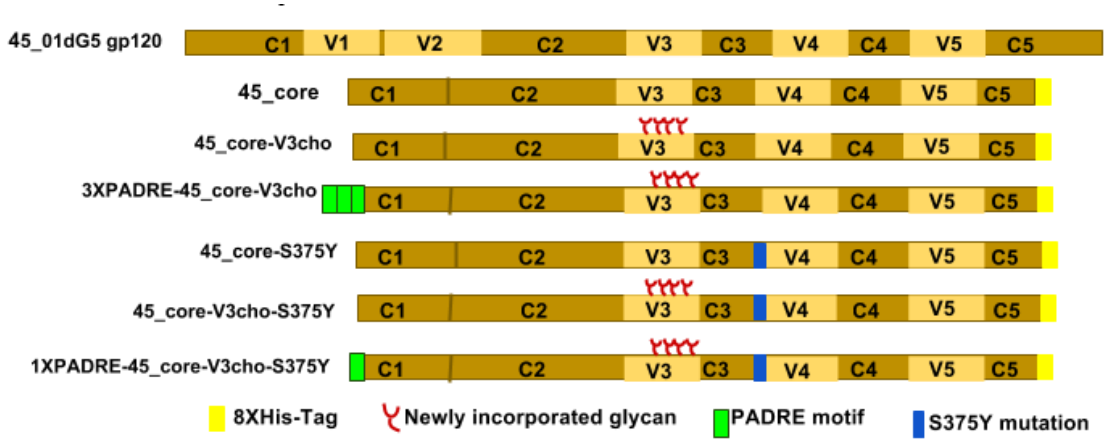

Figure 3.1. Schematic showing the modifications introduced relative to full-length gp120.

Core denotes truncation of the N and C termini at residues 83 and 492, respectively, and portions of the V1V2 loops. V3cho indicates the incorporation of four additional glycans onto the V3 loop [113] 3X and 1X PADRE signifies that three copies or one copy of the PADRE were appended N-terminally to the antigen. S375Y is a Ser-to-Tyr mutation introduced at position 375, which is located in the Phe43 cavity of the CD4bs [174]. The S375Y mutation was expected to stabilize the conformational flexibility of gp120 [175,176].

DNA encoding all constructs was (sub)cloned into the expression plasmid pCMVtag4A [177] or pcDNA-Zeo+ (Invitrogen/Fisher) and verified by Sanger sequencing. CHO-K1 cells were transfected with the resulting plasmids, and stable cell lines were established by limiting dilution in antibiotic-selective media as described previously [151]. Supernatants from limiting dilutions were screened by ELISA and the best-growing clones, having the highest protein expression levels, were expanded to flasks and subsequently to 0.5- or 1-liter cell-stacks (Corning).

The 45_01dG5-derived constructs were purified by means of their HIS-tag using nickel-nitrilotriacetic acid (Ni-NTA) columns (Qiagen) as described previously [151], then buffer-exchanged into phosphate buffer saline (PBS) and flash-frozen in liquid N_2 and stored at -80 ^{o}C until needed. For subsequent purification by size-exclusion chromatography (SEC), the Ni-NTA-purified proteins were thawed at room temperature (RT), buffer-exchanged into a high-salt phosphate buffer (50 mM NaH_2PO_4, 300 mM NaCl, pH 7.2), and concentrated using a centrifugal filter unit (10K Amicon Ultra), then loaded onto a Superdex 200 10/300 GL Increase column (GE), which had been equilibrated with the same buffer and calibrated using a high molecular weight gel filtration calibration kit (GE). The molecular masses of the SEC-purified 45_01dG5-derived protein fractions were determined as *per* the manufacturer's instructions (GE). Protein concentration was determined with a NanoVue spectrophotometer (GE). The molar absorption coefficients of the proteins were calculated based on their amino acid sequence using the ProtParam tool (ExPASY;

http://ca.expasy.org/tools/protparam.html). Samples were aliquoted into cryotubes, flash-frozen in liquid N_2, and stored at -80 ºC until needed.

3.3.2 Recombinant antibody expression

For the expression of cell-surface antibody, 293T cells were transfected with plasmids encoding heavy and light chain genes of VRC01gl, VRC01 mature (VRC01mat), and the Abs, B046, and B053 [178] as described in Chapter 2. Plasmids encoding codon-optimized VRC01mat variable heavy (VH) and variable light chains (VL) were obtained from the National Institutes of Health (NIH) acquired immuno deficiency syndrome (AIDS) Reagent Program, and those encoding for VRC01gl VH and VL were obtained from John Mascola (NIH/Vaccine Research Centre). Regions encoding VL domains were subcloned into pFUSEss-CLIg-hk (Invivogen). Regions encoding VH domains were subcloned into pFUSEss-CHIg-hG1 (Invivogen) for expression of soluble antibody (see below), or into pFUSEss-CHIg- hM*03 (Invivogen), in which the 3' end of the constant-region gene encoding soluble IgM was replaced with that encoding membrane-bound IgM [179], for cell-surface expression. Plasmids encoding the VH of B046-D5 (also termed VRC01c-HuGL2) and B053-p3-E8 (also termed VRC01c-HuGL11) [164] were synthesized by DNA 2.0 and subcloned into the modified pFUSEss-CHIg- hM*03 vectors. Plasmids encoding the VL of these two antibodies were obtained from William Schief (The Scripps Research Institute, La Jolla, CA). 293T cells expressing surface IgM antibody were trypsinized and pelleted at three days post-transfection, as described in Section 3.1, and re-suspended in Hank's Buffer Staining Solution (HBSS; Lonza) supplemented with 10% (v/v) fetal bovine serum (FBS; Thermo Fisher) for flow cytometry.

For the expression of soluble antibody, 293F cells were transfected with plasmids encoding heavy and light chain genes of VRC01mat and B4e8. Cloning of VH and VL genes into expression vectors was performed as described above (VRC01mat) or as in Chapter 2 (B4e8). For transfection, 293F cells that had

been maintained in 293 Freestyle media (Life Technologies) were pelleted by centrifugation (1000 rpm for 5 min at 15º C), re-suspended in 293 Freestyle media, counted, and then seeded into one or more 125-ml shaker flasks (Corning) at a density of $5x10^5$ cells/ml in 50-ml volumes. Following overnight incubation (at 37 ºC, 10% v/v CO_2) on an orbital shaker at 120-150 rpm, cells were transfected with 25 µg of DNA (12.5 µg plasmid of each light chain and heavy chain plasmid) formulated in 2.5 ml 293 Freestyle media containing 50 µl of polyethyleneimine "Max" (PEImax; Polysciences Inc.) or 293fectin (Invitrogen/Thermo Fisher). Cells were pelleted six days post-transfection by centrifugation (3000x*g* for 30 min at 10º C); the supernatant was collected, filtered (0.22-µm filters), and concentrated using 10 or 50 MWCO concentrators (Amicon). Antibody was purified using protein-A agarose spin columns (Piece/Thermo Fisher) as per the manufacturer's recommendations (Pierce). The concentration of purified antibody was measured using a NanoVue spectrophotometer (GE) and stored at 4 ºC until needed.

3.3.3 Immunizations

Approximately 6- to 8-week-old female C57BL/6 mice (n=5/group; Charles River) were used for immunizations. The immunogen formulations were prepared and administered as described in Chapter 2. All experiments were approved by the Animal Care Committee at Simon Fraser University (protocol 1098HS-13).

3.3.4 Flow Cytometry

Membrane-bound VRC01-class antibodies binding to antigen

293T cells expressing cell-surface IgM versions of VRC01gl, VRC01mat, or the VRC01-class precursor antibodies B046 and B053 were trypsinized and pelleted as described for the ELISPOT in Chapter 2, and then re-suspended in Hank's Balanced Salt Solution (HBSS; Lonza) supplemented with 10% (v/v) FBS (Thermo Fisher) (staining buffer). Samples were then incubated with different concentrations of antigen. Bound antigen was detected using an anti-HIS mouse

monoclonal antibody (Qiagen) followed by FITC-conjugated anti-mouse Fc-specific antibody (Jackson ImmunoResearch). APC-conjugated anti-human $F(ab')_2$ (Jackson ImmunoResearch) was used to detect cell surface antibody. All incubation steps were performed for 30 min on ice. Samples were washed and re-suspended in staining buffer between steps. Following staining, data acquisition and analysis were performed as described in Chapter 2.

Analysis of Tfh and B cells following immunization

Preparation of cell suspensions from inguinal lymph nodes (iLNs) and spleens of naïve and immunized mice and GC Tfh and B cell analyses were performed as described in Chapter 2. Staining for memory Tfh cells was performed using mostly the same panel of antibodies as Tfh. However, APC-conjugated PD-1 was replaced with CD62L (APC; MEL-14; Thermo Fisher) since memory Tfh cells down-regulate PD-1 expression and tend to up-regulate CD62L expression [114]. The antibody panel used to identify memory B cells was similar to that used for GC B cells, but the GC B cell-specific markers GL7 and CD95 were replaced with CD38 (PE-Cy7; 281-2; Thermo Fisher), which in the mouse is highly expressed on memory B cells but not on GC B cells or plasma cells [180,181], and anti-HIS (AF647; Qiagen) or anti-KLH (AF647; BioLegend) for antigen detection. To detect antigen-specific memory B cells, splenocytes were incubated with homologous immunogen for 30 min on ice and then with AF647-conjugated anti-HIS antibody (Qiagen), to detect HIV immunogen-specific cells, or with AF647-conjugated anti-KLH (BioLegend) antibody, to detect KLH-specific cells. Incubation with antigen preceded staining with all fluorophore-conjugated antibodies. All reagents were used at manufacturer-recommended concentrations or pre-titrated to determine optimal concentrations for usage. Following staining, data acquisition and analysis were performed as described in Chapter 2.

Table 2 Markers used to identify T and B cell subsets.

Cell type	markers
Tfh cells	CD19- CD4+ CD44hi PD-1+ CXCR5+[20,21]
GC B cells	CD4- CD19+ IgD- GL7+ Fas+[21]
Memory Tfh cells	CD19- CD4+ CD44hi CXCR5+ CD62L+/-[182,183]
Memory B cells	CD4- CD19+ IgD- CD38hi Ag+

Listed here are the markers used to define Tfh cells, GC B cells, memory Tfh cells, and memory B cells by flow cytometry.

3.3.5 Enzyme-Linked Immunosorbent Assays

Binding of anti-HIV antibodies to antigen

Purified 45_01dG5-derived proteins were assessed for binding to antibodies VRC01mat, b6, A32, 412D, and B4e8 in ELISA. VRC01mat and B4e8 were purified from transfected 293F cells as described above. A32 and 412D were obtained from James Robinson (Tulane University) and b6 from Dennis Burton (The Scripps Research Institute, La Jolla, CA). ELISA was performed as described previously [151], with a few modifications. Briefly, 96-well ELISA plates (Corning) were coated in duplicate with antibody in two-fold serial dilutions starting at 250 ng/well. After washing and blocking, antigen was added to plates at 50 ng/well. Bound antigen was detected with mouse monoclonal anti-HIS antibody (Qiagen) (50 ng/well) in conjunction with alkaline phosphatase-conjugated anti-mouse IgG Fc-specific antibody (Jackson ImmunoResearch), diluted 1:1000 in PBS supplemented with 1% bovine serum albumin (BSA) and 0.02% Tween (Bioshop) (PBS-BT), and nitrophenylphosphate substrate (Sigma).

Analysis of serum IgM and IgG

The magnitude of antigen-specific IgM and IgG responses was measured as described in Chapter 2. IgG subclasses 1, 2b, 2c, and 3 in the sera of mice immunized with HA1, KLH, and 45_core-S375Y were detected in a similar manner using subclass-specific alkaline phosphatase (AP)-conjugated secondary antibodies (Jackson ImmunoResearch). Competition ELISA, for assessing the inhibition of the anti-V3 antibody B4e8 binding to 45_core-S375Y by the serum antibodies from immunized mice, was performed by coating microwells with 45_core-S375Y (50 ng/well in PBS) overnight at 4º C. Wells were then washed and blocked with PBS supplemented with 3% BSA [151], followed by incubation with sera from 45_core-S375Y-immunized mice (1:100 in PBS-BT) for 1 h at RT. After washing, B4e8 was added and serially diluted in PBS-BT starting at 100 ng/well. Following a 1-h incubation and washing as before, bound B4e8 was detected using AP-conjugated anti-human IgG Fc-specific antibody (Jackson ImmunoResearch; diluted 1:1000 in PBS-BT) and nitrophenylphosphate substrate.

3.3.6 Enzyme-Linked Immuno Spot Assays

The enumeration of IL-21-secreting cells in iLNs and antibody-secreting cells (ASCs) in spleens of naïve and immunized mice by ELISPOT was performed as described in Chapter 2.

3.3.7 Statistical Analysis

Statistical significance of T and B cell frequencies, and ASCs in naïve and immunized mice were assessed as described in Chapter 2.

3.4 Results

3.4.1 Purification of 45_01dG5-derived antigens by size exclusion chromatography

All 45_01dG5-derived constructs were expressed in stably transfected CHO-K1 cells and initially purified by means of their HIS-tag on a nickel-nitrilotriacetic acid (Ni-NTA) column. The average molecular masses and relative purity of the expected proteins were determined by SDS-PAGE prior to SEC purification. Constructs without the S375Y mutation (Figure 3.1) were purified twice by SEC (Figures 2.2A and 2.2B). The second round of SEC was meant to ensure purity, but resulted in >50% reduction in yield. Furthermore, a single SEC-purification was equally effective at isolating proteins of desired molecular mass (compare Figures 2.2B and 2.2C) with relatively less sample loss. Hence, the S375Y mutants made subsequently were purified only once by SEC after Ni-NTA purification. The SEC profiles contained somewhat broad elution peaks (~2 ml) (Figure 3.2), indicating the presence of protein species of heterogenous molecular mass. Following purification, S375Y protein fractions of ~80 (monomer), ~100 (monomer), and ~160 (dimer/aggregated protein) kDa were recovered for further characterization.

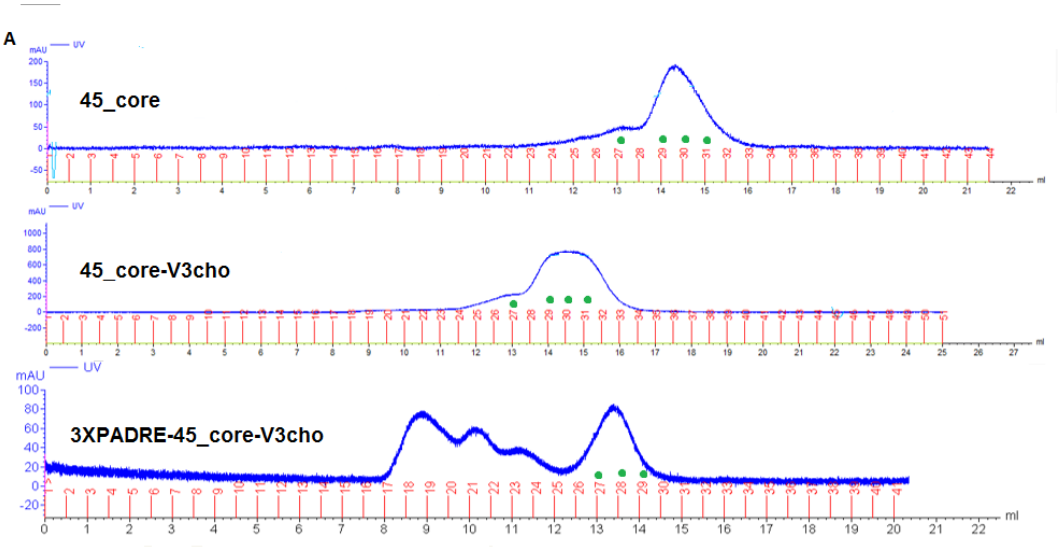

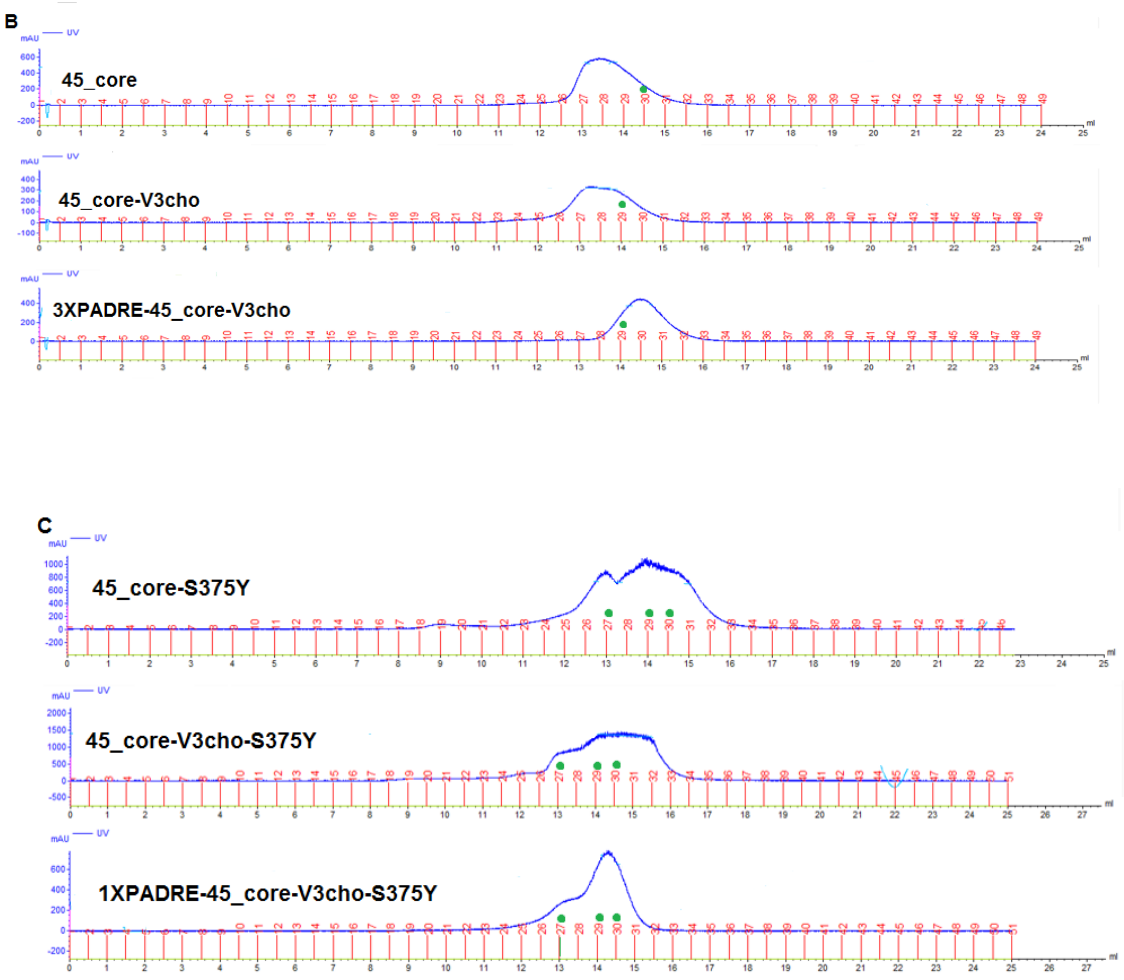

Figure 3.2 SEC purification of 45_01dG5-derived proteins.

The X- and Y-axes indicate elution volume and absorbance at 280 nm, respectively. All fractions (numbers in red) defined by a distinct peak and with an elution volume <15 ml were collected (green dots). A) Shown are representative elution profiles of 45_01dG5-derived proteins without the S375Y mutation after one round of SEC purification. B) Fractions recovered from each construct (from A) were pooled and purified a second time by SEC, and the recovered fractions used in subsequent analyses. C) Shown are the elution profiles of 45_01dG5-derived proteins with the S375Y mutation.

3.4.2 45_01dG5-derived proteins with S375Y substitution are bound with high relative affinity by affinity-matured VRC01 but not by V3 and co-receptor binding site-specific antibodies when glycans are introduced into V3

Affinity-matured VRC01mat was used to assay the first SEC-purified 45_01dG5-derived proteins, which lacked the S375Y mutation, in ELISA. We found that VRC01mat binding to the construct appended with three copies of the PADRE motif (3XPADRE-45_core-V3cho) was diminished relative to the variants without PADRE (*i.e.,* 45_core and 45_core-V3cho), to which the antibody bound with equal affinity (Figure 3.3A). In contrast, VRC01mat bound equally well to all SEC-collected fractions of the 45_01dG5-derived proteins bearing the S375Y substitution (Figure 3.3B). The expected average molecular mass, based on SDS-PAGE, was ~80 kDa for 45_core-S375Y and ~100 kDa for both 45_core-V3cho-S375Y and 1XPADRE-45_core-V3cho-S375Y. The average mass of the heaviest protein species collected for 45_core-S375Y (~160 kDa; fraction #27 in Figure 3.2C) corresponds to a protein dimer, perhaps resulting from aggregation. For the V3cho-S375Y variants, the collected species of ~80 kDa (fraction #30 in Figure 3.2C) might constitute aberrant expression of under-glycosylated forms of these proteins, which can occur when nutrients are depleted in batch cultures such as those used here [184]. To minimize the possible presentation of neo-epitopes, only fractions containing protein species of expected molecular mass (~80 kDa for 45_core-S375Y and ~100 kDa for both 45_core-V3cho-S375Y and 1XPADRE-45_core-V3cho-S375Y) were used for further analyses and immunizations.

To assess the relative accessibility of CD4bs and non-CD4bs epitopes on the S375Y constructs to antibody, we assayed them against a panel of non-CD4bs (A32, 412D, B4e8) and CD4bs (b6, VRC01mat) antibodies in ELISA (Figure 3.3C). The analysis revealed that the binding of 412D (co-receptor binding site; CoRbs) and B4e8 (V3 loop) to 45_core-S375Y was low and absent, respectively. Antibody A32, predictably, did not bind any of the S375Y mutants since it binds to a discontinuous epitope involving the C1 and C2 regions of gp120 [185–187] that

are largely removed in all three constructs. Together, these results indicate that the CD4bs presentation is not obstructed in any of the antigens, and that the glycan-masking of V3 has the intended effect of blocking binding to at least a few non-CD4bs antibodies with epitopes in proximity to the CD4bs. Thus, these S375Y immunogens are unlikely to elicit Abs against (i) the V3 loop, (ii) the coRbs, or (iii) the N or C terminal regions of gp120. This reduces the surface available for the antibody response, making it more likely that targeting of the CD4bs occurs.

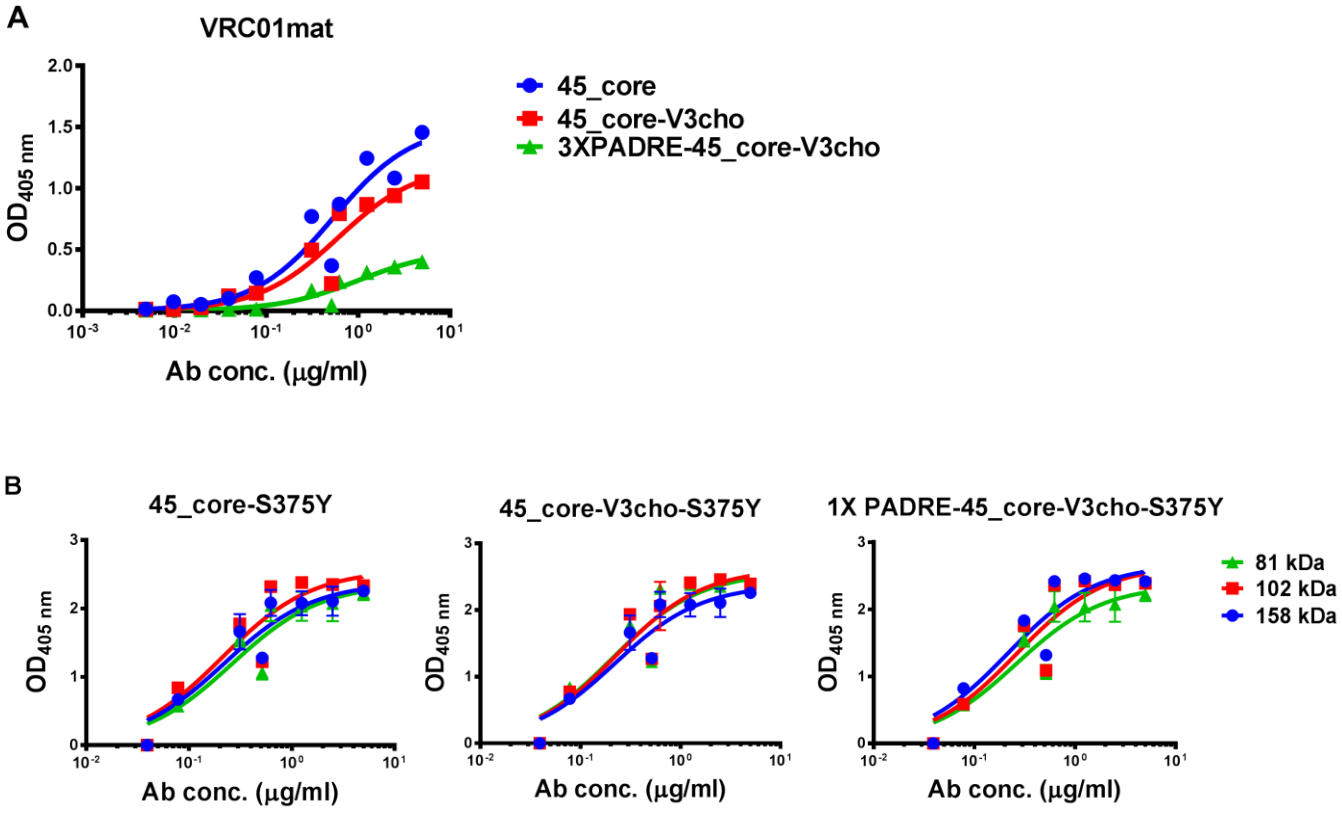

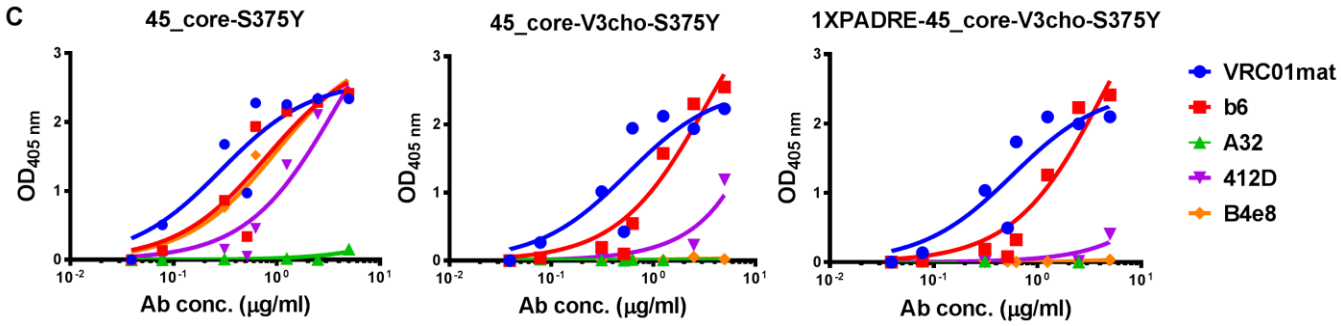

Figure 3.3 Binding assessment of anti-HIV-1 antibodies to 45_01dG5-derived proteins by ELISA.

Data are from a single experiment unless indicated otherwise. A) Affinity-matured VRC01 (VRC01mat) was assayed for binding to the 45_01dG5-derived proteins without the S375Y substitution. B) The binding of VRC01mat to collected fractions of SEC-purified S375Y mutants, as assayed by ELISA. Data are derived from two independent experiments. C) Antibodies A32, 412D, B4e8, and b6 along with VRC01mat were assayed for binding to chosen fractions of SEC-purified 45_core-S375Y (average calculated mass 81 kDa), 45_core-V3cho-S375Y (average calculated mass 100 kDa), and 1XPADRE-45_core-V3cho-S375Y (average calculated mass 102 kDa).

3.4.3 VRC01 germline-reverted and VRC01-class precursor antibodies bind 45_01dG5 antigens with S375Y substitution

To examine the ability of the 45_01dG5-derived proteins to engage cell surface-expressed antibody, as would need to occur *in vivo*, we assayed the antigens by flow cytometry for binding to 293T cells expressing VRC01-class antibodies on their surface. The constructs without S375Y were not bound by VRC01gl when assayed at 200 nM (Figure 3.4A), since there was no increase in fluorescence by VRC01gl. Because of indications that VRC01gl binds 45_01dG5 gp120 with micromolar affinity [78], binding assays at higher concentrations were desirable but could not be accomplished due to limited antigen amounts. However, we were able to assess the subsequently generated S375Y mutants for binding at 1 µM. Binding assays were done with VRC01gl (inferred VRC01 germline antibody) and VRC01-precursor antibodies B046 and B053 (isolated

from healthy individuals using a gl-targeting antigen probe) [164]. S375Y constructs were bound moderately well by mAbs VRC01gl and B046, but not by the B053 antibody (Figure 2.4B). The precursor antibodies B046 and B053 derive from the same VH gene (VH1-2*02), but differ in VL gene usage [164], which could be one reason for the different binding outcomes [82]. Although these results indicate that VRC01gl and B046 bound reasonably well to the S375Y mutants, determination of the exact affinities, for example with bio-layer interferometry (BLI) or surface plasmon resonance (BIAcore), was not pursued further here.

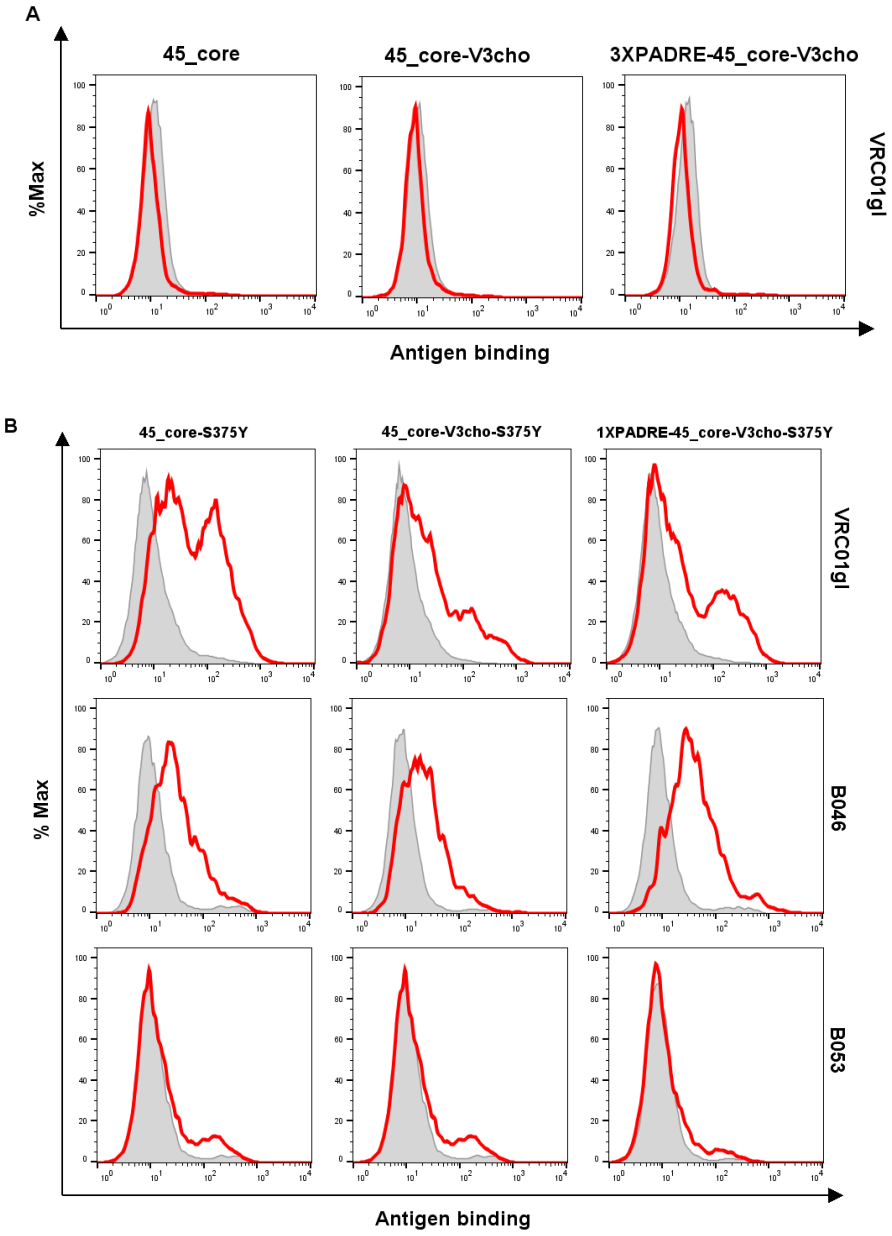
A
45_core
45_core-V3cho
3XPADRE-45_core-V3cho
%Max
VRC01gl
Antigen binding
B
45_core-S375Y
45_core-V3cho-S375Y
1XPADRE-45_core-V3cho-S375Y
% Max
VRC01gl
B046
B053
Antigen binding

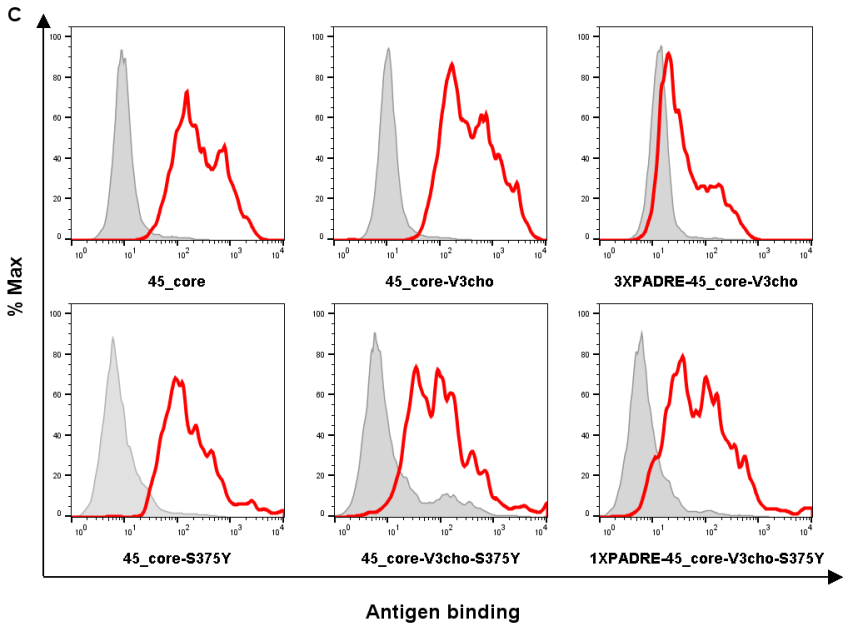

Figure 3.4 VRC01-class antibodies bind 45_01dG5-derived protein constructs by flow cytometry.

A) Protein constructs without the S375Y mutation were assayed at 200 nM for binding to VRC01gl. B) S375Y-containing mutants were assayed at 1 µM for binding to VRC01gl and precursor antibodies B046 and B053. C) Constructs with or without the S375Y mutation were assessed at 200 nM for binding to VRC01mat. A shift in fluorescence intensity ≥ half a log decade was considered positive. Plots are representative of at least three independent experiments.

3.4.4 45_01dG5-derived antigen 45_core-S375Y with unmasked V3 elicits greater frequencies of Tfh cells than variants with masked V3

The *in vitro* binding assessments revealed that S375Y proteins had the desired antigenicity for potential use as priming immunogens for the elicitation of VRC01-class antibodies. To explore their immunogenic potential, we investigated their capacity to elicit T and B cell responses *in vivo*. To this end, we immunized C57BL/6 mice (n=5/group) with candidate immunogens and compared the results with the outcomes from immunizations with KLH and HA1, which we established as sentinel immunogens (Chapter 2). First, we examined the Tfh cell response at seven days post-prime, which is an important component of the GC reaction and

is known to promote GC B cell proliferation, differentiation, and antibody production [6,10,14]. As with KLH and HA1, we used flow cytometry to assess Tfh cell frequencies in samples prepared from the iLNs of immunized mice. We found that 45_core-S375Y elicited Tfh cell levels similar to KLH, and higher than the two V3cho-S375Y variants. The frequency of CD4+ CD44hi cells was similar in all S375Y-immunized mice, indicating that similar proportions of CD4+ T cells had become activated in response to immunization with all S375Y variants, but this stimulation was apparently insufficient to induce Tfh cell responses in animals immunized with the two V3cho-S375Y variants compared to those immunized with 45_core-S375Y.

In addition to Tfh phenotype, we also sought to assess IL-21 secretion, but were unable to detect IL-21-secreting cells even in 45_core-S375Y-immunized mice, implying that our assay might not be suited for *ex vivo* analyses. As explained in Chapter 2, it is commonplace in other protocols for T cells to be incubated with antigen *in vitro* to help stimulate IL-21 secretion; this step was not included in our experimental setup and possibly explains our inability to detect IL-21.

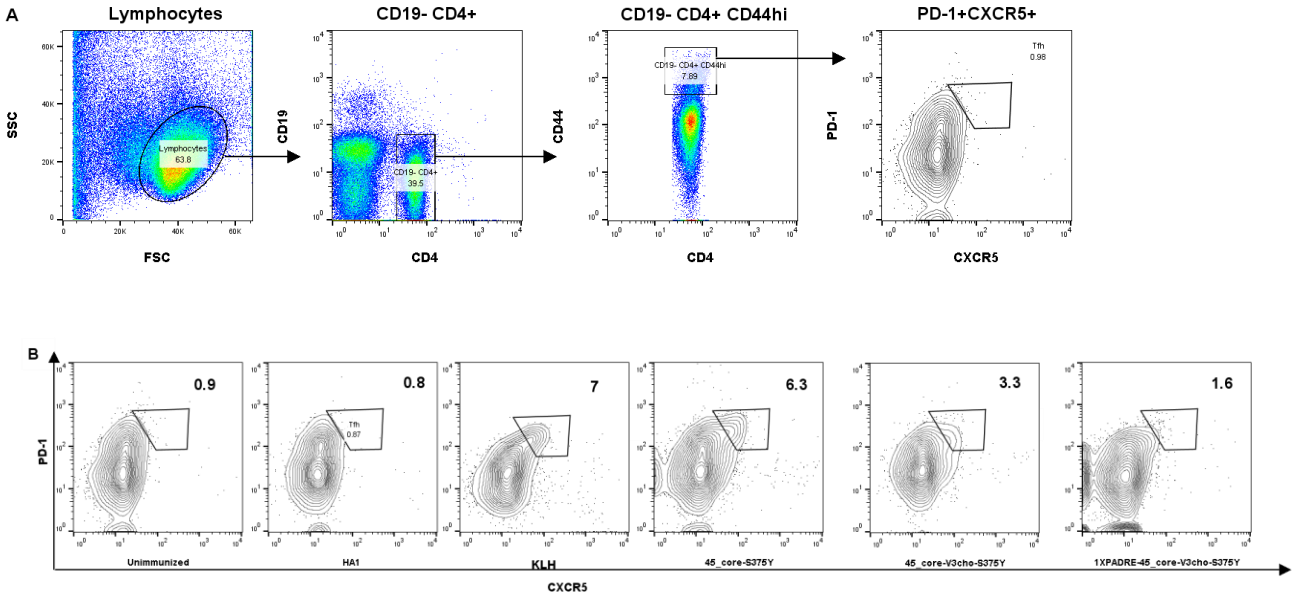

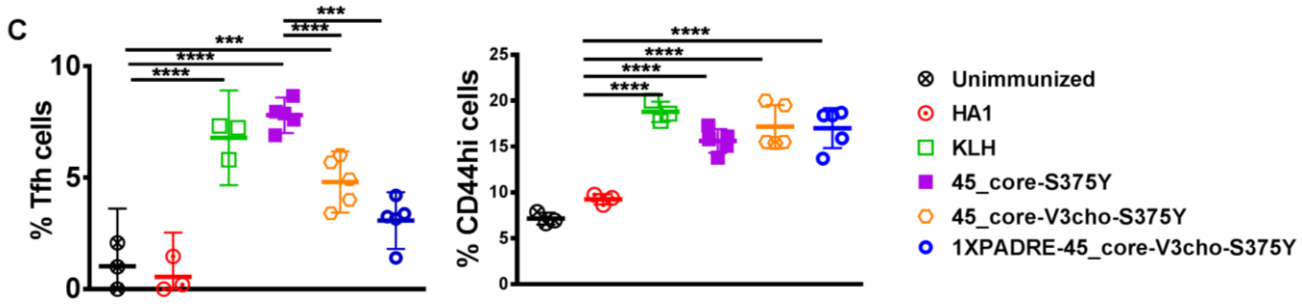

Figure 3.5 Immunization with 45_core-S375Y elicits Tfh cell frequencies comparable to KLH.

Tfh cells were analyzed in iLN samples recovered from unimmunized and immunized C57BL/6 mice at Day 7 post-prime. A) Tfh cells (PD-1+ CXCR5+) were gated on CD19- CD4+ CD44hi T lymphocytes (unimmunized mouse). B) Representative flow cytometry plots showing Tfh cell frequencies (numbers in bold) in unimmunized and immunized mice. C) Dot plots comparing the frequencies of Tfh and CD44hi cells. Data are representative of a single experiment. Statistical significance was assessed by one-way ANOVA followed by Tukey's multiple comparisons test (****p <0.0001, *** p < 0.001, **p < 0.01, *p <0.05). Only significant comparisons are shown.

3.4.5 V3 masking in 45_01dG5-derived antigens results in diminished GC B cell frequencies

In addition to Tfh responses, GC B cell frequencies in iLN were assessed at Day 7 following the priming injection. GC B cells were identified as the GL7+ Fas (CD95)+ subset of antigen-experienced (CD19+ IgD-) B lymphocytes (Figure 3.6A). Although a subset of cells within the GL7+ Fas+ compartment express IgD, they are believed to be a transitional cell type [141,156], and were thus excluded from our gating scheme. These analyses showed that, as with the Tfh cells, GC B cell frequencies were reduced in response to the V3cho- and 1xPADRE-V3cho-S375Y constructs relative to 45_core-S375Y. Despite eliciting similar Tfh cell frequencies, 45_core-S375Y elicited significantly lower GC B cell frequencies than KLH (Figures 3.6B and 3.6C). These data suggest that Tfh cell-mediated B cell help, which promotes GC B cell proliferation [14,188], may have been lower in 45_core-S375Y-immunized mice relative to those primed with KLH.

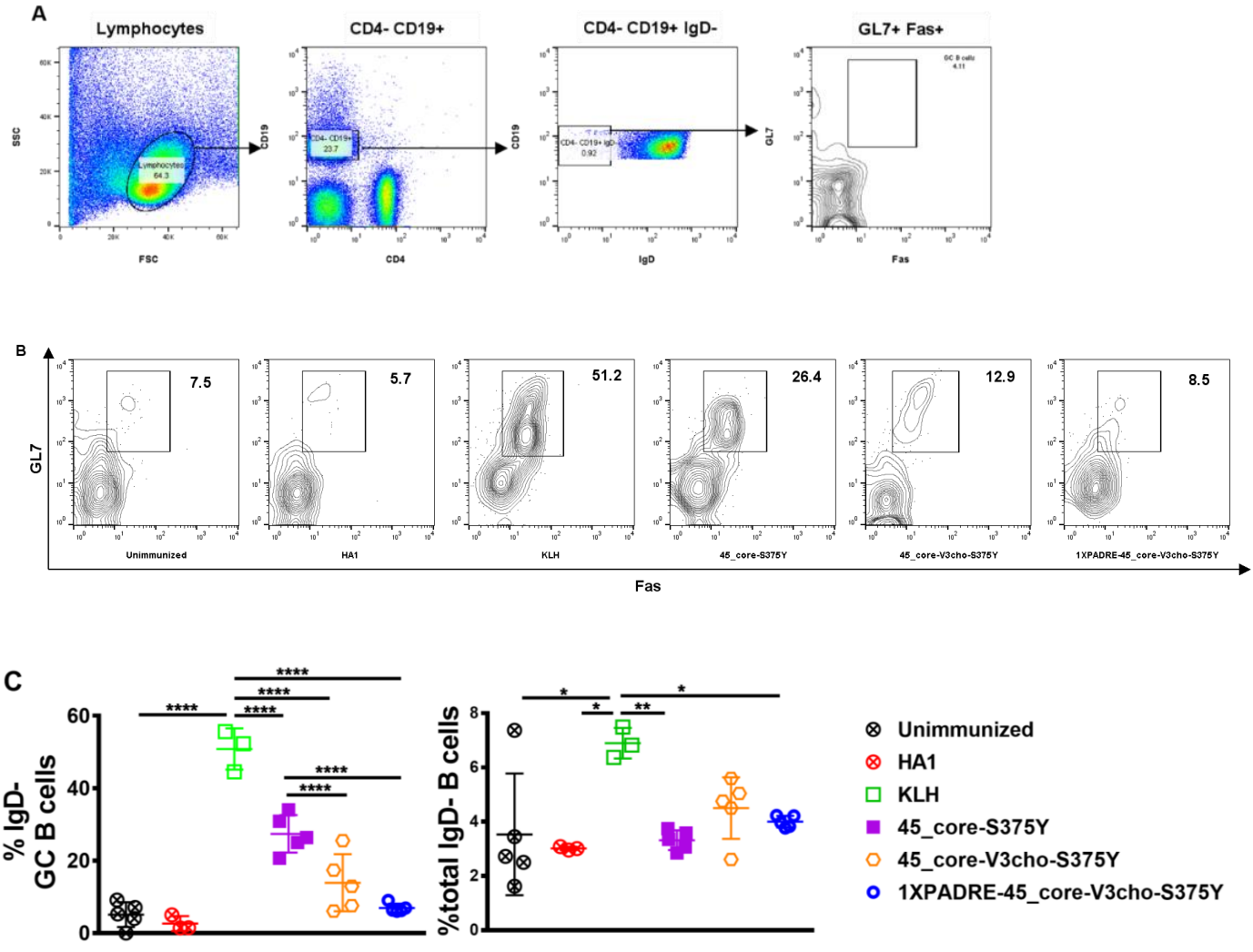

Figure 3.6. 45_core-S375Y elicits greater GC B cell frequencies than the V3cho variants.

Analysis was performed using iLN samples recovered from immunized (seven days previously) and unimmunized C57BL/6 mice. A) GC B cells (GL7+ Fas+) were gated on CD4- CD19+ IgD- B lymphocytes (unimmunized mouse). B) Representative flow cytometry plots showing GC B cell frequencies (numbers in bold) in immunized and unimmunized mice. C) Dot plots comparing the frequencies of GC B and IgD- cells in the different groups of mice. Data are representative of a single experiment. Statistical significance was assessed by one-way ANOVA followed by Tukey's multiple comparisons test (****p <0.0001, *** p < 0.001, **p < 0.01, *p <0.05). Only significant comparisons are shown.

3.4.6 Priming does not yield memory Tfh cells in the spleen at Day 28

To examine if the priming immunizations produced memory Tfh cells in our studies, we analyzed samples prepared from the spleens of mice immunized 28 days previously. Central memory (CM) Tfh cells were defined as CD62Lhi CXCR5+ and effector memory (EM) Tfh cells as CD62Llo/- CXCR5+ subsets of activated (CD44hi) CD4+ T lymphocytes [182,189]. We found both subsets of memory Tfh cells to be below detectable levels in the spleens of all animals (Figure 3.7). This was unexpected, given that previous studies have shown that Tfh cells isolated at the peak of the GC response, *i.e.,* at approximately one week post-prime, and transferred to naïve mice, acquire a CM phenotype within two weeks and can be identified in both the spleen and lymph nodes [114,182]. Although this adoptive transfer model is different from in-host study, it still informed on the migration and development on memory Tfh cells. However, there is also evidence to suggest that memory Tfh cells persist at greater frequencies in local draining lymph nodes relative to other lymphoid sites for several weeks following a priming immunization [183,190,191]. Further investigation with KLH revealed that CM Tfh cells were indeed measurable in the iLN, but at Day 29 post-prime (Figure B4).

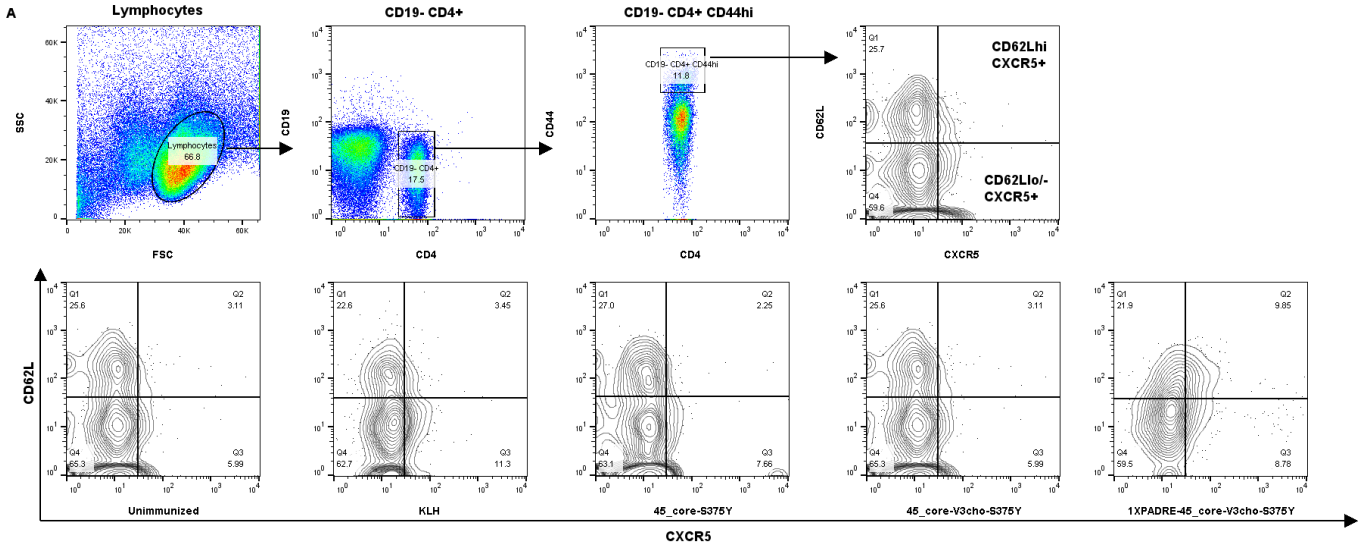

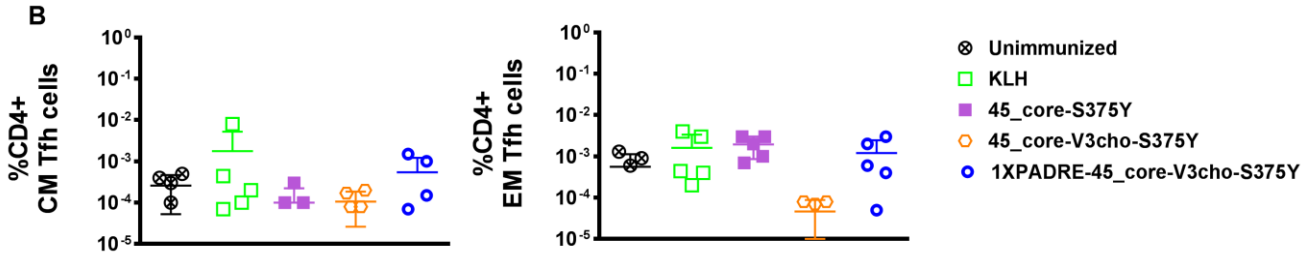

Figure 3.7. Memory Tfh cells are undetectable in the spleens of immunized mice at Day 28 post-prime.

Analysis was performed with spleens recovered from unimmunized and immunized C47BL/6 mice (Day 28 post-prime). A) Memory Tfh cells were gated on CD19- CD4+ CD44hi T lymphocytes (unimmunized mouse). Also shown are representative flow cytometry plots of CM and EM Tfh cells in immunized and unimmunized mice. B) Dot plots comparing the frequencies of memory Tfh cells as a percentage of CD4+ T cells. Data are representative of a single experiment. Statistical significance was assessed by one-way ANOVA followed by Tukey's multiple comparisons test. Comparisons were not significantly different.

3.4.7 Low levels of antigen-specific memory B cells and ASCs in spleen and bone marrow following priming with 45_01dG5-derived antigens

We also examined the frequencies of antigen-specific memory B cells and ASCs in the spleen and bone marrow, respectively. Memory B cells were defined as IgD-CD38hi antigen+ B cells (Figure 3.8A) [192–194], whereas antigen-specific ASCs were enumerated by ELISPOT using the protocol developed in Chapter 2. Strikingly and in contrast to immunization with KLH, we were unable to detect any antigen-specific memory B cells or ASCs in mice immunized with 45_core-S375Y (Figures 3.8B and C), further supporting the hypothesis that Tfh-mediated B cell help, which promotes GC B cell differentiation into memory B cells and ASCs [14], was qualitatively lower in mice immunized with this antigen. However, this assay was not validated for the detection of memory B cells with the relatively weak immunogen, HA1; thus, the assay itself may have lacked the sensitivity to detect memory B cells from 45-core-immunized mice.

Intraperitoneal immunization has been shown previously to elicit memory B cells in the spleen, but studies exploring other routes of antigen administration have suggested that memory B cells preferentially localize to draining lymph nodes and are detectable in the spleen only upon recall [193,195]. Contrary to those findings, Blink and colleagues reported that a recirculating pool of B cells with a memory phenotype can be identified as early as 14 days post-prime [192]. Taken together, these findings suggest that only KLH yielded splenic memory B cells by 28 days post-prime; whether 45_core-S375Y-immunized mice produced memory B cells that might have remained in the iLN requires further investigation.

The absence of antigen-specific ASCs in the bone marrow of 45_core-S375Y-immunized mice was particularly striking considering that a serum IgG response was observed at the same time point (Figure 3.9), and given that the presence of class-switched antibody in the serum following immunization is often considered indicative of ASC generation [143,196,197]. Our findings indicate that perhaps the kinetics of ASC generation and migration were different in 45_core-S375Y-immunized mice relative to KLH- and HA1-immunized mice. Examination of other tissues, such as the draining iLN (site of origin) or blood (route of migration) [192,198,199] in addition to the bone marrow, at Day 28 post-prime, might enable resolution of the ASC response to 45_core-S375Y.

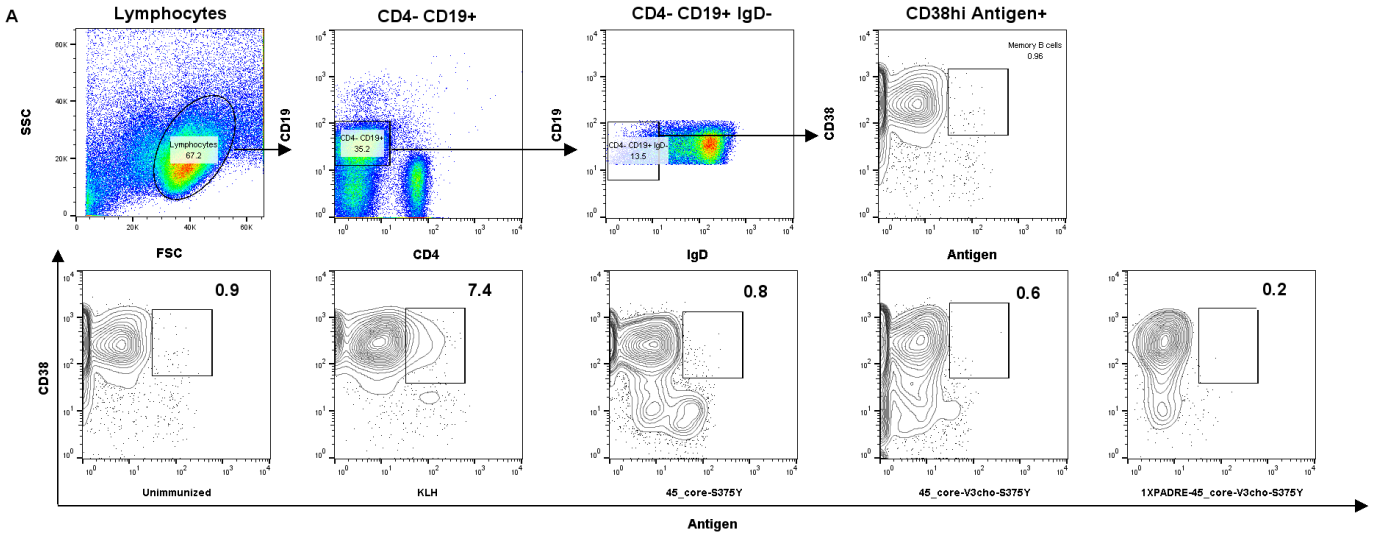

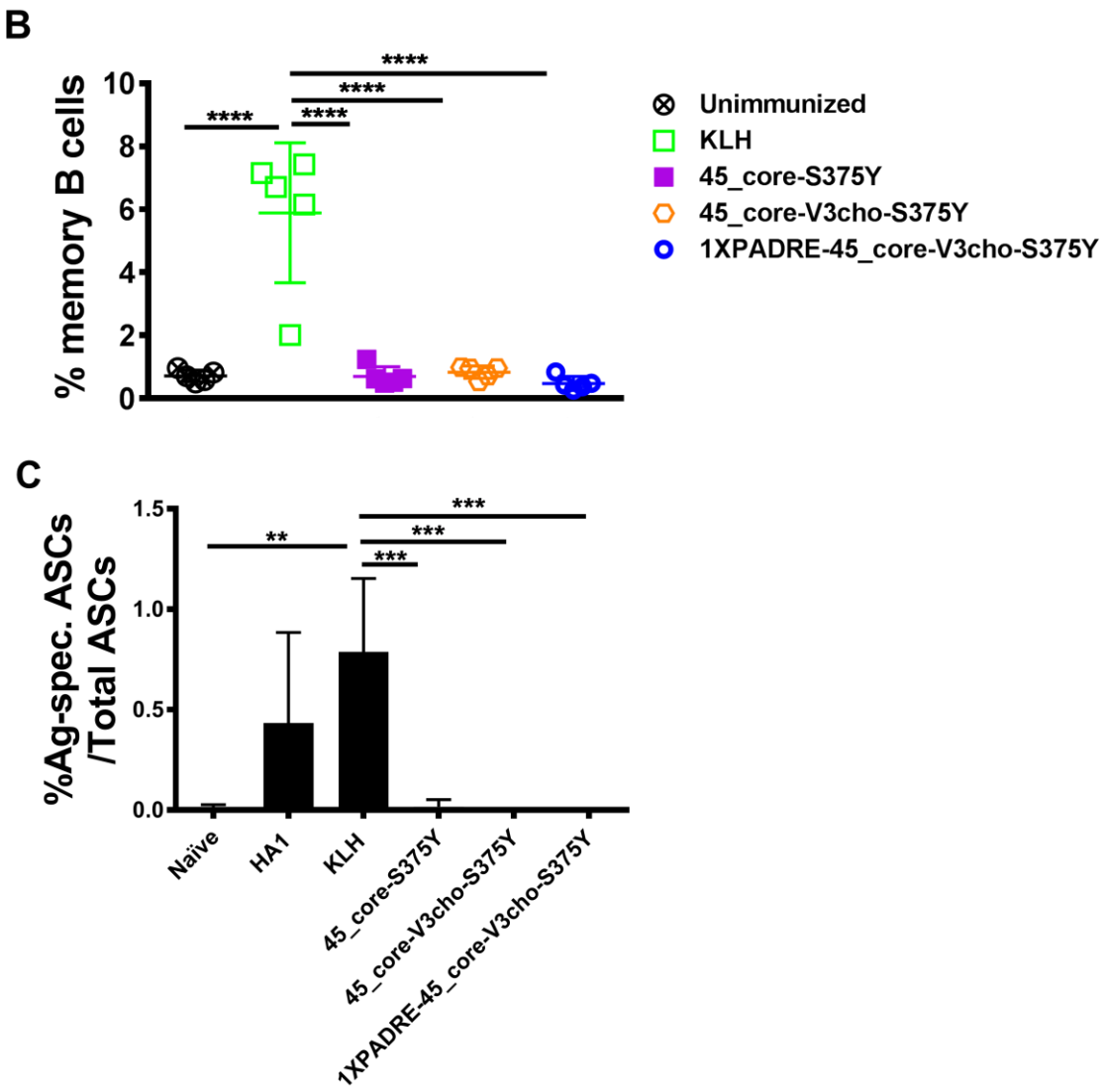

Figure 3.8. Memory B cells and ASCs are undetectable at Day 28 after priming with S375Y mutants.

Analyses were performed with splenocytes. A) Shown is the gating strategy used to identify antigen-specific memory B cells (unimmunized mice) and representative flow plots showing memory B cell frequencies (CD19+ CD4- IgD- CD38hi Antigen+) in unimmunized and immunized mice. B) Dot plots comparing memory B cell frequencies in immunized (n=5/group) and unimmunized (n=3) mice. C) Comparison of the percentage of antigen-specific ASCs in naïve and immunized mice. Data are from a single experiment. Statistical differences determined by one-way ANOVA followed by Tukey's

multiple comparisons test (****p <0.0001, *** p < 0.001, **p < 0.01, *p <0.05). Only significant comparisons are shown.

3.4.8 Antibody responses to the 45_core-S375Y antigen with an unmasked V3 are lower in overall magnitude and IgG1-skewed relative to KLH responses, but not V3 dominant

To examine the antibody responses to the immunogens, we assayed serum samples recovered from immunized animals at 7 and 28 days post-prime, which allowed us to measure the antibody responses during the peak and after the decline of the GC response, respectively. These time points also signify the beginning of antibody production and the accumulation of affinity-matured antibody in the serum [10,200]. The magnitude of IgM and IgG titers in naïve and immunized mice was determined by assaying serum samples in ELISA (Figure 2.9A). IgG was observed at both time points in 45_core-S375Y-immunized mice, and the magnitude of the response increased by Day 28. As expected, the (modest) IgM response observed at Day 7 had diminished by Day 28. The two V3cho-S375Y variants elicited very low antibody responses.

Despite eliciting similar frequencies of Tfh cells, the magnitude of the antibody responses to KLH were greater than those of 45_core-S375Y. The difference in antibody response levels and B cell frequencies (Figures 3.6, 3.8, and 3.9) led us to hypothesize that there was a difference in the quality of Tfh cell help between the animal groups. Tfh cells are a heterogenous population and can have cytokine profiles similar to other T helper subsets such as Th1, Th2, or Th17, which promote class-switching to different IgG subclasses [5,201–203]. As a proxy for potential differences in Tfh help, we assessed the levels of IgG subclasses in the sera of immunized mice. All the antigens were adjuvanted in QuilA, which is known to promote class-switching to IgG1 and IgG2 [204]. Little is known about the influence of QuilA on IgG3 responses, but studies with QS-21, the main adjuvanting fraction of QuilA [205,206], indicate that class-switching to IgG3 also occurs, albeit at lower levels than IgG1 or IgG2 [207–209]. We found that 45_core-S375Y and HA1 elicited IgG1 (Th2/Th17) and IgG2 (Th1/Th17)

antibodies, but no IgG3 (Th17), with 45_core-S375Y eliciting greater IgG1 responses but lower IgG2b responses than HA1. KLH also yielded antibodies from these two subclasses, albeit more robustly for IgG2b, as well as from IgG3. These results further hint at underlying differences in the qualitative nature of the Tfh cell responses induced by each of these immunogens [202,203].

Because antibody responses in animals immunized with the two V3cho-S375Y variants were meager, we asked whether much of the response to 45_core-S375Y, in which the V3 region is not masked by glycans, was directed to epitopes on or near V3. V3-dominant antibody responses have been observed by others when immunizing with recombinant gp120 or other derivatives of the HIV Env spike [21,210–213]. To probe this possibility, we assayed the binding of the anti-V3 antibody B4e8 to variant 45_core-S375Y in the presence or absence of sera from 45_core-S375Y-immunized mice. We found that sera from two of the five animals inhibited B4e8 binding by ~50% relative to the no serum control, indicating that while immunizing with 45_core-S375Y yielded a proportion of anti-V3 responses in several animals, antibody responses to epitopes other than V3 were also elicited in the animals. We conclude from these results that the low antibody responses observed upon immunization with the two V3cho-S375Y variants likely resulted from diminished Tfh help rather than an obscuring of accessible B cell epitopes in V3 due to glycan-masking.

A

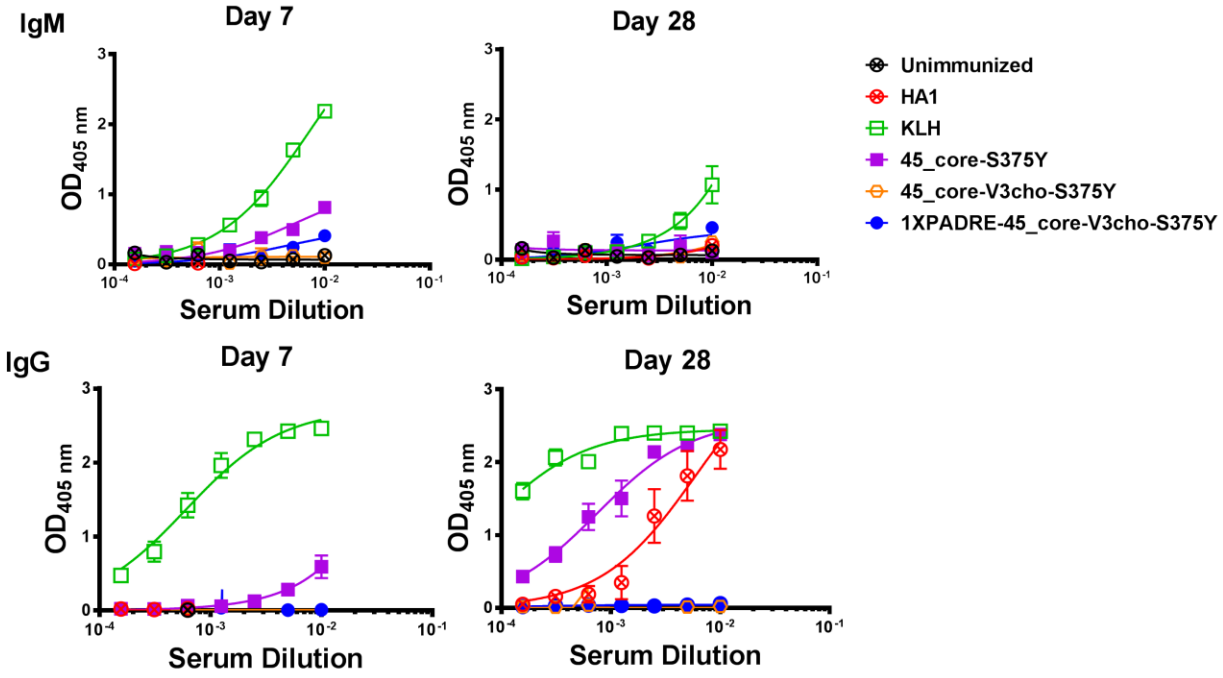
IgM
Day 7
Day 28
IgG
Day 7
Day 28
OD405 nm
Serum Dilution
Unimmunized
HA1
KLH
45_core-S375Y
45_core-V3cho-S375Y
1XPADRE-45_core-V3cho-S375Y

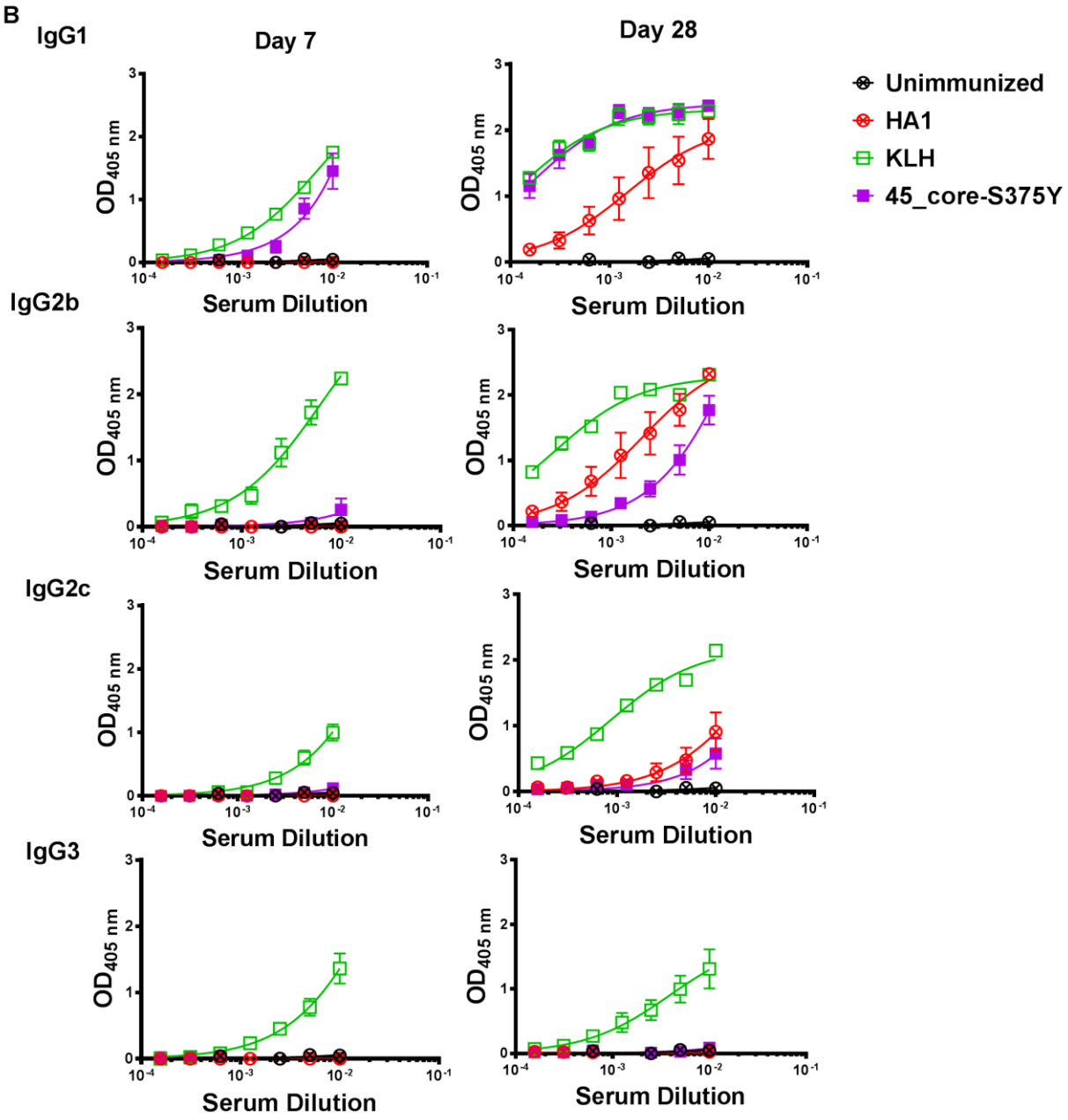
B
IgG1
Day 7
Day 28
Unimmunized
HA1
KLH
45_core-S375Y
IgG2b
IgG2c
IgG3
OD405 nm
Serum Dilution

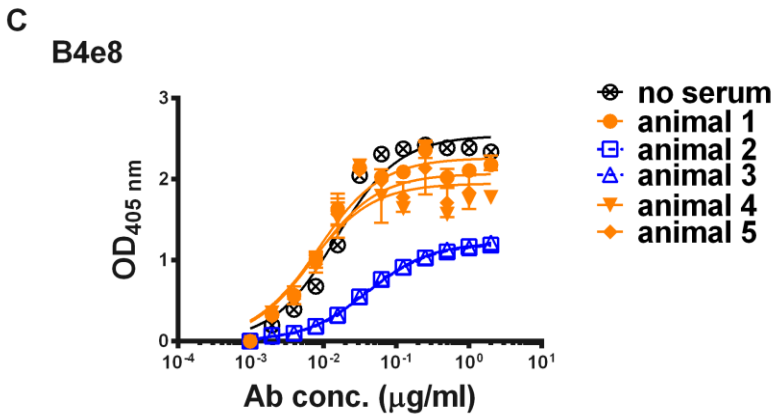

Figure 3.9. The 45_core-S375Y antigen with the unmasked V3 elicits an antibody response to epitopes other than the V3 and is lower in magnitude and different in IgG subclass than KLH.

A) Serum samples were recovered from C57BL/6 mice that were unimmunized (n=5) or immunized with KLH (n=5), HA1 (n=3), or S375Y mutants (n=5/group) at Days 7 and 28 post-prime, and were assayed with homologous antigen in ELISA. B) IgG subclasses were assessed in unimmunized mice, and in mice immunized with HA1 (n=3), KLH (n=5), and 45_core-S375Y (n=5) using sera recovered at Days 7 and 28 post-prime. Each point on a curve is representative of the mean optical density measured at the corresponding serum dilution. C) B4e8 binding to 45_core-S375Y was assessed by assaying sera (at 1:100 dilution) from 45_core-S375Y-immunized mice (n=5) with homologous antigen followed by incubation with B4e8. Each symbol represents data from a different animal. All data are derived from two independent experiments.

3.5 Discussion

This chapter assessed the antigenicity and immunogenicity of VRC01gl-targeting antigens tailored to focus the antibody response to the CD4bs. The core structure that is common to all the antigens we tested was meant to eliminate immunodominant epitopes of the V1V2 loops and portions of the N and C termini (Figure 3.1). Additionally, a subset of the antigens was modified to have additional glycans on the V3 to obscure unwanted B cell epitopes. To compensate for the loss of T helper epitopes from V3 glycan-masking, we appended a PADRE motif to a subset of V3 glycan-covered constructs. The resulting data showed that introducing a S375Y mutation improved binding by mature and gl forms of VRC01 antibodies. The S375Y mutants were also bound by one of two tested VRC01 precursor antibodies. Priming immunizations with

these gl-targeting immunogens revealed that the V3 glycan-masked variants (45_core-V3cho-S375Y and 1XPADRE-45_core-V3cho-S375Y) elicited reduced Tfh cell and B cell responses relative to the V3 unmasked variant (45_core-S375Y), which elicited Tfh cell frequencies comparable to the sentinel immunogen KLH.

Table 3 Responses elicited by immunogens.

Response measured	Immunogen
Tfh cell frequency	KLH, 45_core-S375Y
GC B cell frequency	KLH, 45_core-S375Y
Memory Tfh cell frequency	None
Memory B cell frequency	KLH
ASCs in bone marrow	KLH, HA1
Serum IgG	KLH, HA1, 45_core-S375Y

Following priming with the various immunogens, the frequencies of Tfh cells, GC B cells, memory B cells, and memory Tfh cells, as well as the magnitude of the serum IgG response were measured. Tfh and GC B cell frequencies were observed only in 45_core-S375Y and KLH-immunized mice, and only KLH elicited memory B cells. HA1 did not elicit Tfh and GC B cells at the measured time point, but produced ASC and serum antibody responses.

The HIV-1 antigens used in this thesis were derivatives of the strain 45_01dG5 (Figure 3.1) and were characterized *in vitro* for binding to VRC01-class antibodies. The findings from these binding analyses are in line with previous studies suggesting that the substitution of the Ser at position 375 with a larger hydrophobic residue induces a gp120 conformation close to the CD4-bound state, which is believed to be more stable due to the formation of a bridging sheet between the inner and outer domains [176,214]. This conformational stability could have contributed to the binding by gl-reverted and VRC01-class precursor antibodies observed with all the S375Y mutants. However, only one (B046) of the two tested (B046 and B053) VRC01-precursor antibodies was able to bind these constructs. B046 and B053 were isolated from healthy individuals using the the gl-targeting antigen eOD-GT8, and are believed to be true VRC01-class precursor antibodies [178]. B046 and B053 derive from the same VH gene

(VH1-2*02), but use different κ-chain V genes, VK4-1*01 and VK3-15*01, respectively; this disparity could have contributed to the differences in binding to S375Y mutants. Antigen binding by precursor antibodies was studied using a flow cytometric assay that was somewhat representative of antigen interactions with naïve B cells receptors (BcR) *in vivo,* and required smaller amounts of reagent compared to more traditional methods*,* but it offered a limited amount of information. Perhaps more conventional methods for determining affinity, such as surface plasmon resonance (SPR) and or isothermal calorimetry (ITC), would allow measurement of binding parameters.

Having established binding by gl antibodies, we immunized groups of C57BL/6 mice with the S375Y mutants to further assess their suitability as priming immunogens. As mentioned above, it was evident from the immunizations that introducing additional glycans on the V3 loop dampened the Tfh cell response. The V3 loop was previously described as a hot spot for T helper epitopes [215], which might have been lost when the V3cho modification was introduced, possibly affecting the Tfh cell frequencies. It was also evident from this analysis that appending a single copy of PADRE did not rescue the Tfh response (Figure 3.4). Evidence from the literature suggests that appending a single or multiple copies of PADRE improves the antibody response, possibly by increasing Tfh-mediated B cell help [118,168,133]. However, in the case of the V3-masked immunogens, appending a single PADRE motif might have been insufficient to restore the Tfh cell frequencies. Reduced Tfh cell help could have, in turn, diminished B cell responses such as GC B cell proliferation and antibody production.

Interestingly, the V3-unmasked S375Y (45_core-S375Y) construct elicited a Tfh cell frequency comparable to that elicited by KLH (Figure 3.5), but the GC B cell frequency (Figure 3.6) was relatively lower than that in KLH-immunized mice. Not only was GC B cell proliferation lower, but other B cell functions such as antibody production, and ASC and memory B cell development also appear to have been reduced in 45_core-375Y-immunized mice relative to KLH-immunized mice (Figure 3.8). This suggests that, despite eliciting similar Tfh cell

frequencies, T cell help could stand to be improved. Glimpses at underlying differences in Tfh cell help to B cells were also provided by the analysis of sera from KLH- and 45_core-375Y-immunized mice by ELISA (Figure 3.9C). A majority of the antibody response was directed away from the V3 region. The sera from two of five 45_core-S375Y-immunized mice inhibited binding by the V3 monoclonal antibody B4e8 by ~50% indicating that the binding of the serum antibodies might be weak. This can be assessed further by assaying the sera and B4e8 with V3 peptide.

Despite evidently robust GC responses, KLH surprisingly did not elicit memory Tfh (Figure 3.7) cells in the spleen. Literature evidence suggested that the persistence of memory Tfh cells in the local draining lymph nodes is a strong possibility [114] and should be probed further. However, the presence of memory Tfh cells at the site of origin several weeks post-prime was associated with antigen-depots, suggesting that this localization may not take place without prolonged antigen presentation, as occurs with antigen-depot formation [216]. Conflicting evidence from adoptive transfer experiments suggests that true memory Tfh cells start to appear after the Tfh cell population has contracted, which is well after available antigen has been depleted [182]. Our investigations revealed that CM Tfh cells persisted in iLN following priming and could be measured at Day 29 post-prime (Figure B4) but not Day 28. EM Tfh cells, however, were not measurable at Day 29 (Figure B4), possibly suggesting that they might have migrated from the tissue of origin.

Overall, the work presented in this chapter highlights the influence of the V3 loop on the immunogenicity of the gl-targeting antigens tested here, as well as the necessity to further explore strategies to improve the Tfh cell response to antigens with glycan-covered V3 loops.

3.6 Acknowledgements

We thank John Mascola and Bill Schief for providing the plasmids encoding the VRC01gl VH and VL, and the B046 and B053 VL, respectively. We also thank Joyce Hu and Jonathan Choy for their guidance on performing the

flow cytometry experiments; Kolappan Pillai, Neil Dobson, and Edgar Young for their assistance with the protein purifications, and Ruth Wijaya, Naiomi Lu, Saru Sandhu, and Tim Heslip for assistance with performing the ELISPOT and flow cytometry experiemnts. We further thank Simon Fraser University's Animal Care Facility for assistance with the immunizations, and Ian Bercovitz for his help in performing the statistical analyses.

Chapter 4. Conclusions and future directions

The activation of germline (gl) precursors of broadly neutralizing antibodies (bnAbs) has been identified as one of the hurdles to eliciting bnAbs to HIV-1 [66,217]. The design of immunogens that can activate gl antibodies, dubbed gl-targeting, is currently being explored as part of vaccine strategies aiming to elicit bnAbs, such as those of the CD4-binding site (CD4bs)-specific VRC01 class. The gl-targeting antigens explored in this study derive from the gp120 Env spike subunit of the 45_01dG5 strain of HIV-1, which was reported to bind VRC01gl [78]. Here, we investigated an approach to improve Tfh-mediated B cell help in the context of gl-targeting antigens.

A subset of the immunogens tested here contained a glycan-masked V3 loop to reduce its inherent immunogenicity [218,219]. However, the V3 harbours several T helper epitopes [215] which may have been disrupted by the introduction of additional glycans. We hypothesized that this reduced Tfh cell and B cell responses to the immunogen. To remedy this, we appended a PanDR helper epitope (PADRE) to an antigen with a glycosylated V3. Variants without the PADRE, and those with neither the PADRE nor the glycan-covered V3 were included as comparators (Figure 3.1). We assessed their capacity to engage not only B cells bearing the VRC01gl antibody, but also B cells bearing the VRC01-class precursor antibodies B046 and B053, which were isolated using the gl-targeting immunogen eOD-GT8 [164]. The constructs used for immunizations were engineered to contain a Ser-to-Tyr mutation at position 375 in an attempt to facilitate binding by VRC01-class gl antibodies. We found that these S375Y antigens were bound by VRC01gl, and showed a preference for binding by B046 over B053 (Figure 3.4). These findings are supported by experimental evidence from another gl-targeting antigen, 426c core (reviewed in Section 1.4), suggesting that such disparities in binding can be expected when assaying antigens with VRC01-class precursor antibodies [111].

The immunizations of C57BL/6 mice with the S375Y mutants revealed that the V3-unmasked construct, 45_core-S375Y, elicited Tfh cell frequencies similar to the sentinel T cell immunogen, KLH; in contrast, the Tfh cell responses to the V3 glycan-masked variants, 45_core-V3cho-S375Y and 1XPADRE-45_core-V3cho-S375Y, were substantially reduced (Figure 3.5), possibly leading to the diminished B cell responses observed for these V3 glycan-masked immunogens. The antibody response to 45_core-S375Y was not limited to the V3 loop (Figure 3.9), thus suggesting that B cells were able to access epitopes other than the V3 loop, and that the overall diminished responses to these immunogens probably resulted from the disruption of T helper cell epitopes on the V3. We also found that, despite eliciting similar Tfh cell frequencies, KLH and 45_core-S375Y did not elicit comparable B cell responses. The overall magnitude of the B cell response was relatively lower in 45_core-S375Y-immunized mice (Figures 3.6, 3.8, and 3.9), suggesting that the quality of the Tfh cell response might have differed between the two proteins. A measurement of IgG subclasses in the sera of KLH- *vs*. 45_core-S375Y-immunized mice revealed that KLH elicits Tfh cells with cytokine profiles similar to Th1, Th2, and Th17, whereas 45_core-S375Y appears to favor Th1 and Th2 over Th17 (Figure 3.9). However, the influence of these Tfh cell subsets on the overall magnitude of the B cell response requires further investigation.

In sum, the data presented in this thesis indicates that 45_01dG5-derived gl-targeting immunogens require greater Tfh cell help, especially if the V3 loop is masked. Appending a single copy of the PADRE motif did not restore the Tfh response affected by glycan-masking of the V3, indicating that a greater number or valency of PADRE motifs, or perhaps a different promiscuous T helper cell epitope, might need to be explored. Early binding experiments had revealed that antigens (without the S375Y mutation) when appended with multiple copies of PADRE did not bind CD4bs-directed antibodies as well as the variants without PADRE. However, given the evidence from the literature supporting the abilities of PADRE to enhance Tfh-mediated B cell help (reviewed in Section 1.5), it might

be worthwhile to investigate the immunogenicity of the V3 glycan-masked S375Y construct appended with more copies of the PADRE motif. The adjuvant used in this study, QuilA, was selected based on previous data showing that it supports CD4bs-directed responses [151]. Perhaps substituting QuilA with an adjuvant that is known to strongly promote Tfh cell induction [128], e.g. MF59, might also improve the immunogenicity of the 45_01dG5 constructs. Additionally, booster injections with second-step designer antigens might provide further insight into the memory response generated during priming.

Table 4 Summary of conclusions.

Response measured	**Conclusion**
Tfh cell frequency	Dampened by V3 glycan-masking.
GC B cell frequency	Relatively lower in 45_core-S375Y-immunized mice relative to the KLH group.
Memory B cell frequency	Undetectable in 45_core-S375Y-immunized mice at Day 28. Day 29 post-prime might be more suitable for measurement.
Memory Tfh cells	Assessing iLN at Day 29 post-prime might enable measurement of CM Tfh cells.
IgG subclass	Varied preference for IgG subclass in KLH and 45_core-S375Y-immunized mice, possibly indicating difference in the Tfh sub-populations elicited in each case.
Specificity of the Ab response	Elicited weak V3-directed antibodies in a minority of animals.

Although the main purpose of this undertaking was to assess the influence of the PADRE motif on early immune responses in the context of gl-targeting immunogens, we significant caveat is the priming with VRC01-class targeting immunogens in a wild-type mouse model (C57BL/6) with an antibody repertoire that is incapable of generating VRC01-like antibodies [220]. Although these mice

did enable assessment of the immunogenicity of the immunogens, the use of human antibody transgenic mice might better inform the ability of these immunogens to prime VRC01 antibodies *in vivo*. However, while the use of such transgenic mice might seem a viable alternative, recent studies with mice expressing 3BNC60gl found that these antibodies were autoreactive [82].

In conclusion, this work highlights the features of the early immune response, such as Tfh cell-mediated B cell help, that might be critical to the downstream development of VRC01-class bnAbs, and provides impetus for further investigation into the improvement of the Tfh cell response and subsequent B cell responses.

References

1. Burton, D. R. Antibodies, viruses and vaccines. *Nat. Rev. Immunol.* **2,** 706–713 (2002).

2. Berry, J. D. & Gaudet, R. G. Antibodies in infectious diseases: Polyclonals, monoclonals and niche biotechnology. *N. Biotechnol.* **28,** 489–501 (2011).

3. Swanson, C. L., Pelanda, R. & Torres, R. M. Division of labor during primary humoral immunity. *Immunol. Res.* **55,** 277–286 (2013).

4. Berkowska, M. a *et al.* Human memory B cells originate from three distinct germinal center-dependent and -independent maturation pathways Human memory B cells originate from three distinct germinal center- dependent and -independent maturation pathways. *Blood* **118,** 2150–2159 (2011).

5. Reinhardt, R. L.*et al*. Cytokine-secreting follicular T cells shape the antibody repertoire. *Nat. Immunol.* **10,** 385–393 (2009).

6. McHeyzer-Williams, L. & Pelletier, N. Follicular helper T cells as cognate regulators of B cell immunity. *Curr. Opin. Immunol.* **21,** 266–273 (2009).

7. Heesters, B. A.*et al*. Follicular dendritic cells : dynamic antigen libraries. *Nat. Rev. Immunol.* **14,** (2014).

8. Okada, T. *et al.* Antigen-engaged B cells undergo chemotaxis toward the T zone and form motile conjugates with helper T cells. *PLoS Biol.* **3,** 1047–1061 (2005).

9. Paus, D. *et al.* Antigen recognition strength regulates the choice between extrafollicular plasma cell and germinal center B cell differentiation. *J. Exp. Med.* **203,** 1081–1091 (2006).

10. Victora, G. D. & Nussenzweig, M. C. Germinal centers. *Annu Rev Immunol.* **30,** 429–457 (2012).

11. Hauser, A. E. *et al*. Cellular choreography in the germinal center: new visions from *in vivo* imaging.*Semin. Immunopathol.* **144,** 724–732 (2008).

12. Schwickert, T. a. *et al.* A dynamic T cell-limited checkpoint regulates affinity-dependent B cell entry into the germinal center. *J. Exp. Med.* **208,** 1243–1252 (2011).

13. Rajewsky, K. Clonal selection and learning in the antibody system. *Nature* **381,** 751–758 (1996).

14. Crotty, S. Follicular helper CD4 T cells (TFH). *Annu. Rev. Immunol.* **29,** 621–663 (2011).

15. Arnold, C. N. *et al*. The germinal center response is impaired in the absence of T cell-expressed CXCR5. *Eur. J. Immunol.* **37,** 100–109 (2007).

16. Yu, D. *et al.* The transcriptional repressor Bcl-6 directs T follicular helper cell lineage commitment. *Immunity* **31,** 457–468 (2009).

17. Qi, H. *et al*. SAP-controlled T-B interactions underlie germinal center formation. *Nature* **455,** 764–769 (2009).

18. Zotos, D. *et al.* IL-21 regulates germinal center B cell differentiation and proliferation through a B cell – intrinsic mechanism. **207,** 365–378 (2010).

19. Wang, Y. *et al.* Germinal-center development of memory B cells driven by IL-9 from follicular helper T cells. *Nat. Immunol.* **18,** 921–930 (2017).

20. Leddon, S. *et al.* The peptide specificity of the endogenous T follicular helper cell repertoire generated after protein immunization. *PLoS One* **7,** (2012).

21. Hu, J. K. *et al.* Murine antibody responses to cleaved soluble HIV-1 envelope trimers are highly restricted in specificity. *J. Virol.* **89,** 10383–10398 (2015).

22. Vinuesa, C. G. *et al*. Follicular helper T cells. *Annu. Rev. Immunol.* **34,** annurev-immunol-041015-055605 (2016).

23. Douek, D. C. *et al.* HIV preferentially infects HIV-specific CD4+ T cells. *Nature* **417,** 95–98 (2002).

24. Hemelaar, J. The origin and diversity of the HIV-1 pandemic. *Trends Mol. Med.*

18, 182–192 (2012).

25. Campbell-Yesufu, O. T. & Gandhi, R. T. Update on human immunodeficiency virus (HIV)-2 infection. *Clin. Infect. Dis.* **52,** 780–787 (2011).

26. Barre-Sinoussi, F. Isolation of a T-lymphotropic retrovirus from a patient at risk for Acquired Immuno Deficiency Syndrome (AIDS). *Science*. **54,** 155–161 (2014).

27. Coffin, J. *et al.* Human Immunodeficiency Virus. *Science*. 232: 697 (1986).

28. Marx, J. L. Strong new candidate for AIDS agent. *Science* **226,** 475–477 (2017).

29. Yukl, S. a. *et al.* Challenges in detecting HIV persistence during potentially curative interventions: A study of the Berlin patient. *PLoS Pathog.* **9,** (2013).

30. Who, Unicef & Unaids. Global HIV/AIDS response progress report 2011. *Vasa* 1–233 (2011).

31. Adejumo, O. A. *et al.* Contemporary issues on the epidemiology and antiretroviral adherence of HIV-infected adolescents in sub-Saharan Africa : a narrative review. *J. Int. AIDS Soc.* 18, 200049 (2015).

32. Rankin, W. W. *et al*. The stigma of being HIV-positive in Africa. *PLoS Med.* **2,** e247 (2005).

33. Deeks, S. G. *et al.* International AIDS society global scientific strategy: towards an HIV cure 2016. *Nat. Med.* **22,** 839–50 (2016).

34. Chan, E. *et al.* Gene therapy strategies to exploit TRIM derived restriction factors against HIV-1. *Viruses* **6,** 243–263 (2014).

35. Jones, R. B. *et al.* A Subset of latency-reversing agents expose HIV-infected resting CD4+T cells to recognition by cytotoxic T lymphocytes. *PLoS Pathog.* **12,** 1–25 (2016).

36. Leibman, R. S. & Riley, J. L. Engineering T cells to functionally cure HIV-1 infection. *Mol. Ther.* **23,** 1149–1159 (2015).

37. Weiss, R. a & Esparza, J. The prevention and eradication of smallpox: a

commentary on Sloane (1755) ‘An account of inoculation’. *Philos. Trans. R. Soc. B Biol. Sci.* **370,** 20140378–20140378 (2015).

38. Barouch, D. H. Challenges in the development of an HIV-1 vaccine. *Nature* **455,** 613–619 (2008).

39. Kwong, P. D., Mascola, J. R. & Nabel, G. J. Broadly neutralizing antibodies and the search for an HIV-1 vaccine: the end of the beginning. *Nat. Rev. Immunol.* **13,** 693–701 (2013).

40. Tran, E. E. H. *et al.* Structural mechanism of trimeric HIV-1 envelope glycoprotein activation. *PLoS Pathog.* **8,** 37 (2012).

41. Pancera, M. *et al.* Structure and immune recognition of trimeric pre-fusion HIV-1 Env. *Nature* **514,** 455–61 (2014).

42. Checkley, M. A. *et al*. HIV-1 envelope glycoprotein biosynthesis, trafficking, and incorporation. *J. Mol. Biol.* **410,** 582–608 (2011).

43. Varchetta, S. *et al.* Sialic acid-binding Ig-like lectin-7 interacts with HIV-1 gp120 and facilitates infection of CD4pos T cells and macrophages. *Retrovirology* **10,** 154 (2013).

44. Perez, L. G. *et al*. Envelope Glycoprotein Binding to the Integrin 4 7 Is Not a General Property of Most HIV-1 Strains. *J. Virol.* **88,** 10767–10777 (2014).

45. Wilen, C. B. *et al*. HIV: Cell binding and entry. *Cold Spring Harb. Perspect. Med.* **2,** 1–13 (2012).

46. Wyss, S. *et al.* Regulation of Human Immunodeficiency Virus type 1 envelope glycoprotein fusion by a membrane-interactive domain in the gp41 cytoplasmic tail. *J. Virol.* **79,** 12231–12241 (2005).

47. Viard, M. *et al.* Photoinduced reactivity of the HIV-1 glycoprotein with a membrane-embedded probe reveals insertion of portions of the HIV-1 gp41 cytoplasmic tail into the viral membrane. *Biochemistry* **454,** 42–54 (2007).

48. Burton, D. *et al.* Antibody responses to HIV-1 glycoproteins in HIV-1 infection.

Nat.Immunol. **16,** 571–576 (2015).

49. Moore PL *et al.* Nature of nonfunctional envelope proteins on the surface of human immunodeficiency virus type 1. *J. Virol.* **80,** 2515–2528 (2006).

50. Fouts, T. R. *et al*. Neutralization of the human immunodeficiency virus type 1 primary isolate JR-FL by human monoclonal antibodies correlates with antibody binding to the oligomeric form of the envelope glycoprotein complex. *J. Virol.* **71,** 2779–85 (1997).

51. Yasmeen, A. *et al.* Differential binding of neutralizing and non-neutralizing antibodies to native-like soluble HIV-1 Env trimers, uncleaved Env proteins, and monomeric subunits. *Retrovirology* **11,** 41 (2014).

52. Forthal, D. N. *et al.* Antibody-dependent cellular cytotoxicity independently predicts survival in severely immunocompromised human immunodeficiency virus-infected patients. *J Infect Dis* **180,** 1338–1341 (1999).

53. Gilbert, P. *et al.* Magnitude and breadth of a nonprotective neutralizing antibody response in an efficacy trial of a candidate HIV-1 gp120 vaccine. *J. Infect. Dis.* **202,** 595–605 (2010).

54. Burton, D. R. *et al.* Limited or no protection by weakly or nonneutralizing antibodies against vaginal SHIV challenge of macaques compared with a strongly neutralizing antibody. *Proc. Natl. Acad. Sci. U. S. A.* **108,** 11181–11186 (2011).

55. Moog, C. *et al.* Protective effect of vaginal application of neutralizing and nonneutralizing inhibitory antibodies against vaginal SHIV challenge in macaques. *Mucosal Immunol.* **7,** 46–56 (2014).

56. Dugast, A. S. *et al.* Lack of protection following passive transfer of polyclonal highly functional low-dose non-neutralizing antibodies. *PLoS One* **9,** (2014).

57. Walker, L. M. *et al.* A limited number of antibody specificities mediate broad and potent serum neutralization in selected HIV-1 infected individuals. *PLoS Pathog.* **6,** 11–12 (2010).

58. Cubas, R. a *et al.* Inadequate T follicular cell help impairs B cell immunity during

HIV infection. *Nat. Med.* **19,** 494–9 (2013).

59. Boswell, K. L. *et al.* Loss of circulating CD4 T cells with B cell helper function during chronic HIV infection. *PLoS Pathog.* **10,** 1–14 (2014).

60. Havenar-Daughton, C. *et al*. Tfh cells and HIV bnAbs, an immunodominance model of the HIV neutralizing antibody generation problem. *Immunol. Rev.* **275,** 49–61 (2017).

61. Bar, K. J. *et al.* Early low-titer neutralizing antibodies impede HIV-1 replication and select for virus escape. *PLoS Pathog.* **8,** (2012).

62. McGuire, A. T. *et al.* HIV antibodies. Antigen modification regulates competition of broad and narrow neutralizing HIV antibodies. *Science* **346,** 1380–3 (2014).

63. Briney, B. *et al.* Tailored Immunogens Direct Affinity Maturation toward HIV Neutralizing Antibodies. *Cell* **166,** 1459–1470.e11 (2016).

64. Sather, D. N. *et al.* Emergence of broadly neutralizing antibodies and viral coevolution in two subjects during the early stages of infection with human immunodeficiency virus type 1. *J. Virol.* **88,** 12968–81 (2014).

65. Nourmohammad, A., Otwinowski, J. & Plotkin, J. B. Host-Pathogen Coevolution and the Emergence of Broadly Neutralizing Antibodies in Chronic Infections. *PLoS Genet.* **12,** 1–23 (2016).

66. Burton, D. R. & Hangartner, L. Broadly Neutralizing Antibodies to HIV and Their Role in Vaccine Design. *Annu. Rev. Immunol.* **34,** 635–659 (2016).

67. Mascola, J. R. & Montefiori, D. C. The Role of Antibodies in HIV Vaccines. *Annu. Rev. Immunol.* **28,** 413–444 (2010).

68. Stephenson, K. E. & Barouch, D. H. Broadly Neutralizing Antibodies for HIV Eradication. *Curr. HIV/AIDS Rep.* **13,** 31–37 (2016).

69. Gautam, R. *et al.* A single injection of anti-HIV-1 antibodies protects against repeated SHIV challenges. *Nature* **533,** 105–9 (2016).

70. Gruell, H. *et al.* Antibody and antiretroviral preexposure prophylaxis prevent cervicovaginal HIV-1 infection in a transgenic mouse model. *J. Virol.* **87,** 8535–44 (2013).

71. Shingai, M. *et al.* Passive transfer of modest titers of potent and broadly neutralizing anti-HIV monoclonal antibodies block SHIV infection in macaques. *J. Exp. Med.* **211,** 2061–74 (2014).

72. Saunders, K. O. *et al.* Sustained Delivery of a Broadly Neutralizing Antibody in Nonhuman Primates Confers Long-Term Protection against Simian/Human Immunodeficiency Virus Infection. *J. Virol.* **89,** 5895–903 (2015).

73. King, D. F. L. *et al.* Broadly Neutralizing Antibodies Display Potential for Prevention of HIV-1 Infection of Mucosal Tissue Superior to That of Nonneutralizing Antibodies. *J. Virol.* **91,** 1–16 (2017).

74. Bournazos, S. *et al.* Broadly Neutralizing Anti-HIV-1 Antibodies Require Fc Effector Functions for In Vivo Activity. *Cell* **158,** 1243–1253 (2014).

75. Bruel, T. *et al.* Elimination of HIV-1-infected cells by broadly neutralizing antibodies. *Nat. Commun.* **7,** 10844 (2016).

76. Scheid, J. F. *et al.* Antibodies That Mimic CD4 Binding. *Science* **333,** 1633–1637 (2012).

77. Zhou, T. *et al.* Structural repertoire of HIV-1-neutralizing antibodies targeting the CD4 supersite in 14 donors. *Cell* **161,** 1280–1292 (2015).

78. Wu, X. *et al.* Maturation and diversity of the VRC01-antibody lineage over 15 years of chronic HIV-1 infection. *Cell* **161,** 480–485 (2015).

79. Zhou, T. *et al.* Multidonor analysis reveals structural elements, genetic determinants, and maturation pathway for HIV-1 neutralization by VRC01-class antibodies. *Immunity* **39,** 245–258 (2013).

80. Jardine, J. G. *et al.* Minimally Mutated HIV-1 Broadly Neutralizing Antibodies to Guide Reductionist Vaccine Design. *PLoS Path*. **2011,** 1–23 (2016).

81. He, Q., Johnston, J., Zeitlinger, J., City, K. & City, K. HHS Public Access. **33,** 395–401 (2015).

82. McGuire, A. T. *et al.* Specifically modified Env immunogens activate B-cell precursors of broadly neutralizing HIV-1 antibodies in transgenic mice. *Nat. Commun.* **7,** 10618 (2016).

83. de Taeye, S. W., Moore, J. P. & Sanders, R. W. HIV-1 Envelope Trimer Design and Immunization Strategies To Induce Broadly Neutralizing Antibodies. *Trends Immunol.* **37,** 221–232 (2016).

84. Jardine, J. Rational HIV Immunogen Design to Target Specific Germline B Cell Receptors. *Science (80-.).* **340,** 711–716 (2013).

85. Mann, J. K. & Ndung'u, T. HIV-1 vaccine immunogen design strategies. *Virol. J.* **12,** 3 (2015).

86. Scharf, L. *et al.* Structural basis for germline antibody recognition of HIV-1 immunogens. *Elife* **5,** 1–24 (2016).

87. Tian, M. *et al.* Induction of HIV Neutralizing Antibody Lineages in Mice with Diverse Precursor Repertoires. *Cell* **166,** 1471–1484.e18 (2016).

88. Moore, P. L. & Williamson, C. Approaches to the induction of HIV broadly neutralizing antibodies. *Curr. Opin. HIV AIDS* 1 (2016).

89. Day, T. a & Kublin, J. G. Lessons learned from HIV vaccine clinical efficacy trials. *Curr. HIV Res.* **11,** 441–9 (2013).

90. Montefiori, D. C. *et al.* Magnitude and breadth of the neutralizing antibody response in the RV144 and Vax003 HIV-1 vaccine efficacy trials. *J. Infect. Dis.* **206,** 431–441 (2012).

91. Tomaras, G. D. & Haynes, B. F. Advancing toward HIV-1 vaccine efficacy through the intersections of immune correlates. *Vaccines* **2,** 15–35 (2014).

92. Flynn, N. *et al.* Placebo-controlled phase 3 trial of a recombinant glycoprotein 120 vaccine to prevent HIV-1 infection. *J. Infect. Dis.* **191,** 654–665 (2005).

93. Karnasuta, C. *et al.* Comparison of Antibody Responses Induced by RV144, VAX003 and VAX004 Vaccination Regimens. 1–54 (2016).

94. Rerks-Ngram, P. *et al.* Vaccination with ALVAC and AIDSVAX to prevent HIV-1 infection in Thailand. *New Engl. J. Med*. 361: 23 (2009).

95. Seaman, M. S. *et al.* Tiered categorization of a diverse panel of HIV-1 Env pseudoviruses for assessment of neutralizing antibodies. *J Virol* **84,** 1439–1452 (2010).

96. Gottardo, R. *et al.* Plasma IgG to linear epitopes in the V2 and V3 regions of HIV-1 gp120 correlate with a reduced risk of infection in the RV144 vaccine efficacy trial. *PLoS One* **8,** 1–16 (2013).

97. Haynes, B. F. *et al.* Immunoe-correlates analysis of an HIV-1 vaccine efficacy trial. *New Eng. J. Med.* 339–354 (2008).

98. Bekker, L. G. & Gray, G. E. Hope for HIV control in southern Africa: The continued quest for a vaccine. *PLoS Med.* **14,** 10–12 (2017).

99. Buchbinder, S. P. *et al.* Efficacy assessment of a cell-mediated immunity HIV-1 vaccine (the Step Study): a double-blind, randomised, placebo-controlled, test-of-concept trial. *Lancet* **372,** 1881–1893 (2009).

100. Gray, G., Buchbinder, S. & Duerr, A. Overview of STEP and Phambili trial results: two phase IIb test of concept studies investigating the efficacy of MRK ad5 gag/pol/nef subtype B HIV vaccine. *Curr opin HIV AIDS* **5,** 357–361 (2011).

101. Barouch, D. H. & Korber, B. HIV-1 vaccine development after STEP. *Annu. Rev. Med.* **61,** 153–67 (2010).

102. Benlahrech, A. *et al.* Adenovirus vector vaccination induces expansion of memory CD4 T cells with a mucosal homing phenotype that are readily susceptible to HIV-1. *Proc. Natl. Acad. Sci. U. S. A.* **106,** 19940–5 (2009).

103. Catanzaro, A. T. *et al.* Phase I clinical evaluation of a six-plasmid multiclade HIV-1 DNA candidate vaccine. *Vaccine* **25,** 4085–4092 (2007).

104. Hammer, S. M. *et al.* Efficacy trial of a DNA/rAd5 HIV-1 preventive vaccine. *N. Engl. J. Med.* **369,** 2083–2092 (2014).

105. Huang, J. *et al.* Identification of a CD4-Binding-Site Antibody to HIV that Evolved Near-Pan Neutralization Breadth. *Immunity* **45,** 1108–1121 (2016).

106. Euler, Z. & Schuitemaker, H. Cross-reactive broadly neutralizing antibodies: Timing is everything. *Front. Immunol.* **3,** 1–11 (2012).

107. Burton, D. R. *et al.* A blue print for HIV vaccine discovey. *Cell Host Microbe.* **12,** 396–407 (2013).

108. Asbach, B. *et al.* Potential To Streamline Heterologous DNA Prime and NYVAC/Protein Boost HIV Vaccine Regimens in Rhesus Macaques by Employing Improved Antigens. *J. Virol.* **90,** 4133–49 (2016).

109. Zurawski, G. *et al.* Targeting HIV-1 env gp140 to LOX-1 elicits immune responses in rhesus macaques. *PLoS One* **11,** 1–23 (2016).

110. Stamatatos, L., Pancera, M. & McGuire, A. T. Germline-targeting immunogens. *Immunol. Rev.* **275,** 203–216 (2017).

111. Mcguire, A. T. *et al.* Engineering HIV envelope protein to activate germline B cell receptors of broadly neutralizing anti-CD4 binding site antibodies. *J. Exp. Med.* **210,** 655–663 (2013).

112. Safrit, J. T. & Koff, W. C. Novel approaches in preclinical HIV vaccine. *Curr. Opin. HIV AIDS* **11,** 601–606 (2016).

113. Pantophlet, R., Wilson, I. a. & Burton, D. R. Improved design of an antigen with enhanced specificity for the broadly HIV-neutralizing antibody b12. *Protein Eng. Des. Sel.* **17,** 749–758 (2004).

114. Weber, J. P., Fuhrmann, F. & Hutloff, A. T-follicular helper cells survive as long-term memory cells. *Eur. J. Immunol.* **42,** 1981–1988 (2012).

115. Crotty, S. T follicular helper cell diffreentiation, function and roles in disease. *Immunity* **41,** 529–542 (2015).

116. Linterman, M. a & Hill, D. L. Can follicular helper T cells be targeted to improve vaccine efficacy? *F1000Research* **5,** (2016).

117. Silva-Flannery, L. M., Cabrera-Mora, M., Dickherber, M. & Moreno, A. Polymeric linear peptide chimeric vaccine-induced antimalaria immunity is associated with enhanced in vitro antigen loading. *Infect. Immun.* **77,** 1798–1806 (2009).

118. Lahoud, M. H. *et al.* Targeting antigen to mouse dendritic cells via Clec9A induces potent CD4 T cell responses biased toward a follicular helper phenotype. *J. Immunol.* **187,** 842–850 (2011).

119. Bentebibel, S. *et al.* Induction of ICOS+CXCR3+CXCR5+ Th cells correlates with antibody responses to influenza vaccination. *Sci. Transl. Med.* **5,** 1–19 (2014).

120. Baumjohann, D. *et al.* Persistent Antigen and Germinal Center B Cells Sustain T Follicular Helper Cell Responses and Phenotype. *Immunity* **38,** 596–605 (2013).

121. Li, S. *et al.* Synthetic peptides containing B- and T-cell epitope of dengue virus-2 E domain III provoked B- and T-cell responses. *Vaccine* **29,** 3695–3702 (2011).

122. Decroix, N., Quan, C. P., Pamonsinlapatham, P. & Bouvet, J. P. Mucosal immunity induced by intramuscular administration of free peptides in-line with PADRE: IgA antibodies to the ELDKWA epitope of HIV gp41. *Scand. J. Immunol.* **56,** 59–65 (2002).

123. Calvo-Calle, J. M. *et al.* A linear peptide containing minimal T- and B-cell epitopes of Plasmodium falciparum circumsporozoite protein elicits protection against transgenic sporozoite challenge. *Infect. Immun.* **74,** 6929–6939 (2006).

124. De Groot, A.Immunogenic consensus sequences T helper epitopes for a Pan Brkholderia biodefense vaccine.*Immunome Res*. **44,** 735–745 (2008).

125. Nezafat, N. *et al.* Production of a novel multi-epitope peptide vaccine for cancer immunotherapy in TC-1 tumor-bearing mice. *Biologicals* **43,** 11–17 (2015).

126. Hanagata, N. Structure-dependent immunostimulatory effect of CpG oligodeoxynucleotides and their delivery system. *Int. J. Nanomedicine* **7,** 2181–2195 (2012).

127. Gupta, N., Vedi, S., Kunimoto, D. Y., Agrawal, B. & Kumar, R. Novel lipopeptides of ESAT-6 induce strong protective immunity against Mycobacterium tuberculosis: Routes of immunization and TLR agonists critically impact vaccine's efficacy. *Vaccine* **34,** 5677–5688 (2016).

128. Mastelic Gavillet, B. *et al.* MF59 mediates its B cell adjuvanticity by promoting T follicular helper cells and thus germinal center responses in adult and early life. *J. Immunol.* **194,** 4836–45 (2015).

129. Alexander, J. *et al.* The optimization of helper T lymphocyte (HTL) function in vaccine development. *Immunol. Res.* **18,** 79–92 (1998).

130. Wilson, J. T. *et al.* pH responsive nanoparticle vaccines for dual discovery of antigens and immunostimulatory oligonucleotides. *ACS Nano*. **7,** 3912–3925 (2014).

131. Sledz, C. a, Holko, M., de Veer, M. J., Silverman, R. H. & Williams, B. R. Activation of the interferon system by short-interfering RNAs. *Nat Cell Biol* **5,** 834–839 (2003).

132. Alexander, J. *et al.* Development of experimental carbohydrate-conjugate vaccines composed of Streptococcus pneumoniae capsular polysaccharides and the universal helper T-lymphocyte epitope (PADRE). *Vaccine* **22,** 2362–7 (2004).

133. Rosa, D. S., Tzelepis, F., Cunha, M. G., Soares, I. S. & Rodrigues, M. M. The pan HLA DR-binding epitope improves adjuvant-assisted immunization with a recombinant protein containing a malaria vaccine candidate. *Immunol. Lett.* **92,** 259–68 (2004).

134. Guenaga, J. *et al.* Heterologous epitope-scaffold prime: Boosting immuno-focuses B cell responses to the HIV-1 gp41 2F5 neutralization determinant. *PLoS One* **6,** (2011).

135. Schaerli, P. *et al.* CXC chemokine receptor 5 expression defines follicular homing T cells with B cell helper function. *J. Exp. Med.* **192,** 1553–62 (2000).

136. Francisco, L. M., Sage, P. T. & Sharpe, A. H. The PD-1 pathway in tolerance and

autoimmunity. *Immunol. Rev.* **236,** 219–242 (2010).

137. Haynes, N. M. *et al.* Role of CXCR5 and CCR7 in follicular Th cell positioning and appearance of a programmed cell death gene-1high germinal center-associated subpopulation. *J. Immunol.* **179,** 5099–5108 (2007).

138. Locci, M. *et al.* Human circulating PD-1+CXCR3-CXCR5+ memory Tfh cells are highly functional and correlate with broadly neutralizing HIV antibody responses. *Immunity* **39,** 758–769 (2013).

139. Linterman, M. A. *et al.* Foxp3+ follicular regulatory T cells control the germinal center response. *Nat. Med.* **17,** 975–82 (2011).

140. Chung, Y. *et al.* Follicular regulatory T (Tfr) cells with dual Foxp3 and Bcl6 expression suppress germinal center reactions. *Nat. Med.* **17,** 983–988 (2011).

141. Shinall, S. M., Gonzalez-Fernandez, M., Noelle, R. J. & Waldschmidt, T. J. Identification of murine germinal center B cell subsets defined by the expression of surface isotypes and differentiation antigens. *J. Immunol.* **164,** 5729–5738 (2000).

142. Hao, Z. *et al.* Fas Receptor Expression in germinal center B cells is essential for T and B lymphocyte homeostasis. *Immunity* **29,** 615–627 (2008).

143. Nutt, S. L., Hodgkin, P. D., Tarlinton, D. M. & Corcoran, L. M. The generation of antibody-secreting plasma cells. *Nat. Rev. Immunol.* **15,** 160–171 (2015).

144. Fazilleau, N., Mark, L., McHeyzer-Williams, L. J. & McHeyzer-Williams, M. G. Follicular Helper T Cells: Lineage and Location. *Immunity* **30,** 324–335 (2009).

145. Ma, C. S., Deenick, E. K., Batten, M. & Tangye, S. G. The origins, function, and regulation of T follicular helper cells. *J. Exp. Med.* **209,** 1241–1253 (2012).

146. Tellier, J. & Nutt, S. L. The unique features of follicular T cell subsets. *Cell. Mol. Life Sci.* **70,** 4771–84 (2013).

147. Liu, F. *et al.* Expression and Functional Activity of Isotype and Subclass Switched Human Monoclonal Antibody Reactive with the base of the V3 loop of HIV-1

gp120. *AIDS Res. Hum. Retroviruses*. **19,** 597–607 (2003).

148. Pantophlet, R., Aguilar-sino, R. O., Wrin, T., Cavacini, L. A. & Burton, D. R. Analysis of the neutralization breadth of the anti-V3 antibody F425-B4e8 and re-assessment of its epitope fine specificity by scanning mutagenesis. *Protein Eng. Des. Sel.* **364,** 441–453 (2007).

149. Ekiert, D. C. *et al.* Antibody recognition of conserved influenza virus epitope. *Scienec* **1857,** 246–252 (2009).

150. Liu, F. *et al.* Expression and functional activity of isotype and subclass switched human monoclonal antibody reactive with the base of the V3 loop of HIV-1 gp120. *AIDS Res. Hum. Retroviruses* **19,** 597–607 (2003).

151. Ahmed, F. K., Clark, B. E., Burton, D. R. & Pantophlet, R. An engineered mutant of HIV-1 gp120 formulated with adjuvant Quil A promotes elicitation of antibody responses overlapping the CD4-binding site. *Vaccine* **30,** 922–30 (2012).

152. Toomer, K. H. *et al.* Developmental Progression and Interrelationship of Central and Effector Regulatory T Cell Subsets. *J. Immunol.* 196: 3665-3676 (2017).

153. Byrd, D., Amet, T., Hu, N., Lan, J. & Hu, S. Primary Human Leukocyte Subsets Differentially Express Vaccinia Virus Receptors Enriched in Lipid Rafts. *J. Virol.* **87,** 9301–9312 (2013).

154. Kantele, a. *et al.* Humoral immune response to keyhole limpet haemocyanin, the protein carrier in cancer vaccines. *Clin. Dev. Immunol.* **2011,** (2011).

155. Blanchfield, K. *et al.* Recombinant influenza H7 hemagglutinins induce lower neutralizing antibody titers in mice than do seasonal hemagglutinins. *Influenza Other Respi. Viruses* **8,** 628–635 (2014).

156. Kraal, G., Weissman, I. L. & Butcher, E. C. Germinal centre B cells: antigen specificity and changes in heavy chain class expression. *Nature* **298,** 377–379 (1982).

157. Meyer-Hermann, M. E., Maini, P. K. & Iber, D. An analysis of B cell selection mechanisms in germinal centers. *Math. Med. Biol.* **23,** 255–77 (2006).

158. Fooksman, D. R. *et al.* Development and migration of pre-palsma cells in the mouse lymph node. *Immunity* **33,** 118–127 (2011).

159. Zhang, Y., Garcia-Ibanez, L. & Toellner, K. M. Regulation of germinal center B-cell differentiation. *Immunol. Rev.* **270,** 8–19 (2016).

160. Huang, J., Ehrnfelt, C., Paulie, S., Zuber, B. & Ahlborg, N. ELISpot and ELISA analyses of human IL-21-secreting cells: Impact of blocking IL-21 interaction with cellular receptors. *J. Immunol. Methods* **417,** 60–66 (2015).

161. Harrell, M. I., Iritani, B. M. & Ruddell, A. Lymph node mapping in the mouse. *J. Immunol. Methods* **332,** 170–174 (2008).

162. Good-Jacobson, K. L., O'Donnell, K., Belz, G. T., Nutt, S. L. & Tarlinton, D. M. c-Myb is required for plasma cell migration to bone marrow after immunization or infection. *J. Exp. Med.* **212,** 1001–9 (2015).

163. Peterhoff, D. & Wagner, R. Guiding the long way to broad HIV neutralization. *Curr. Opin. HIV AIDS* **12,** 257–264 (2017).

164. Jardine, J. G. *et al.* HIV-1 broadly neutralizing antibody precursor B cells revealed by germline-targeting immunogen. *Science* **351,** 1458–1463 (2016).

165. Steichen, J. M. *et al.* HIV Vaccine Design to Target Germline Precursors of Glycan-Dependent Broadly Neutralizing Antibodies. *Immunity* **45,** 483–496 (2016).

166. Steichen, J. M. *et al.* HIV Vaccine Design to Target Germline Precursors of Glycan-Dependent Broadly Neutralizing Antibodies. *Immunity* **45,** 483–496 (2016).

167. De Groot, A. S. *et al.* Engineering immunogenic consensus T helper epitopes for a cross-clade HIV vaccine. *Methods* **34,** 476–487 (2004).

168. Alexander, J. *et al.* Linear PADRE T helper epitope and carbohydrate B cell epitope conjugates induce specific high titer IgG antibody responses. *J. Immunol.* **164,** 1625–1633 (2000).

169. Franke, E. D. *et al.* Pan DR binding sequence provides T-cell help for induction of protective antibodies against Plasmodium yoelii sporozoites. *Vaccine* **17,** 1201–1205 (1999).

170. Wu, X. *et al.* Maturation and diversity of the VRC01-antibody lineage over 15 years of chronic HIV-1 infection. *Cell* **161,** 470–485 (2016).

171. Wyatt, R. *et al.* Functional anf immunological characterization of human immunodeficiency virus type 1 envelope glycoproteins containing deletions of the major variable regions. *J. Virol.* **67,** 4557–4565 (1993).

172. Ren, X., Sodroski, J. & Yang, X. An unrelated monoclonal antibody neutralizes human immunodeficiency virus type 1 by binding to an artificial epitope engineered in a functionally neutral region of the viral envelope glycoproteins. *J. Virol.* **79,** 5616–5624 (2005).

173. Stamatatos, L. & Cheng-Mayer, C. An envelope modification that renders a primary, neutralization-resistant clade B human immunodeficiency virus type 1 isolate highly susceptible to neutralization by sera from other clades. *J. Virol.* **72,** 7840–5 (1998).

174. Kwong, P. D. *et al.* Structure of an HIV gp120 envelope glycoprotein in complex with the CD4 receptor and a neutralizing human antibody. *Nature* **393,** 648–659 (1998).

175. Dey, B. *et al.* Characterization of human immunodeficiency virus type 1 monomeric and trimeric gp120 glycoproteins stabilized in the CD4-bound state: antigenicity, biophysics, and immunogenicity. *J. Virol.* **81,** 5579–5593 (2007).

176. Xiang, S. *et al.* Mutagenic stabilization and/or disruption of a CD4-bound state reveals distinct conformations of the human immunodeficiency virus type 1 gp120 envelope glycoprotein. *J. Virol.* **76,** 9888–99 (2002).

177. Pantophlet, R. *et al.* Fine mapping of the interaction of neutralizing and nonneutralizing monoclonal antibodies with the CD4 binding site of human immunodeficiency virus type 1. *J. Virol.* **77,** 642–658 (2003).

178. Jardine, J. G. *et al.* HIV-1 broadly neutralizing antibody precursor B cells revealed by germline-targeting immunogen. *Science (80-.).* **351,** 1458–1463 (2016).

179. Friedlander, R. M., Nussenzweig, M. C. & Leder, P. Complete nucleotide sequence of the membrane form of the human IgM heavy chain. *Nucleic Acids Res.* **18,** 4278 (1990).

180. Oliver, a M., Martin, F. & Kearney, J. F. Mouse CD38 is down-regulated on germinal center B cells and mature plasma cells. *J. Immunol.* **158,** 1108–15 (1997).

181. Ridderstad, a & Tarlinton, D. M. Kinetics of establishing the memory B cell population as revealed by CD38 expression. *J. Immunol.* **160,** 4688–4695 (1998).

182. Hale, J. S. & Ahmed, R. Memory T follicular helper CD4 T cells. *Front. Immunol.* **6,** 1–9 (2015).

183. Fazilleau, N. *et al.* Lymphoid reservoirs of antigen-specific memory T helper cells. *Nat. Immunol.* **8,** 753–761 (2007).

184. Butler, M. Optimisation of the cellular metabolism of glycosylation for recombinant proteins produced by mammalian cell systems. *Cytotechnology* **50,** 57–76 (2006).

185. Moore, J. P. & Sodroski, J. Antibody cross-competition analysis of the human immunodeficiency virus type 1 gp120 exterior envelope glycoprotein. *J. Virol.* **70,** 1863–72 (1996).

186. Kwong, P. D. *et al.* HIV-1 evades antibody-mediated neutralization through conformational masking of receptor-binding sites. *Nature* **420,** 678–682 (2002).

187. Tolbert, W. D. *et al.* Paring down HIV Env: design and crystal structure of a stabilized inner domain of HIV-1 gp120 displaying a major ADCC target of the A32 region. *Structure* **24,** 697–709 (2016).

188. Rolf, J. *et al.* Phosphoinositide 3-kinase activity in T cells regulates the magnitude of the germinal center reaction. *J. Immunol.* **185,** 4042–52 (2010).

189. Fazilleau, N., McHeyzer-Williams, L. J., Rosen, H. & McHeyzer-Williams, M. G.

The function of follicular helper T cells is regulated by the strength of T cell antigen receptor binding. *Nat. Immunol.* **10,** 375–384 (2009).

190. Suan, D. *et al.* T follicular helper cells have distinct modes of migration and molecular signatures in naive and memory immune responses. *Immunity* **42,** 704–718 (2015).

191. Liang, F. *et al.* Vaccine priming is restricted to draining lymph nodes and controlled by adjuvant-mediated antigen uptake. **2094,** (2017).

192. Blink, E. J. *et al.* Early appearance of germinal center–derived memory B cells and plasma cells in blood after primary immunization. *J. Exp. Med.* **201,** 545–554 (2005).

193. McHeyzer-Williams, L. J., Milpied, P. J., Okitsu, S. L. & McHeyzer-Williams, M. G. Class-switched memory B cells remodel BCRs within secondary germinal centers. *Nat. Immunol.* **16,** 296–305 (2015).

194. Anderson, S. M., Tomayko, M. M., Ahuja, A., Haberman, A. M. & Shlomchik, M. J. New markers for murine memory B cells that define mutated and unmutated subsets. *J. Exp. Med.* **204,** 2103–2114 (2007).

195. Kaji, T. *et al.* Distinct cellular pathways select germline-encoded and somatically mutated antibodies into immunological memory. *J. Exp. Med.* **209,** 2079–2097 (2012).

196. Fischer, N. O. Conjugation to nickel-chelating nanolipoprotein particles increases the potency and efficacy of subunit vaccines to prevent West Nile encephelitis .*Bioconjug. Chem.* **29,** 997–1003 (2012).

197. He, X.-S. *et al.* Plasmablast-derived polyclonal antibody response after influenza vaccination. *J. Immunol. Methods* **365,** 67–75 (2011).

198. Acetyl, V., Takahashi, B. Y., Dutta, P. R. & Cerasoli, D. M. In Situ Studies of the Primary Immune Response to . Affinity Maturation Develops in Two Stages of Clonal Selection. **187,** (1998).

199. Radbruch, A. *et al.* Competence and competition: the challenge of becoming a

long-lived plasma cell. *Nat. Rev. Immunol.* **6,** 741–50 (2006).

200. Silva, N. S. De, Klein, U., Irving, H., Cancer, C. & Biology, C. HHS Public Access. **15,** 137–148 (2015).

201. Toellner, K. M. *et al.* T helper 1 (Th1) and Th2 characteristics start to develop during T cell priming and are associated with an immediate ability to induce immunoglobulin class switching. *J. Exp. Med.* **187,** 1193–1204 (1998).

202. McHeyzer-Williams, L. J. & McHeyzer-Williams, M. G. Antigen-Specific Memory B Cell Development. *Annu. Rev. Immunol.* **23,** 487–513 (2005).

203. Mitsdoerffer, M. *et al.* Proinflammatory T helper type 17 cells are effective B-cell helpers. *Proc. Natl. Acad. Sci.* **107,** 14292–14297 (2010).

204. Lefeber, D. J. *et al.* Th1-Directing Adjuvants Increase the Immunogenicity of Oligosaccharide-Protein Conjugate Vaccines Related to Streptococcus pneumoniae Type 3. *Infect. Immun.* **71,** 6915–6920 (2003).

205. Kaba, S. a. *et al.* Immune responses of mice with different genetic backgrounds to improved multiepitope, multitarget malaria vaccine candidate antigen FALVAC-1A. *Clin. Vaccine Immunol.* **15,** 1674–1683 (2008).

206. Marty-Roix, R. *et al.* Identification of QS-21 as an inflammasome-activating molecular component of saponin adjuvants. *J. Biol. Chem.* **291,** 1123–1136 (2016).

207. Beck, Z. *et al.* Differential immune responses to HIV-1 envelope protein induced by liposomal adjuvant formulations containing monophosphoryl lipid A with or without QS21. *Vaccine* **33,** 5578–5587 (2015).

208. Rivera, F. & Espino, A. M. Adjuvant-enhanced antibody and cellular responses to inclusion bodies expressing FhSAP2 correlates with protection of mice to Fasciola hepatica. *Exp. Parasitol.* **160,** 31–38 (2016).

209. Zhu, D. & Tuo, W. QS-21: A potent vaccine adjuvant. *Nat. Prod. Chem. Res.* **3,** 3–4 (2016).

210. Du, S. X. *et al.* A directed molecular evolution approach to improved immunogenicity of the HIV-1 envelope glycoprotein. *PLoS One* **6,** (2011).

211. De Taeye, S. W. *et al.* Immunogenicity of Stabilized HIV-1 Envelope Trimers with Reduced Exposure of Non-neutralizing Epitopes. *Cell* **163,** 1702–1715 (2015).

212. Smith, D. H. *et al.* Comparative immunogenicity of HIV-1 clade c envelope proteins for prime/boost studies. *PLoS One* **5,** (2010).

213. Chen, H., Xu, X. & Jones, I. M. Immunogenicity of the outer domain of a HIV-1 clade C gp120. *Retrovirology* **4,** 33 (2007).

214. Li, H. *et al.* Envelope residue 375 substitutions in simian-human immunodeficiency viruses enhance CD4 binding and replication in rhesus macaques. *Proc. Natl. Acad. Sci. U. S. A.* **113,** E3413-22 (2016).

215. Surman, S. *et al.* Localization of CD4+ T cell epitope hotspots to exposed strands of HIV envelope glycoprotein suggests structural influences on antigen processing. *Proc. Natl. Acad. Sci. U. S. A.* **98,** 4587–92 (2001).

216. Jelley-Gibbs, D. M. *et al.* Unexpected prolonged presentation of influenza antigens promotes CD4 T cell memory generation. *J. Exp. Med.* **202,** 697–706 (2005).

217. Haynes, B. F., Kelsoe, G., Harrison, S. C. & Kepler, T. B. B-cell–lineage immunogen design in vaccine development with HIV-1 as a case study. *Nat. Biotechnol.* **30,** 423–433 (2012).

218. Jacob, R. A. *et al.* Anti-V3/Glycan and Anti-MPER Neutralizing Antibodies, but Not Anti-V2/Glycan Site Antibodies, Are Strongly Associated with Greater Anti-HIV-1 Neutralization Breadth and Potency. *J. Virol.* **89,** 5264–75 (2015).

219. Hioe, C. E. *et al.* Anti-V3 monoclonal antibodies display broad neutralizing activities against multiple HIV-1 subtypes. *PLoS One* **5,** (2010).

220. West, A. P., Diskin, R., Nussenzweig, M. C. & Bjorkman, P. J. Structural basis for germ-line gene usage of a potent class of antibodies targeting the CD4-binding site of HIV-1 gp120. *Proc. Natl. Acad. Sci.* **109,** E2083–E2090 (2012).

221. Goo, L. *et al.* Early development of broadly neutralizing antibodies in HIV-1-infected infants. *Nature Medicine* 20, 655-658 (2014).

Appendix A. Supplemental figures for Chapter 2

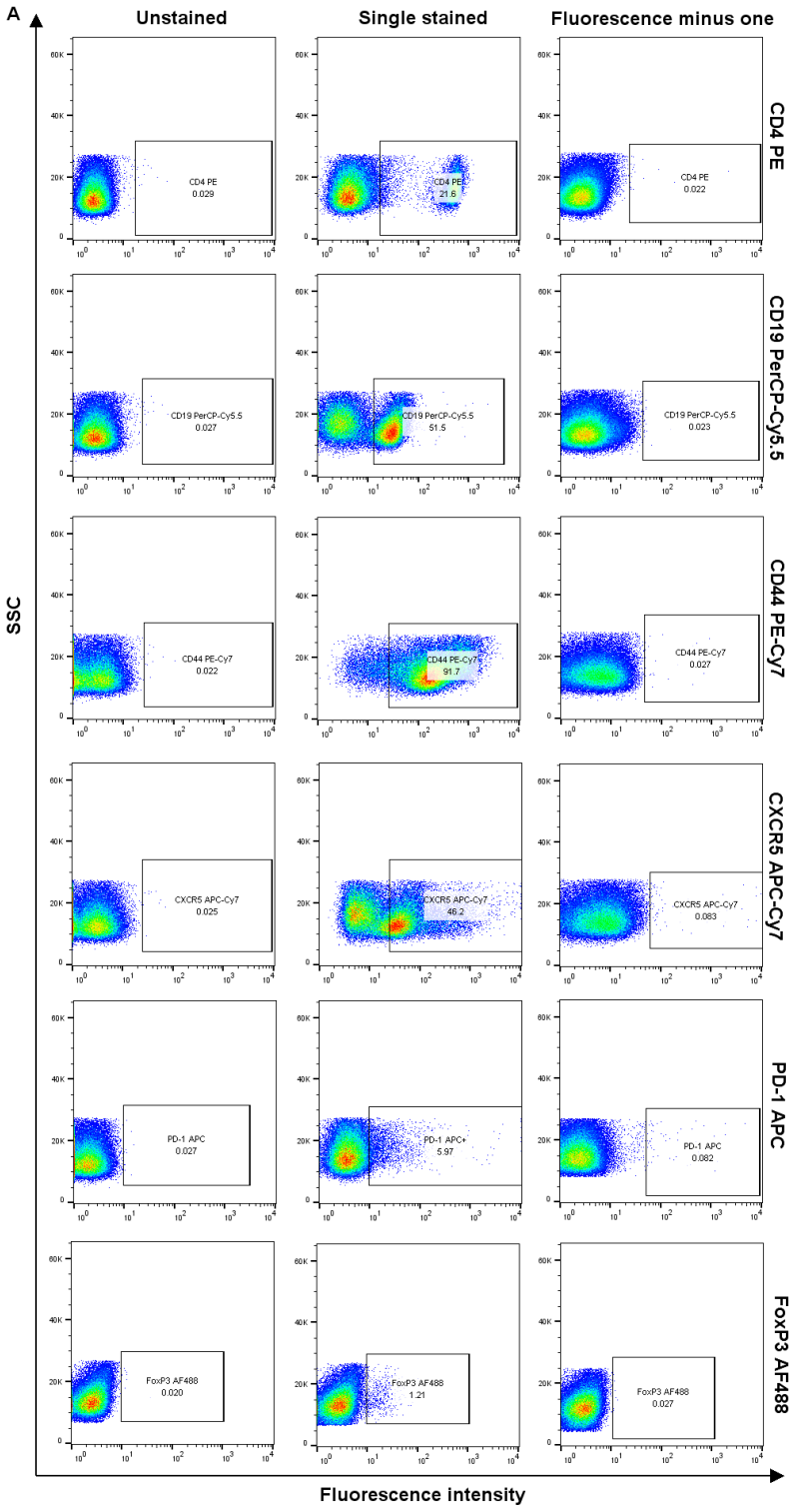

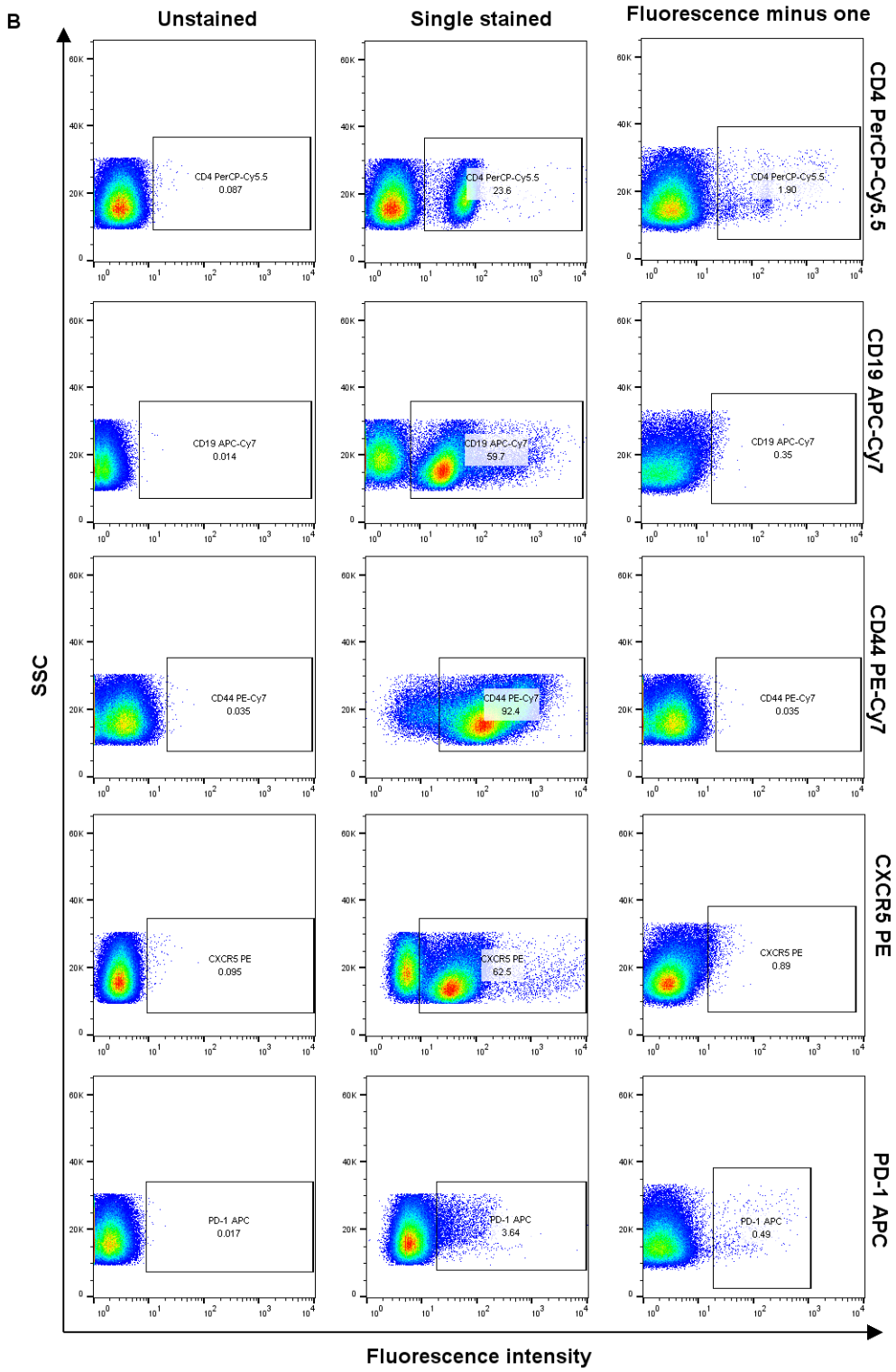
B
Unstained
Single stained
Fluorescence minus one
CD4 PerCP-Cy5.5
CD19 APC-Cy7
CD44 PE-Cy7
CXCR5 PE
PD-1 APC
CD4 PerCP-Cy5.5 0.087
CD4 PerCP-Cy5.5 23.6
CD4 PerCP-Cy5.5 1.90
CD19 APC-Cy7 0.014
CD19 APC-Cy7 59.7
CD19 APC-Cy7 0.35
CD44 PE-Cy7 0.035
CD44 PE-Cy7 92.4
CD44 PE-Cy7 0.035
CXCR5 PE 0.095
CXCR5 PE 62.5
CXCR5 PE 0.89
PD-1 APC 0.017
PD-1 APC 3.64
PD-1 APC 0.49
SSC
Fluorescence intensity

Figure A1 Gating controls for flow cytometric analysis of Tfh and GC B cells. Shown here are the unstained, single stained, and fluorescence minus one (FMO) controls for each fluorophore-conjugated antibody used to phenotypically identify Tfh and memory Tfh cells (A), and GC B and memory B cells (B) according to the gating schemes discussed in Chapter 2. The population expressing the cell surface antigen was identified using the unstained and single controls. The position of this gate was further adjusted based on the background observed in the FMO plots and in unimmunized controls.

Appendix B. Supplemental figures for Chapter 3

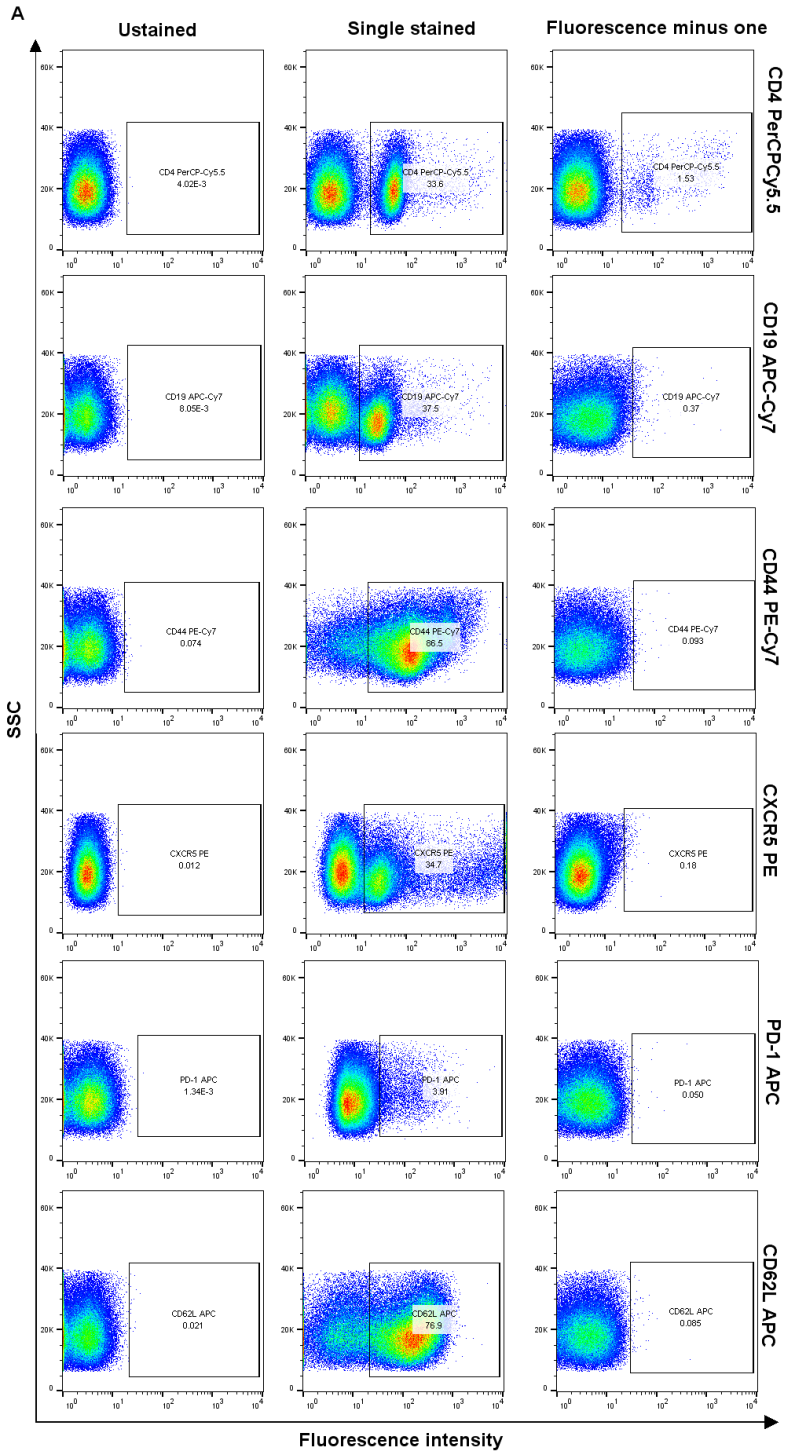

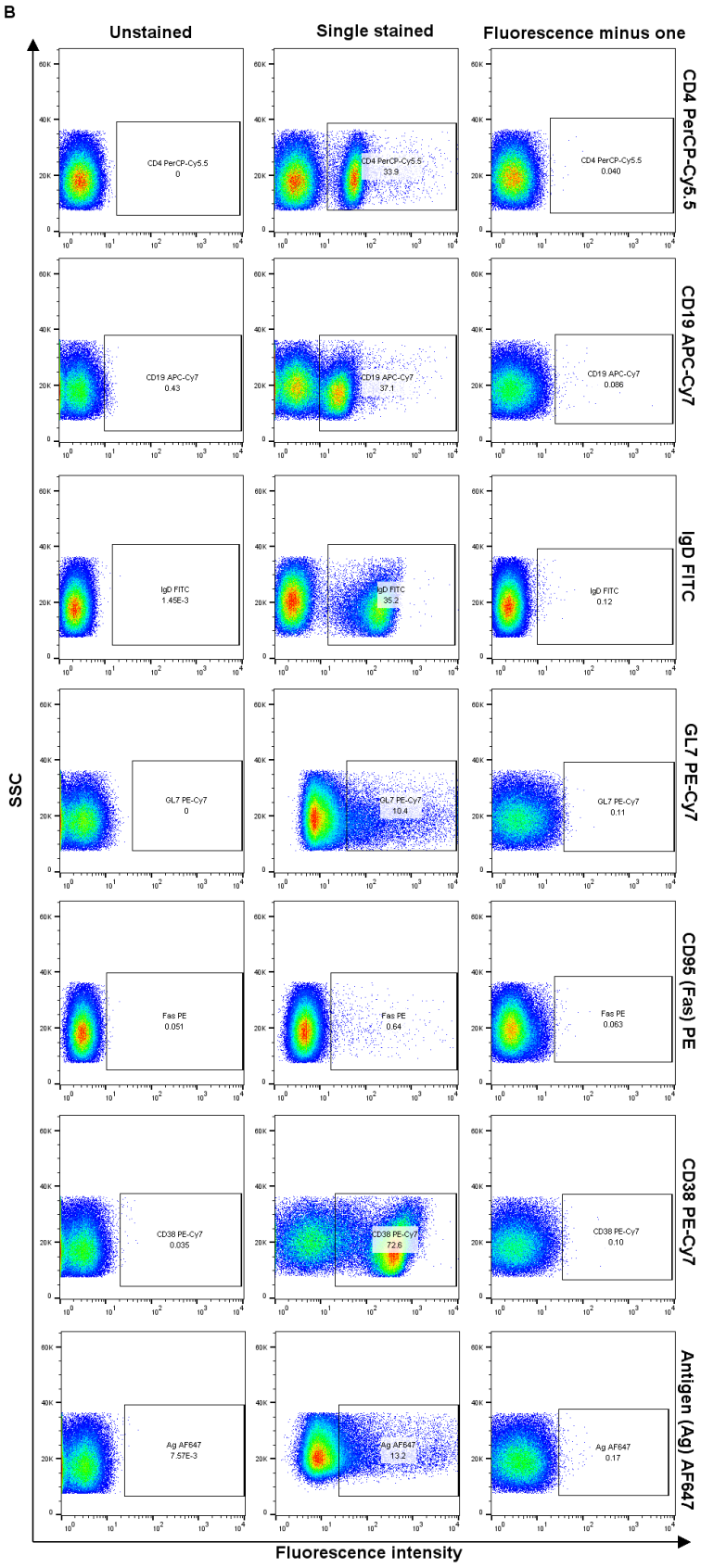
B
Unstained
Single stained
Fluorescence minus one
CD4 PerCP-Cy5.5
CD19 APC-Cy7
IgD FITC
GL7 PE-Cy7
CD95 (Fas) PE
CD38 PE-Cy7
Antigen (Ag) AF647
SSC
Fluorescence intensity

Figure B1. Gating controls for flow cytometric analysis of T and B cell subsets. Shown here are the unstained, single stained, and FMO controls for each fluorophore-conjugated antibody used to phenotypically identify Tfh and memory Tfh cells (A), and GC B and memory B cells (B) according to the gating schemes discussed in Chapter 3. The population expressing the cell surface antigen was identified using the unstained and single controls. The background was eliminated with the help of the FMO control. The position of this gate was further adjusted based on the background observed in unimmunized controls.

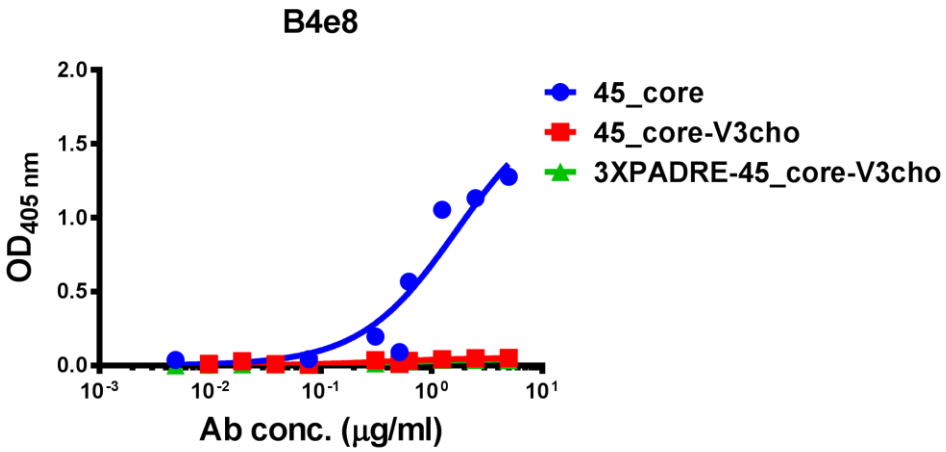

Figure B2. Binding of B4e8 to antigens without the S375Y mutation. The anti-V3 antibody B4e8 was assayed in ELISA with 45_01dG5-derived antigens lacking the S375Y mutation**.** As expected, the antibody bound only to the 45_core antigen, in which V3 is not masked by added glycans.

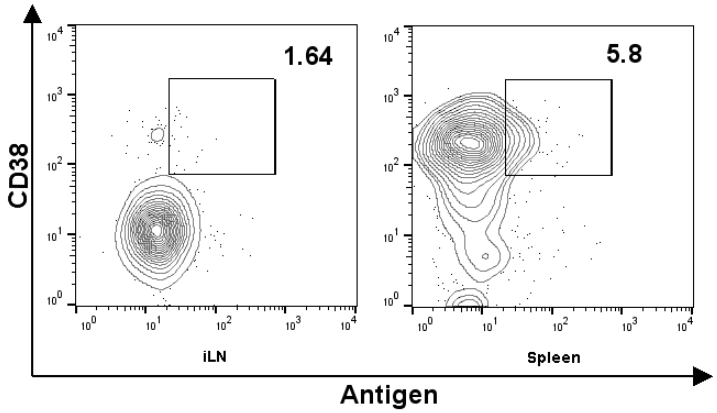

Figure B3. Comparison of memory B cells in iLN and spleens.

Shown here are the representative plots showing memory B cell frequencies in mice immunized 28 days previously with adjuvanted KLH. The memory B cells in iLN samples were lower than in the spleens, implying that this population was possibly not localized to the site of origin (iLN).

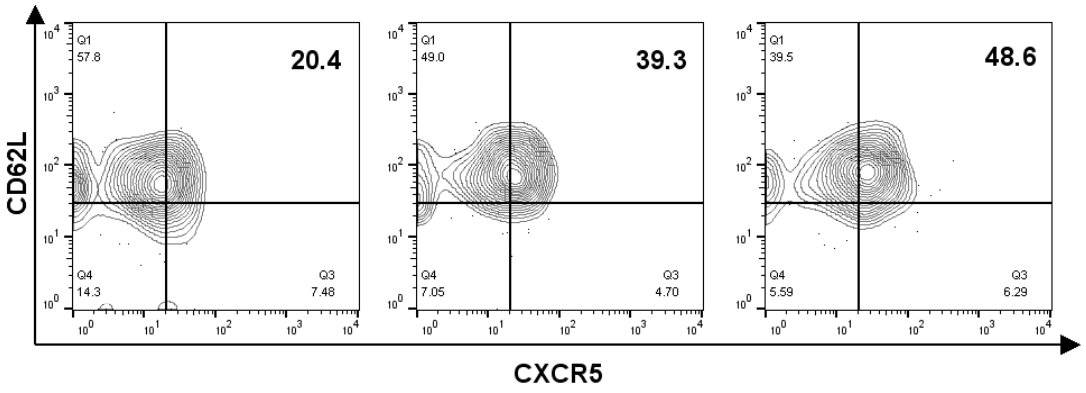

Figure B4. Meausrement of memory Tfh cells in iLN of KLH-immunized mice at Day 29 post-prime.

Memory Tfh cells were stained and measured according to the gating scheme discussed in Chapter 3. CM Tfh cells were measurable in the iLN at Day 29 post-prime.